Photo-detectors

technologies at comparison and in perspective

G.Collazuol
Dipartimento di Fisica ed Astronomia
Universita` di Padova

Overview
- Introduction
- Principles, characteristics and some developments of
  - vacuum based detectors (focusing on PMT)
  - solid state detectors (focusing on Silicon PM)
- Comparisons

Photo-detection steps

1. Photo-electric conversion with or without emission in vacuum

"external" photoemission

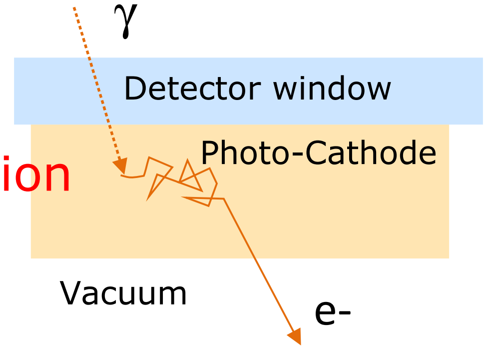

Emission in vacuum implies

☺ → low detection efficiency

☹ → low dark count rate

"internal" photoemission

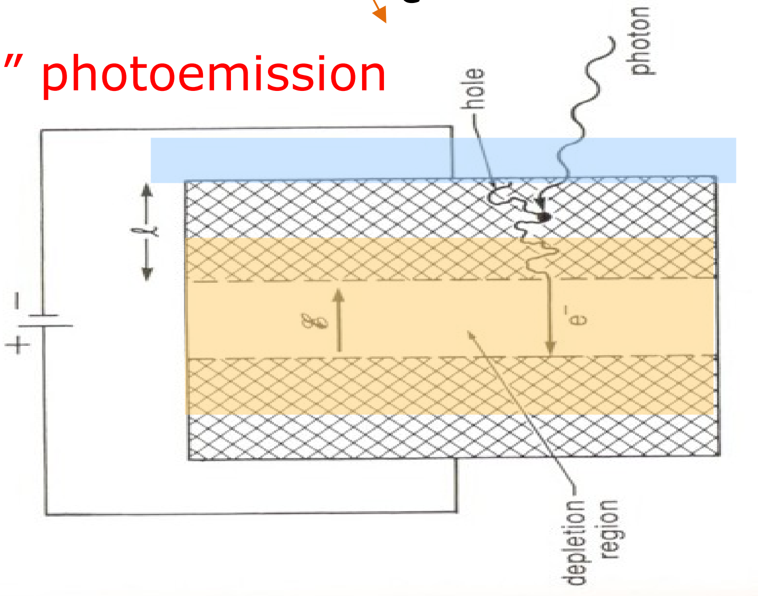

...source of main differences between vacuum and semiconductor devices also concerning multiplication...

2. Internal charge multiplication

Charge multiplication in the device implies

☺ → better S/N

☹ → intrinsic fluctuations in amplitude and timing (depending on the multiplication method)

Photo-detector family tree

Gas
External photoemission

gas photoionization
(TMAE, TEA, ...)

and/or

multiplication in gas
by avalanche
(MWPC, GEM, ...)

Vacuum devices
External photoemission

secondary electron multiplication

Dynodes:
- discrete (PMT)
- continuous dynode (channeltron, MCP)

Anode:
- multi-anode
- strip lines RF

hybrid

multiplication by
ionization in Silicon
(HPD, HAPD, ...)
or
multiplication by
luminescent anodes
(light amplifiers:
SMART/Quasar,
X-HPD, ...)

Solid state
Internal photoemission

- PIN-Photo-diode
- APD, GM-APD (SiPM)
- Imaging CMOS, CCD

- Quantum well detectors
- Supercond. Tunnel Junc.

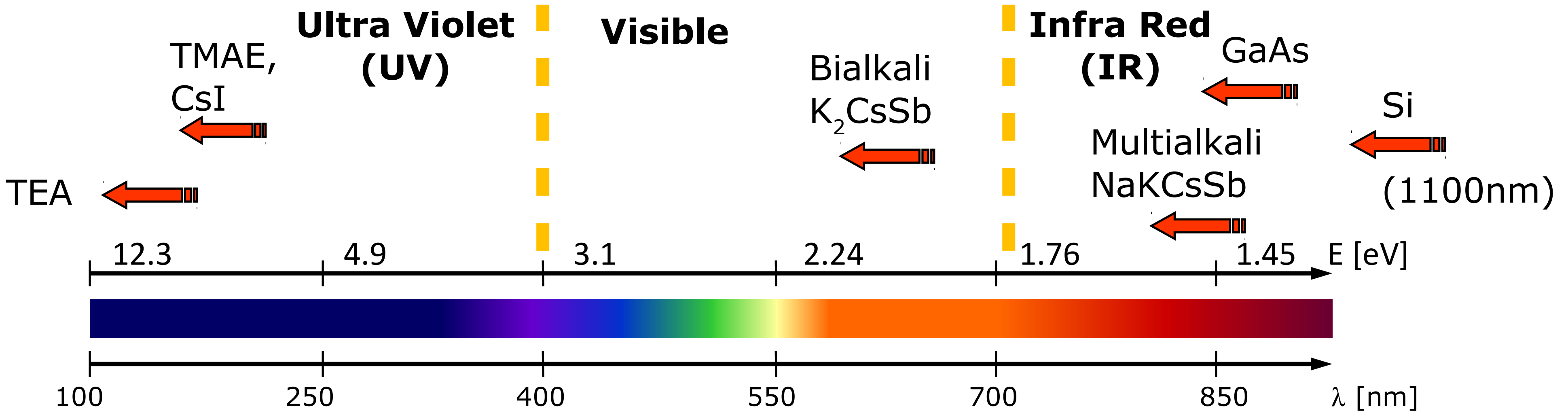

Vacuum based Photo-Detectors

Based on two fundamental phenomena:

1) photo-emission

2) secondary emission

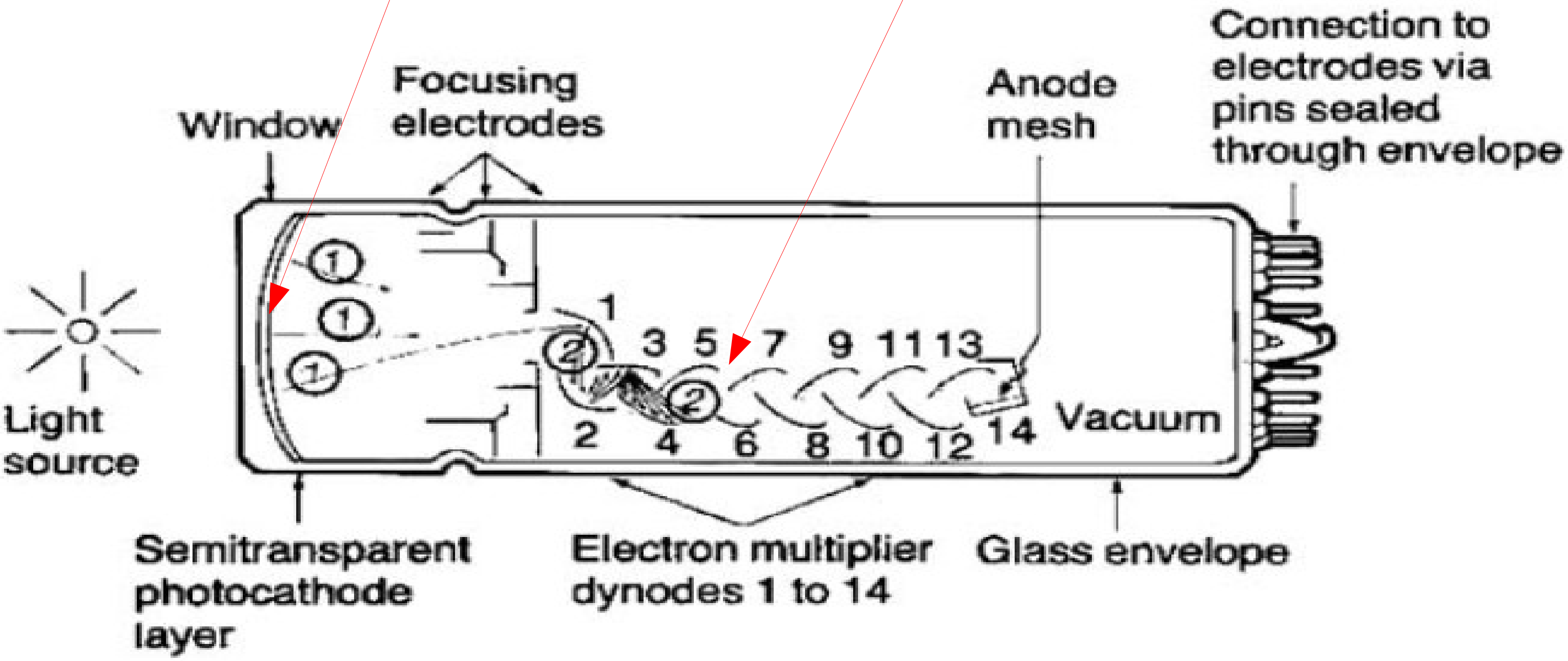

Vacuum PD fundamental parameters

Photo-Detection Efficiency

→ **PDE = QE * CE**

QE = quantum efficiency
CE = collection efficiency

Gain and Signal formation

→ **$G = g_1 g_2 \dots g_n$**

g_n = single stage gain

Noise sources

→ **Dark count**
→ **After-Pulsing**

fluctuations in measurement of

- **Amplitude** (number of photons)
- **Position** (photon impact position)
- **Timing** (photon arrival time)

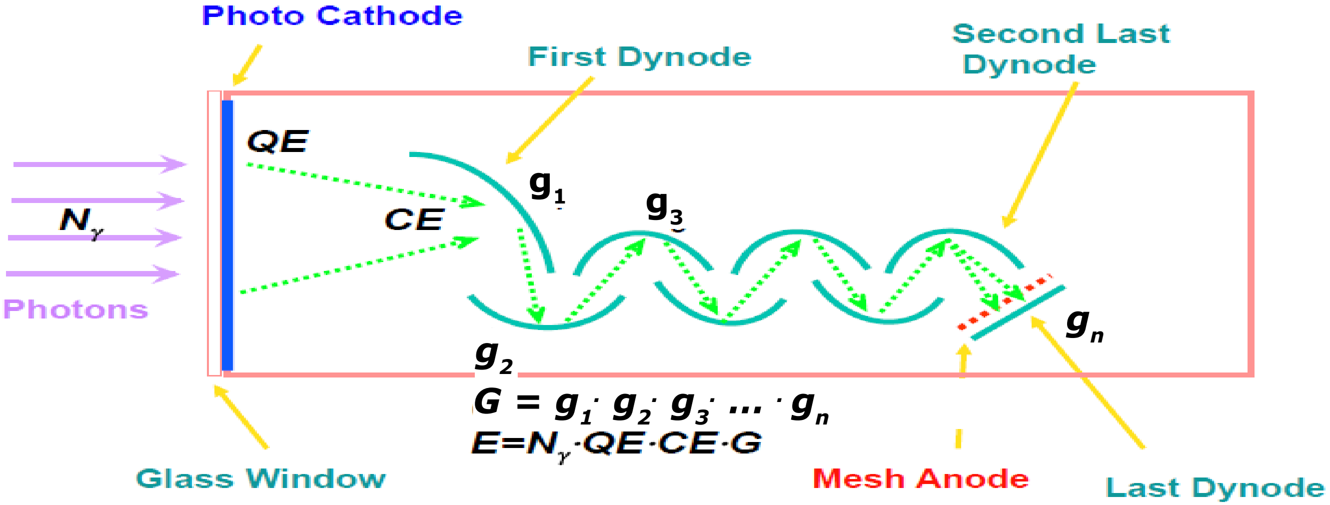

Photo Detection Efficiency (PDE)

$$\frac{\#\text{emitted photo-electrons}}{\#\text{incident photons}} \qquad \frac{\#\text{ph.e captured by } 1^{st} \text{ dynode}}{\#\text{emitted ph.e}}$$

$$PDE = QE \times CE$$

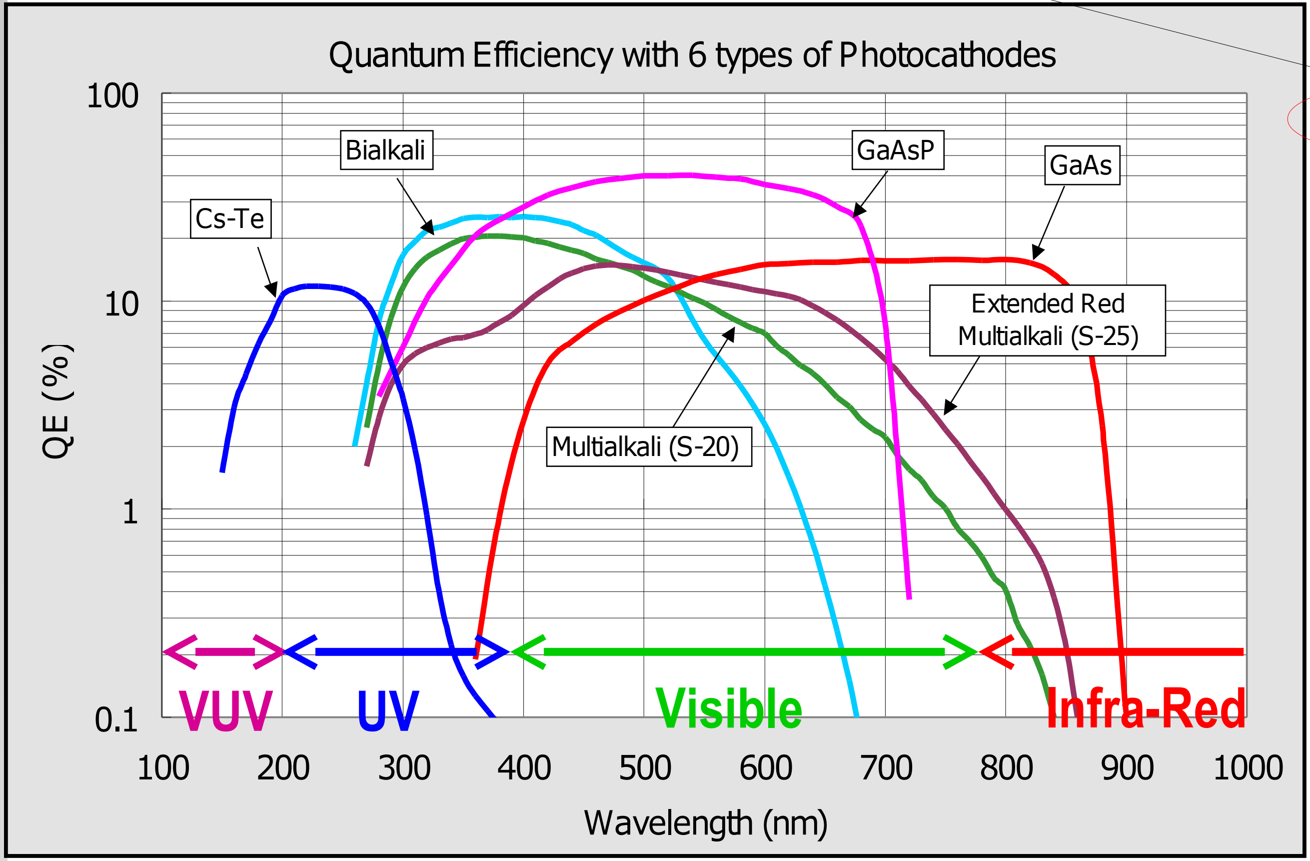

Photo-cathode determines

- quantum efficiency QE(λ)
- angular and momentum distribution of 1st photo-electron
- noise behavior
- part of timing fluctuations

Photo-cathode: most crucial element in any PMT type
→ still **room for improvement** !
→ since last 10 years revived interest in R&D for new photo-cathodes

Photo-emission: a bulk process in 3 steps

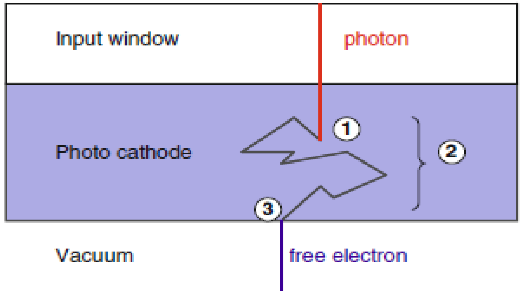

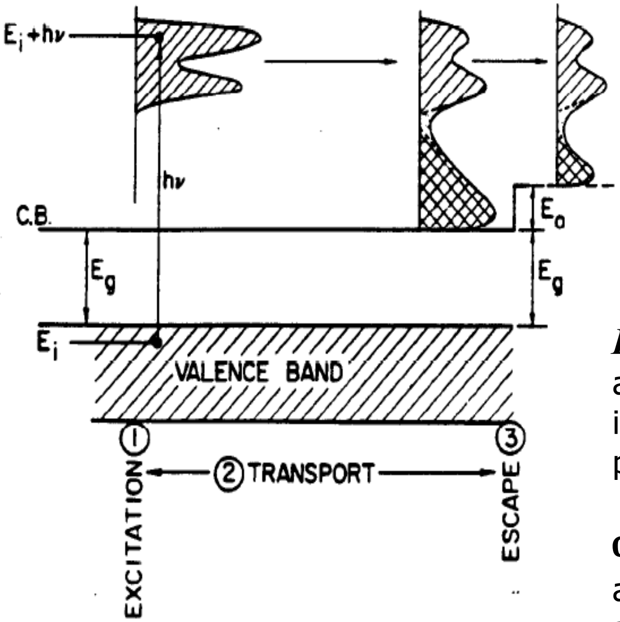

W.E.Spicer, Phys. Rev.112 (1958) 114

$$QE = (1-R)\frac{\alpha_{PE}P_E}{\alpha}\frac{1}{1+{l_a}/{L}}$$

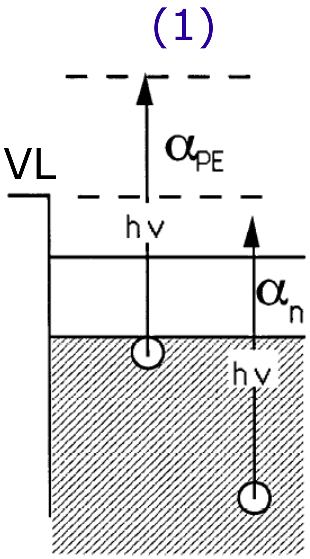

Absorption and Excitation

R = reflection coeff. is a function of angle of incidence and polarization

α_{PE}/α = fraction of the absorbed electrons that are **excited above the vacuum level** (VL)

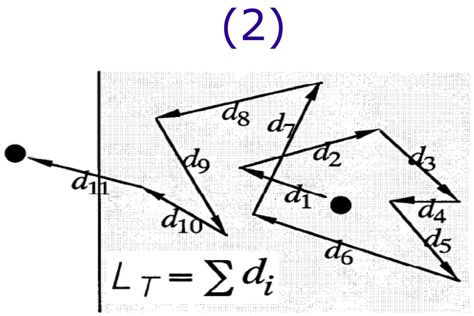

Transport

from conversion location to vacuum interface by **diffusion.** In presence of band bending (BB) near interface then also **drift** (outward BB help escape)

During transport :
1) E loss (**thermalization**) down towards bottom CB by scattering (hundreds of collisions)

2) Electron **losses** due to:
- trapping due to inward BB at vacuum interface or outward BB at window itface
- **recombination** due to impurities (cristallinity is a crucial factor)

l_a/L = photon absorption length over electron scattering length (wide range 1-10^4) The lower **l_a/L** the less recombination

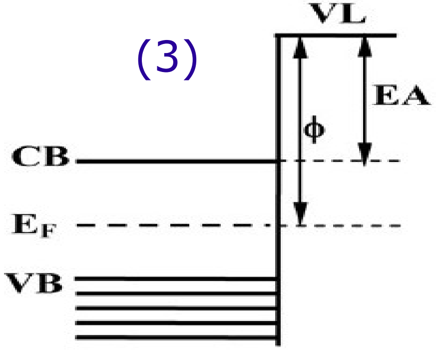

Escape to vacuum

P_E = fraction of electrons that reach the surface keeping sufficient energy E to escape (usually P_E <0.5)

E > electron affinity (EA)
EA = E vacuum – E CB bulk
(work function for metals)

Longest wavelength cutoff in QE due to Ebandgap + EA

Special semiconductor threatment → negative EA

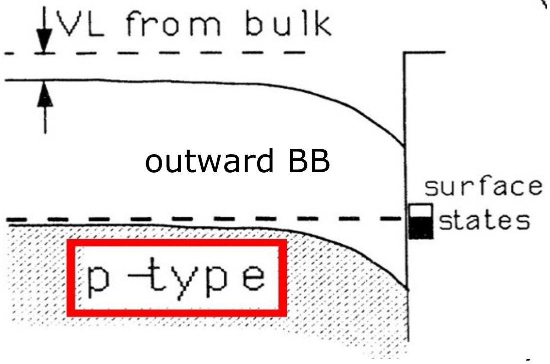

Photocathodes

Most efficient bulk material for **photocathode are semiconductors**

Metal photocathodes show much lower QE due to:

- energy-momentum conservation forbid absorption on free e- in CB → high reflectivity

- electrons suffer e-e scattering → escape depth L very short (large l_a/L)
  NOTE: in semiconductors e-e is not allowed for optical excitations due to bandgap → only energy loss via electron-phonon → small l_a/L

- work function ϕ > 2eV (metals) compares with smaller E_A (few 0.1eV) or (even better) negative in semiconductors (NEA)

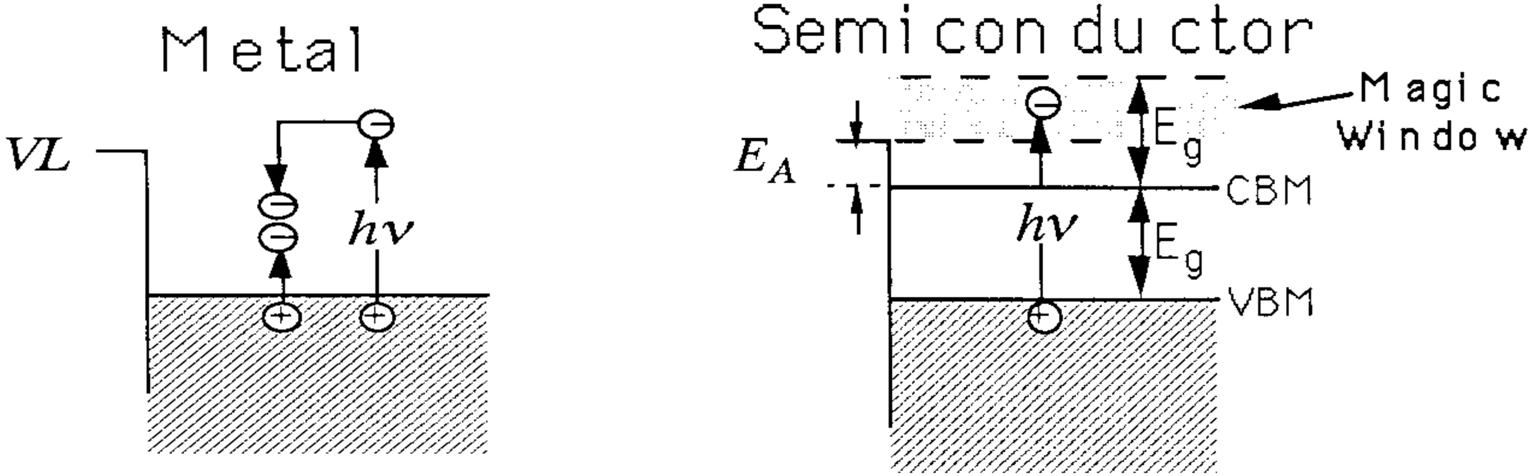

W.E.Spicer, A.Herrera-Gomez SLAC-PUB-6306 (1993)

Photocathodes – Negative Electron Affinity

Cs plays a large role for NEA:

1) band bending (BB) through donor surface states → vacuum level shifted down

- Cs-induced donor-like surface states contribute their electrons to the bulk
- Hole depleted region (negatively charged acceptors) lead to BB region
  → internal built-in electric field (acceletation in BB region)

2) dipole surface layer from polarized Cs atoms

- Majority of Cs atoms become only polarized forming a dipole layer (e- Cs+)
  → external electric field (cusp barrier → tunneling)

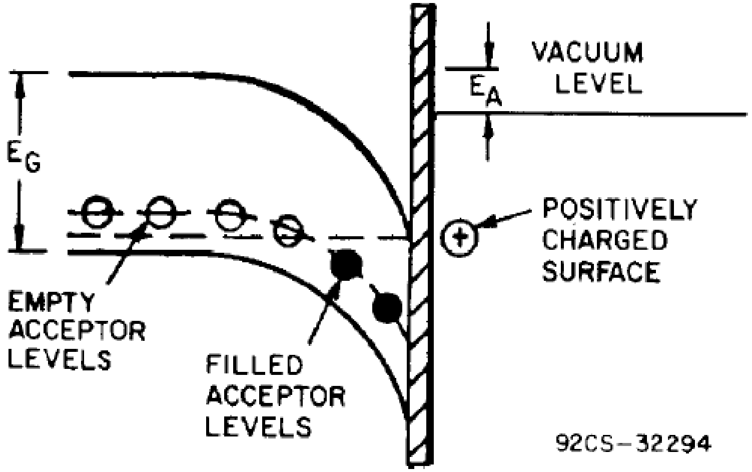

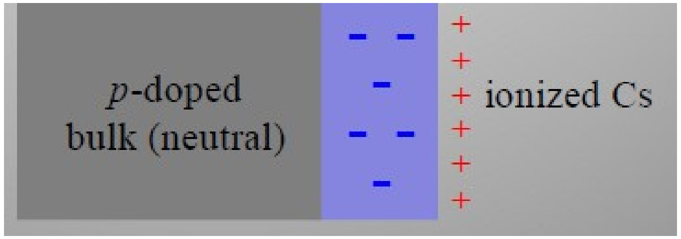

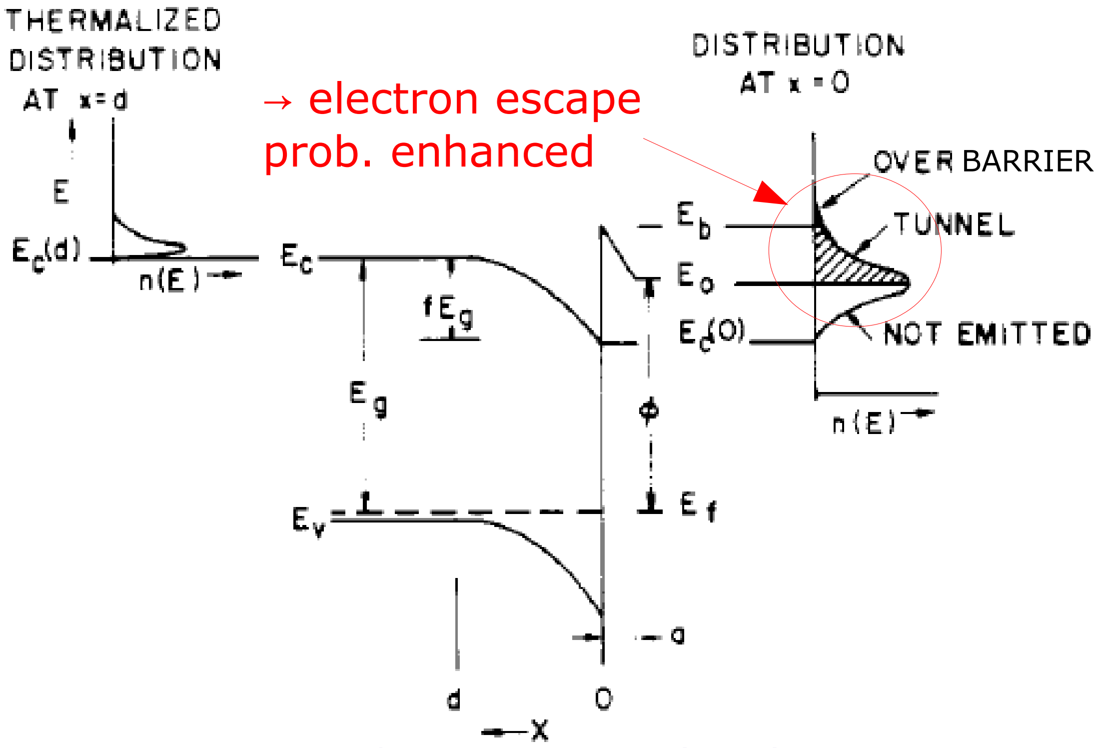

→ electron escape prob. enhanced

R.Martinelli, D.G.Fisher IEEE Procs 62 (1974)

Most common photocathodes

1) Bi/Multi-alkali-antimonides

→ K/Na + Sb in bulk + Cs/Rb at surface

→ poly-cristalline layers w/ high carrier lifetime

→ very good absorbers for photons 200-850nm

eg. Na_3Sb, K_3Sb (Bialkali), Na_2KSb (S20, S25)

Weak points:

- recombination centers in poly-crystalline struct.
- active layer directly deposited on window
  → electron sink due to outward band bending

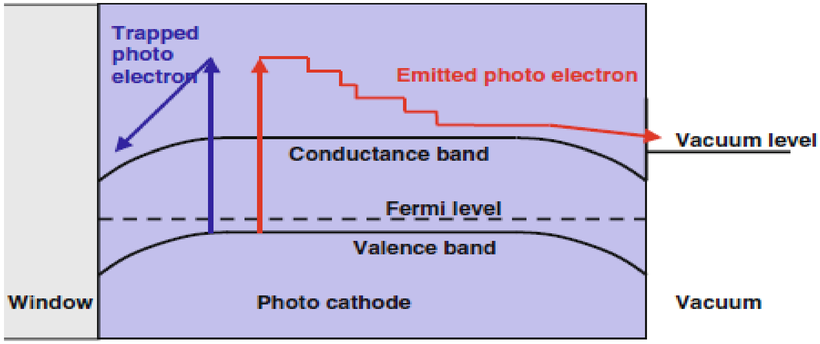

Examples:

- S20 has PEA (cutoff at 820nm)

☹ only hot e- escape → thin layer (60nm)

☺ low dark rate (<Khz/cm²)

- S25 has NEA (cutoff at bandgap, 890nm)

☺ → thick layer (170nm)

☹ higher dark rate (10KHz/cm²)

2) III-V semiconductors

→ GaAs, GaAsP bulk + Cs for NEA

→ very pure mono-crystalline layers

→ easy doping and hetero junctions

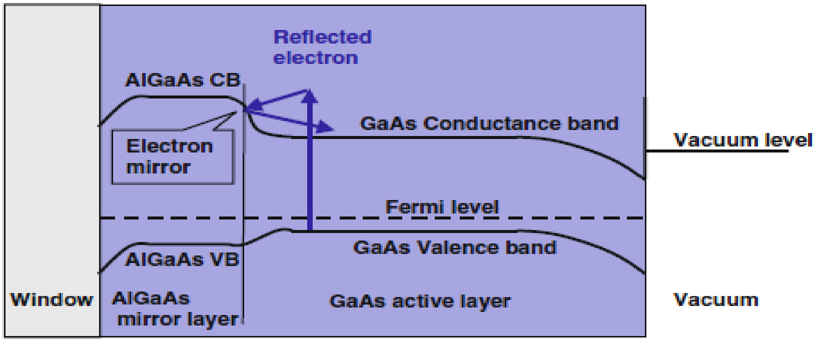

Weak points:

- extreme sensitivity to over-exposure and ion feed-back
- high dark rate (10KHz/cm²)

Note: alkali metals are very strong oxidizers

→ the smallest amount of O_2or H_2O totally burn any cathode

→ ultra high vacuum (10^{-9} mbar) needed

Most recent high QE photocathodes

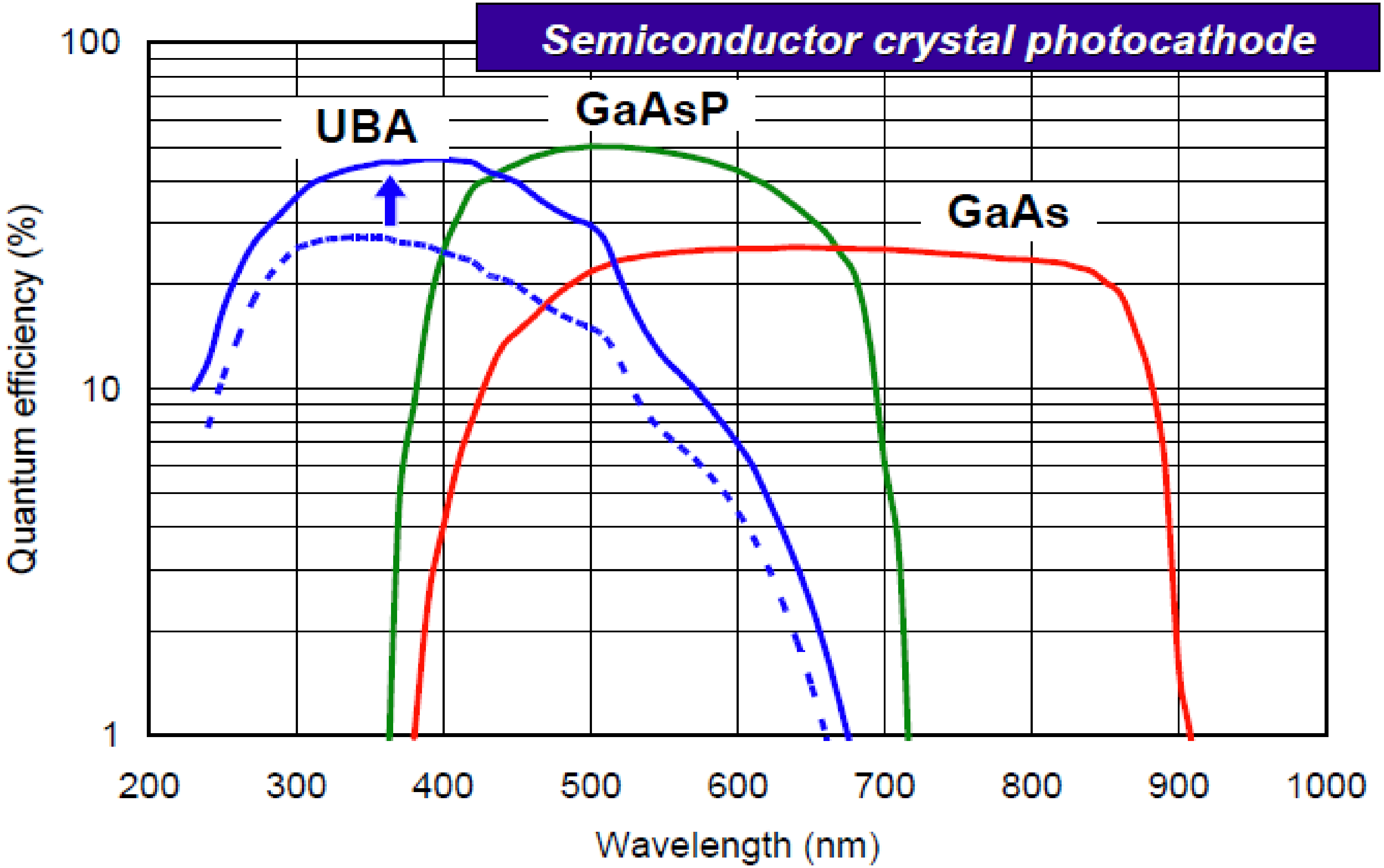

Hamamatsu - HPK

Future photocathodes

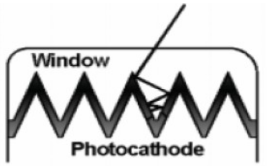

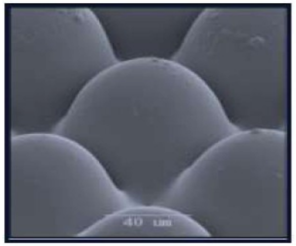

1) Search for new photocathode (PC) materials
- bi- and multi-alkali revisited (eg. Li_2CsSb)
- III-Nitrides (eg. GaN, $Al_xGa_{1-x}N$)
- II-VI (eg. ZnO, $Zn_{1-x}Mg_xO$)

2) Electron emission enhancement
- Piezoelectrically enhanced PC (no Cs)
- Electric field assisted emission
- anti-reflecting structures (eg nanowires)

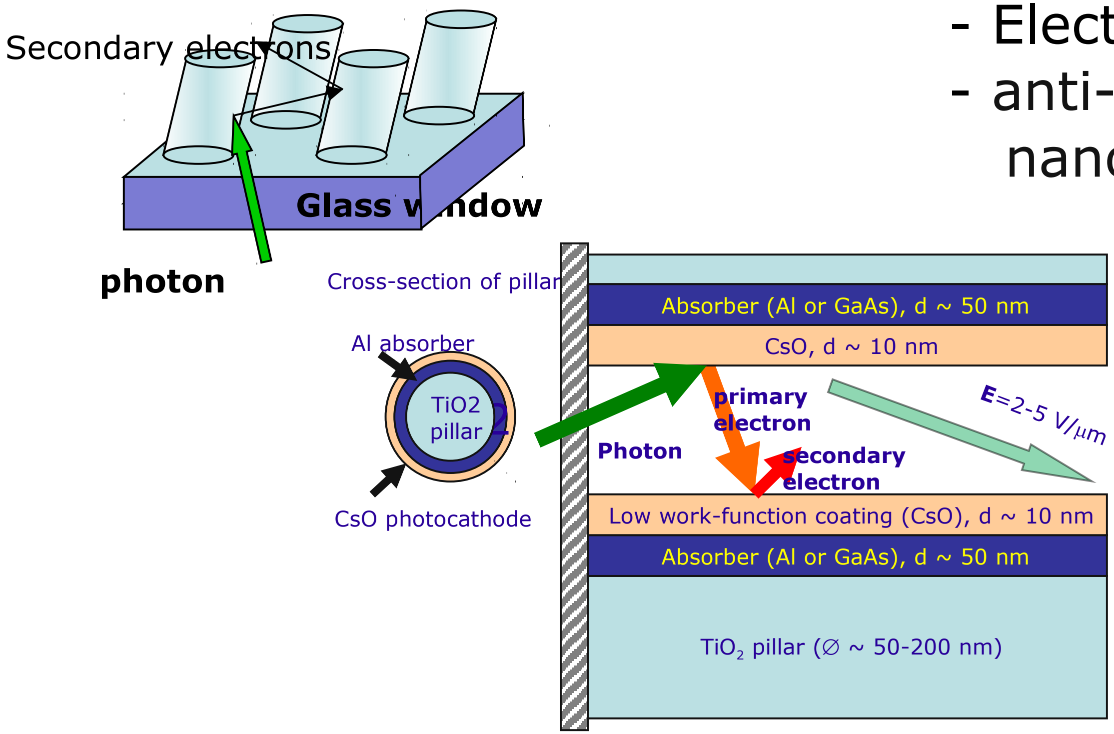

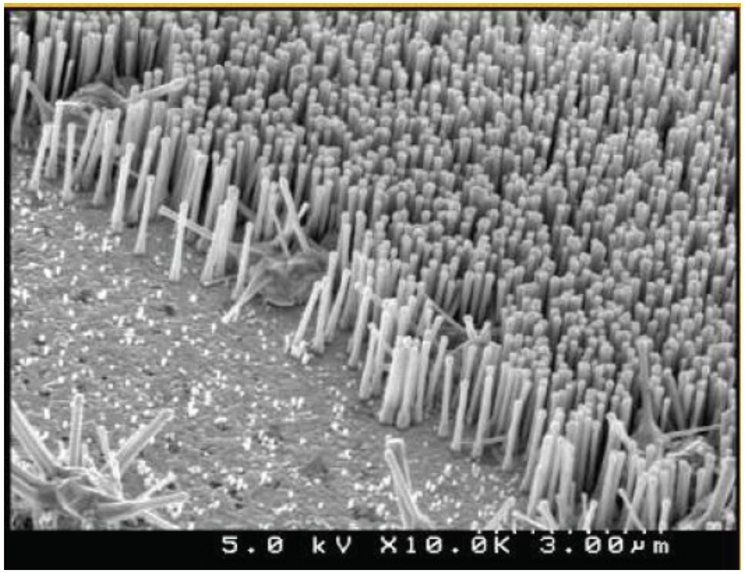

Photocathode Workshop
University of Chicago July 2009
http://psec.uchicago.edu/photocathodeConference/

Gain mechanisms: electron multiplication

Secondary emission from n dynodes → primary ph.e. multiplication

$$\text{Gain} = \frac{\text{\#electrons delivered to the anode}}{\text{\#ph.e captured by } 1^{st} \text{ dynode}}$$

dynode gain g~3-50 (function of incoming electron energy E)
→ total gain **$G = g_1 g_2 \ldots g_n \sim g^n$**
Example: 10 dynodes with g=4 → $g = 4^{10}$ **~**10^6

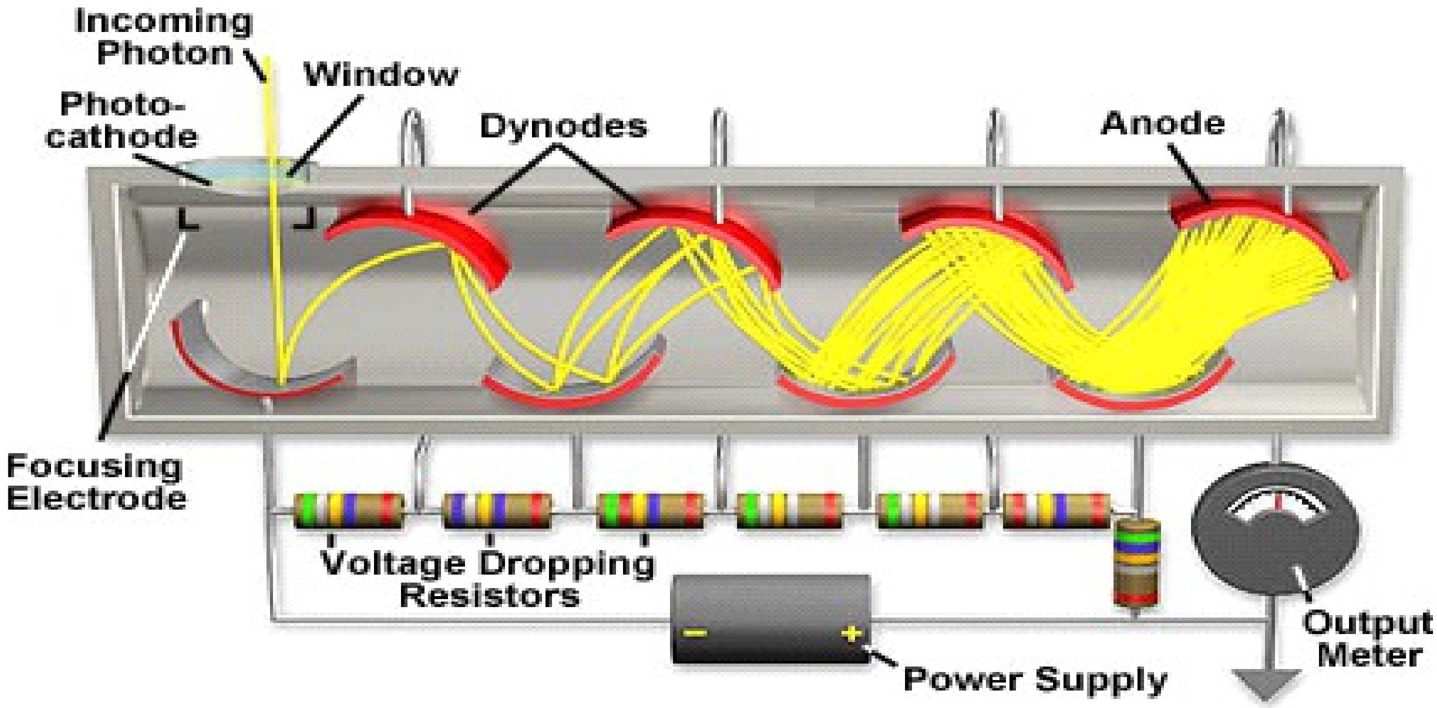

Potential difference between adjacent dynodes typically
→ΔV ~ 100V

Secondary electron multiplication

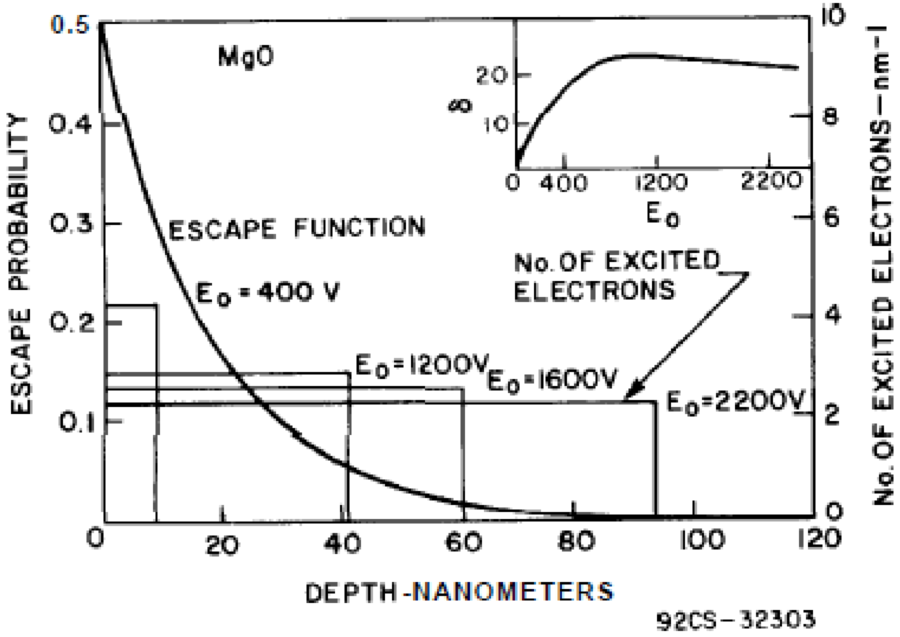

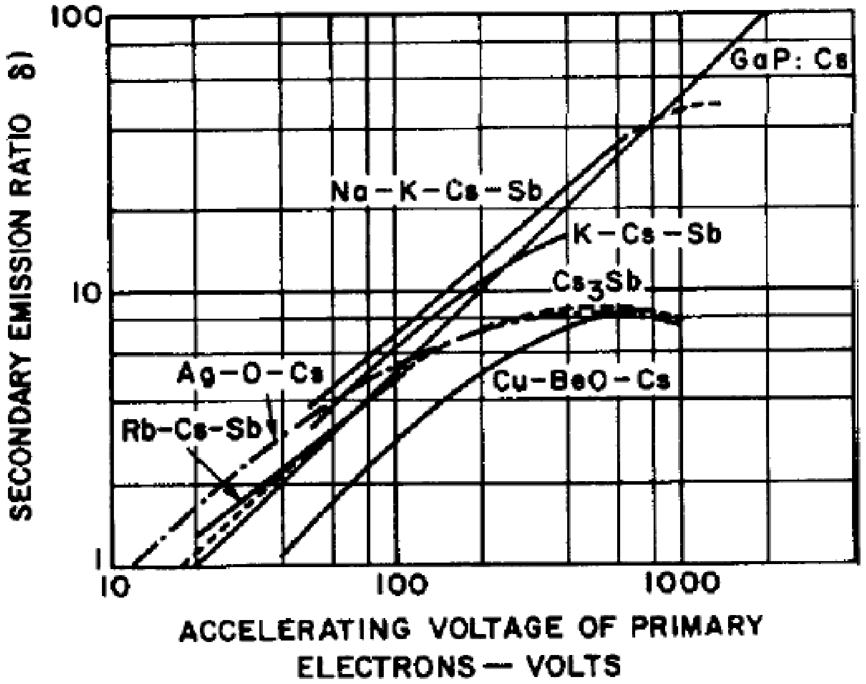

Process in 3 steps (again):

1) absorbed primary electrons impart energy to electrons in the material (depending on their energy, primary electrons may back-scatter)

2) energized electrons diffuse through the material

3) electrons reaching the surface with sufficient excess energy escape into the vacuum

Steps 2 and 3 are similar to photoemission:

→ **best materials are semiconductors (activated by Cs)**

→ **NEA improves secondary production**

$g \sim HV^{\alpha} \rightarrow G \sim HV^{\alpha n}$

g = dynode gain

α = 0.65-0.75

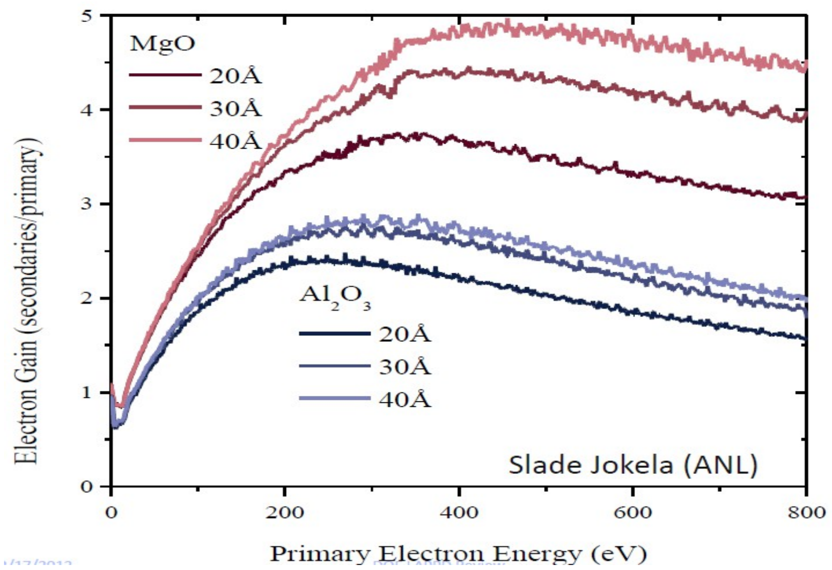

Slade Jokela (ANL)

Electron multiplier types

discrete multiplication

continuous multiplication

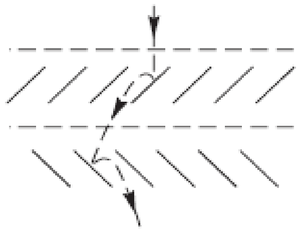

venetian blind

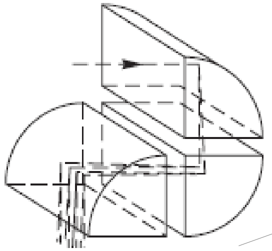

box & grid

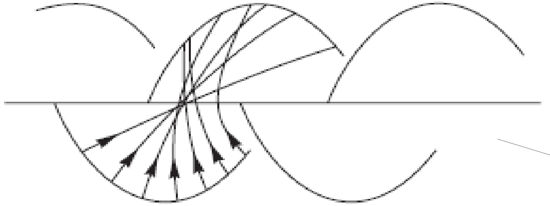

linear focus

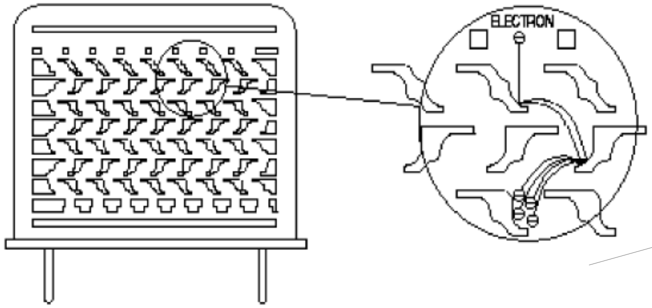

metal channel

PDE (CE)	Gain stability	Timing	B field immun.
🙂	🙂	☹	☹
😐	😐	🙂	🙂
☹	😐	🙂	☹
🙂	😐	😐	🙂

micro-channel plate (MCP)

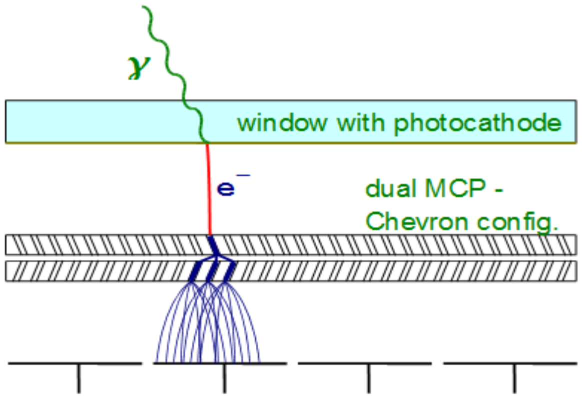

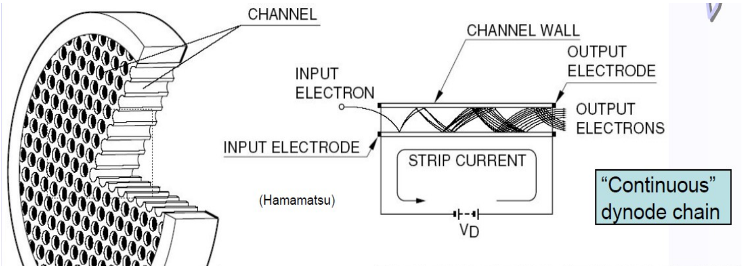

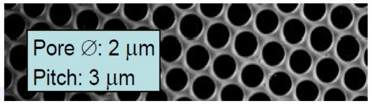

Pore length: 400μm

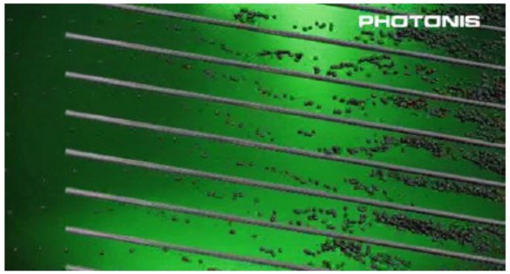

...plus a number of variants...

Gain fluctuations: single electron spectrum

Secondary emission process → **large amplitude fluctuations**
→ measure **single electron response** (SER) in amplitude

SER relative variance

$$\frac{\sigma_A^2}{A^2} = \frac{1}{g_1} + \frac{1}{g_1 g_2} + \ldots + \frac{1}{g_1 g_2 \ldots g_n}$$

Note: dynode multiplication is assumed Poisson process (only a first approximation; consider for instance dynodes non-uniformity

Main contribution is from 1st dynode
→ improvement when higher $V_{K\text{-}Dy1}$

Excess Noise Factor (ENF)
for a multiplication process

$$ENF \equiv \frac{\sigma_{output}^2}{\sigma_{input}^2} = 1 + \frac{\sigma_M^2}{M^2}$$

Multiplication noise

ENF in the case of PMT:

$$ENF = 1 + \frac{1}{g_1} + \frac{1}{g_1 g_2} + \ldots + \frac{1}{g_1 g_2 \ldots g_n}$$

SER variance is multiplication variance !

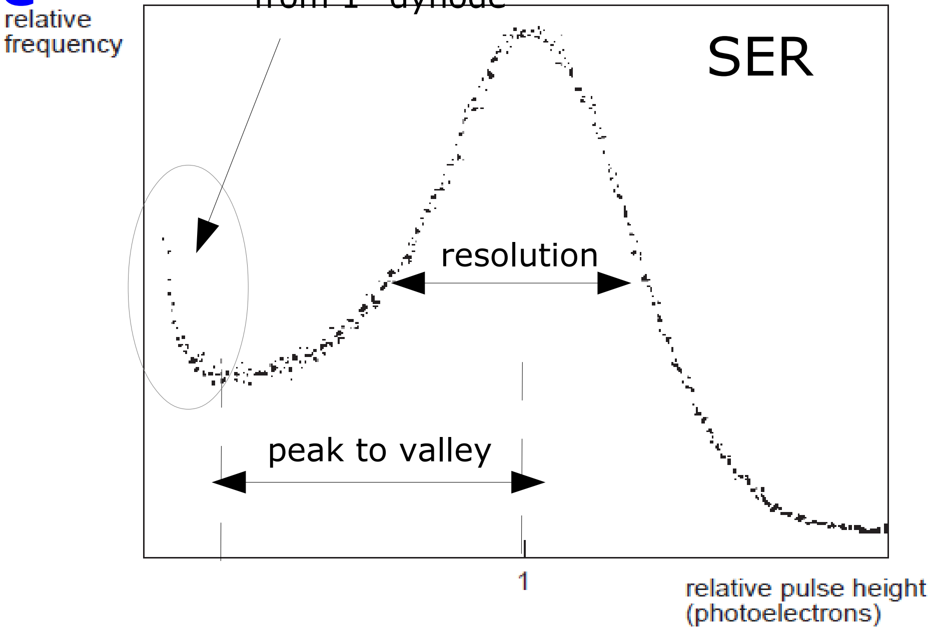

Note: small amplitudes due to photoelectrons back-scattered from 1st dynode

Fig.2.4 Typical single-electron spectrum. Resolution 67% FWHM. Peak-to-valley ratio 2.8:1

Flyckt and Marmorier –
"PMT principles and applications"

Gain fluctuations: single photon resolution

Single photon resolution
only when **$g_1 \geq 12$**

either 1) **higher $V_{K\text{-}Dy1}$** (modify divider ratio)
or 2) use PMT with **NEA for 1st dynode**
… anyway the price is **higher dark noise**

PMT (Hamamatsu R5600)

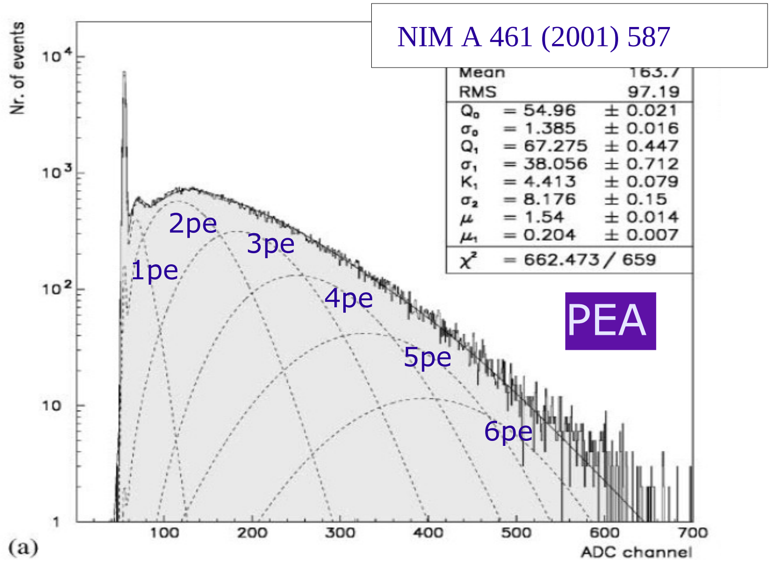

NIM A 461 (2001) 587

NIM 112 (1974) 121

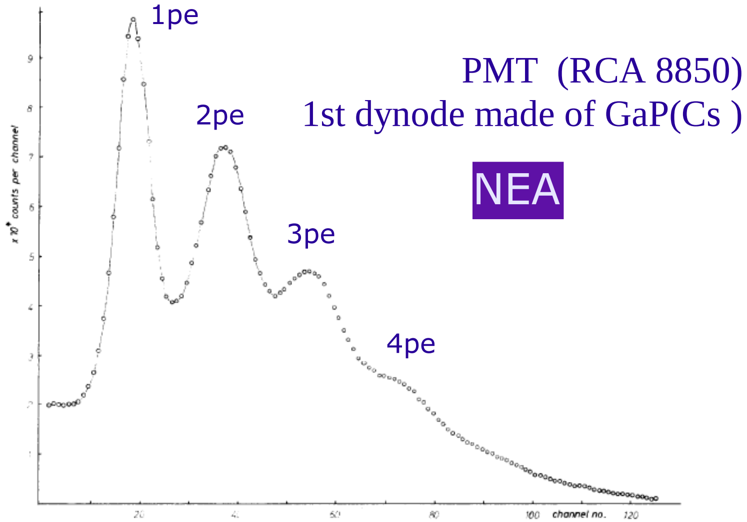

PMT (RCA 8850)
1st dynode made of GaP(Cs)

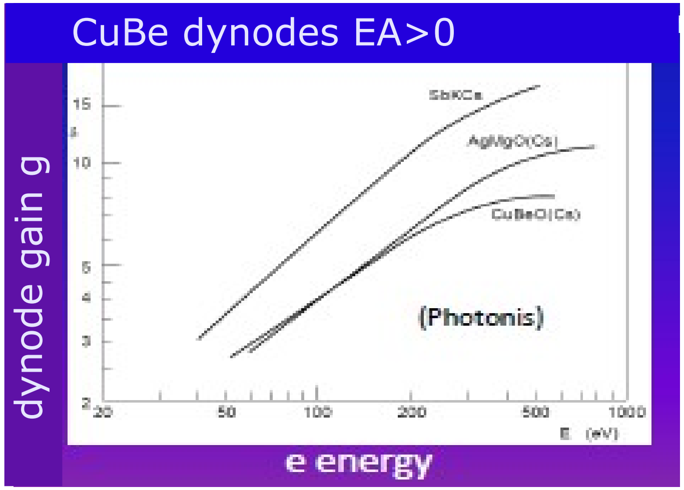

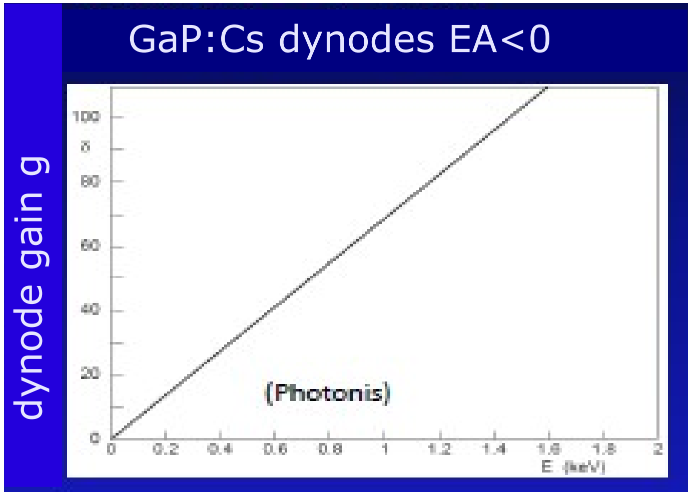

Gain and photo-conversion fluctuations

→ Amplitude resolution (eg in Energy measurement)

Combining **Photo-conversion fluctuations** (binomial statistics)
and **Gain fluctuations** (Poisson, in good approximation)
→ get PMT contribution to **amplitude resolution** (E = Nγ PDE G)

$$\frac{\sigma_E}{E} = \frac{\sigma_{N_\gamma}}{N_\gamma} = \sqrt{\frac{ENF - PDE}{N_\gamma \; PDE}} = \sqrt{\frac{ENF - (QE \;\; CE)}{N_\gamma \; QE \;\; CE}}$$

Question: **how to measure Nγ** ?
Answer: must measure QE, CE, G and ENF before !

1) **measure QE** from the ratio of cathode currents I_C for PMT and calibrated detector (known QE)
→ $QE = QE_{cal} \; I_C / I_{C\,cal}$ (All dynodes connected to anode at +100V wrt cathode)

2) **measure CE** from the ratio between single ph.e counting rate $R_{ph.e}$ and cathode current I_C
→ $CE = q_e \, R_{ph.e} / I_C$ (need calibrated neutral filter when counting single ph.e)

3) **measure G** from SER → G = <A>
Alternative: measure G x CE from ratio between anode and cathode currents → $G \times CE = I_A / I_C$

4) **measure ENF** from SER relative variance
→ $\frac{\sigma_A}{A} = \sqrt{ENF - 1}$

Dynamic range – pulse linearity

Deviation from linear response due to

1) **space charge** between last and 2nd to last dynode ← anode current saturation
2) multiplication current ~ divider current → gain unstable
3) slow photocathode recharge (eg at low T) ← cathode current saturation

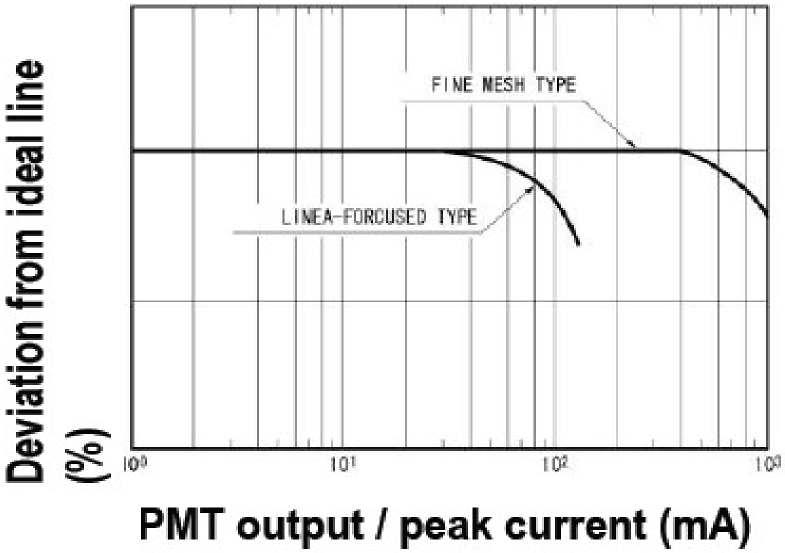

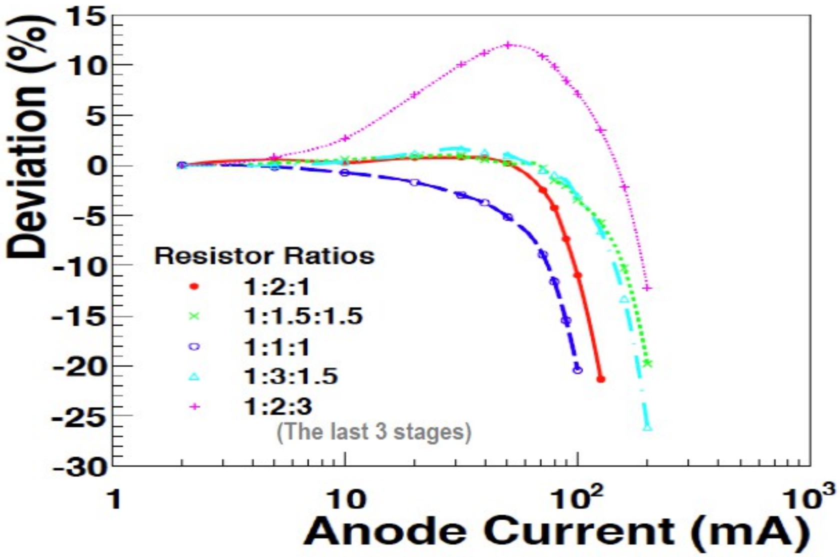

Tapered voltage divider

K.Arisaka – PMT lecture at IEEE NSS 2012 (Anaheim)

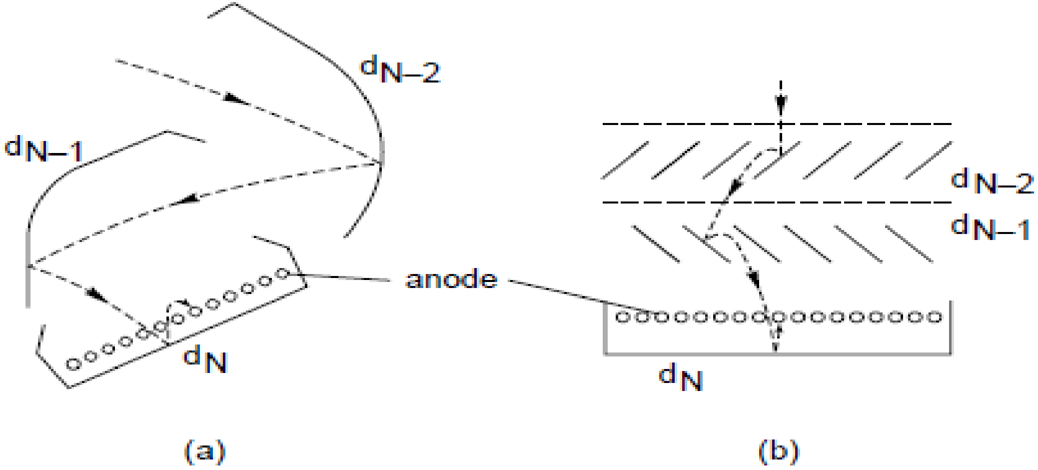

Anode shape: grid positioned close to the last dynode → allow **high electric field** between the last dynode and anode → reduce the space charge effect in the last stage

Flyckt and Marmorier – “PMT principles and applications”

Dynamic range – pulse linearity

Passive Voltage Divider

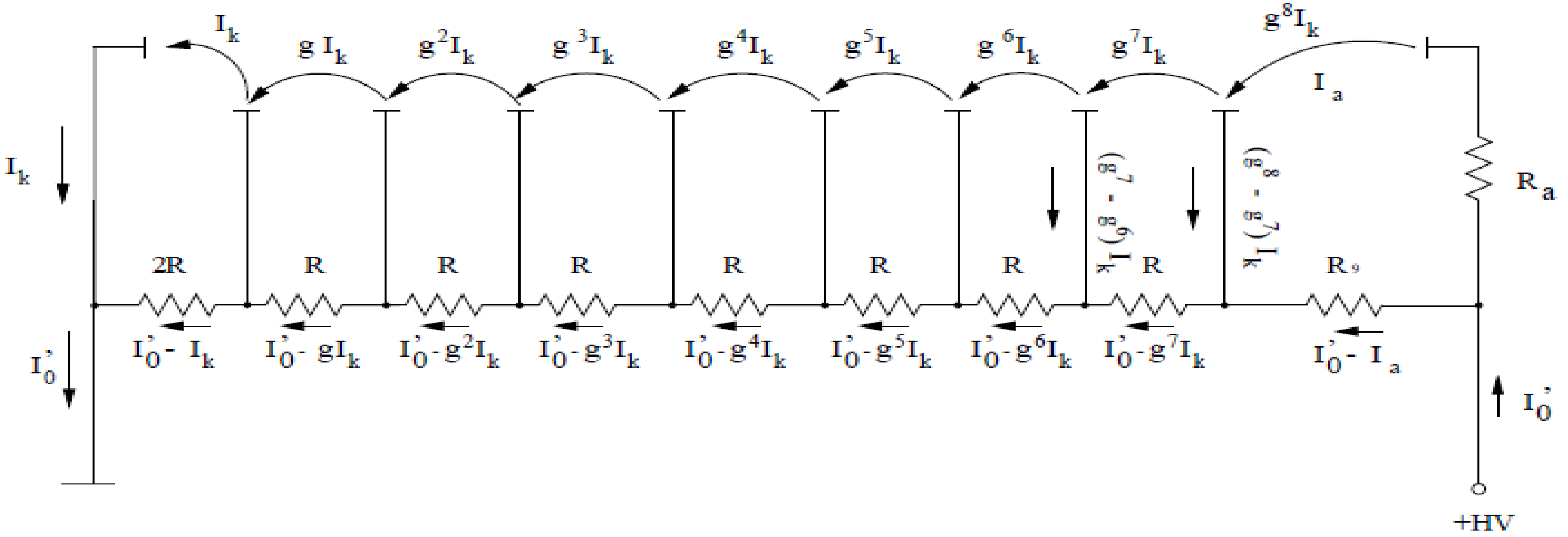

1) Tapered voltage divider reduces effects due to space-charge

Active Voltage Divider

2) Charge storage capacitors give prompt charge

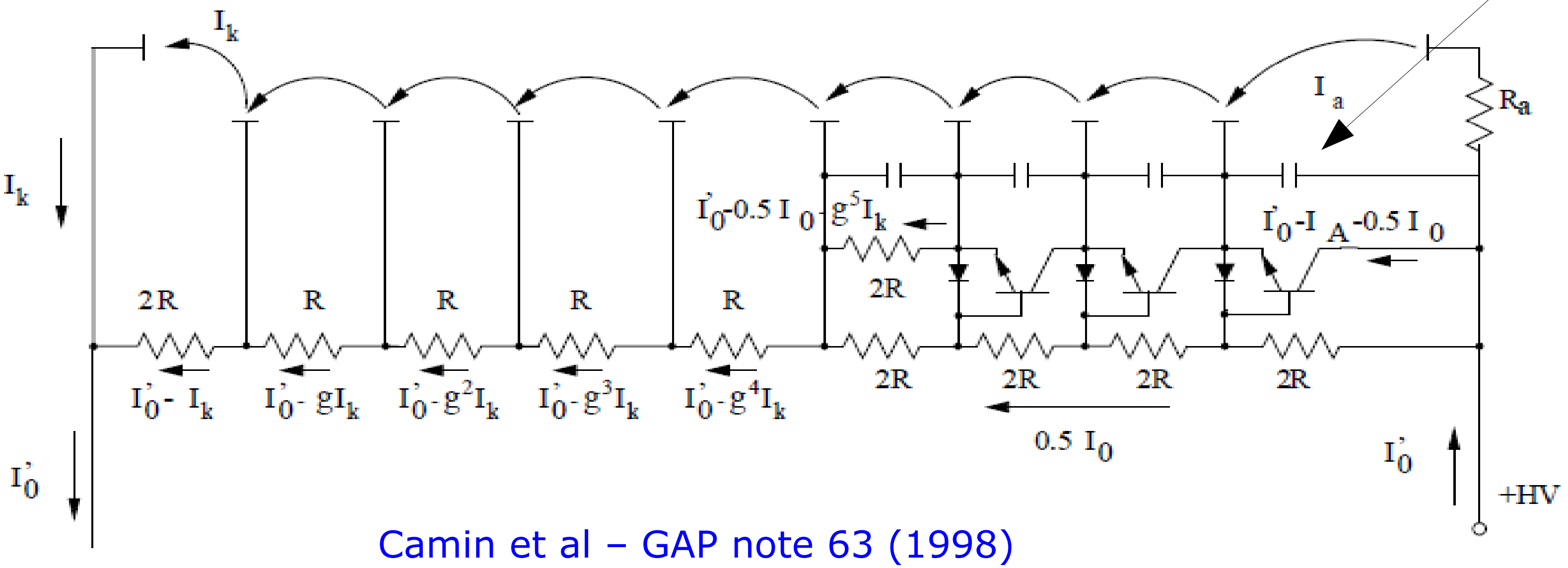

3) Transistors keep constant collector-emitter voltage (ie fix dynode potential) independent of the divider current

Camin et al – GAP note 63 (1998)

Effects of magnetic fields

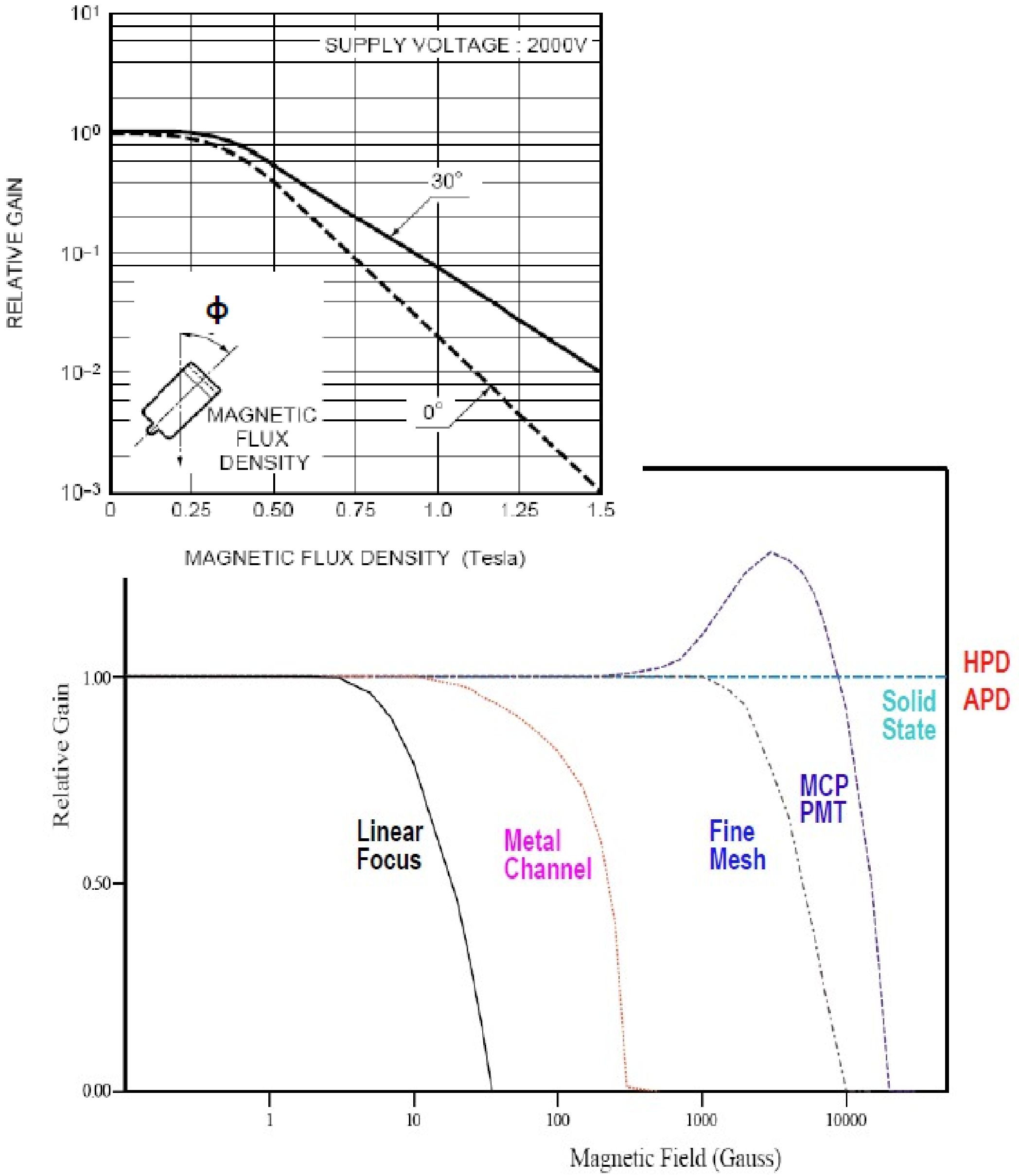

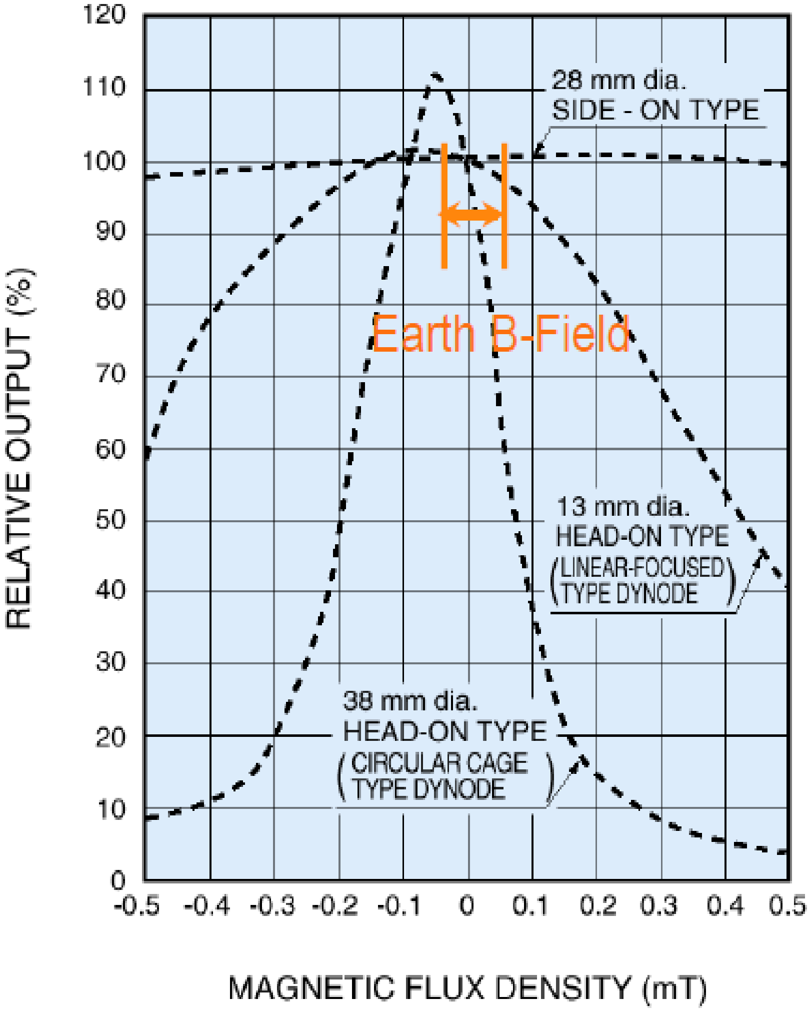

PMT is very sensitive to B fields → need shield (μ metal)

Dark Noise sources in PMT

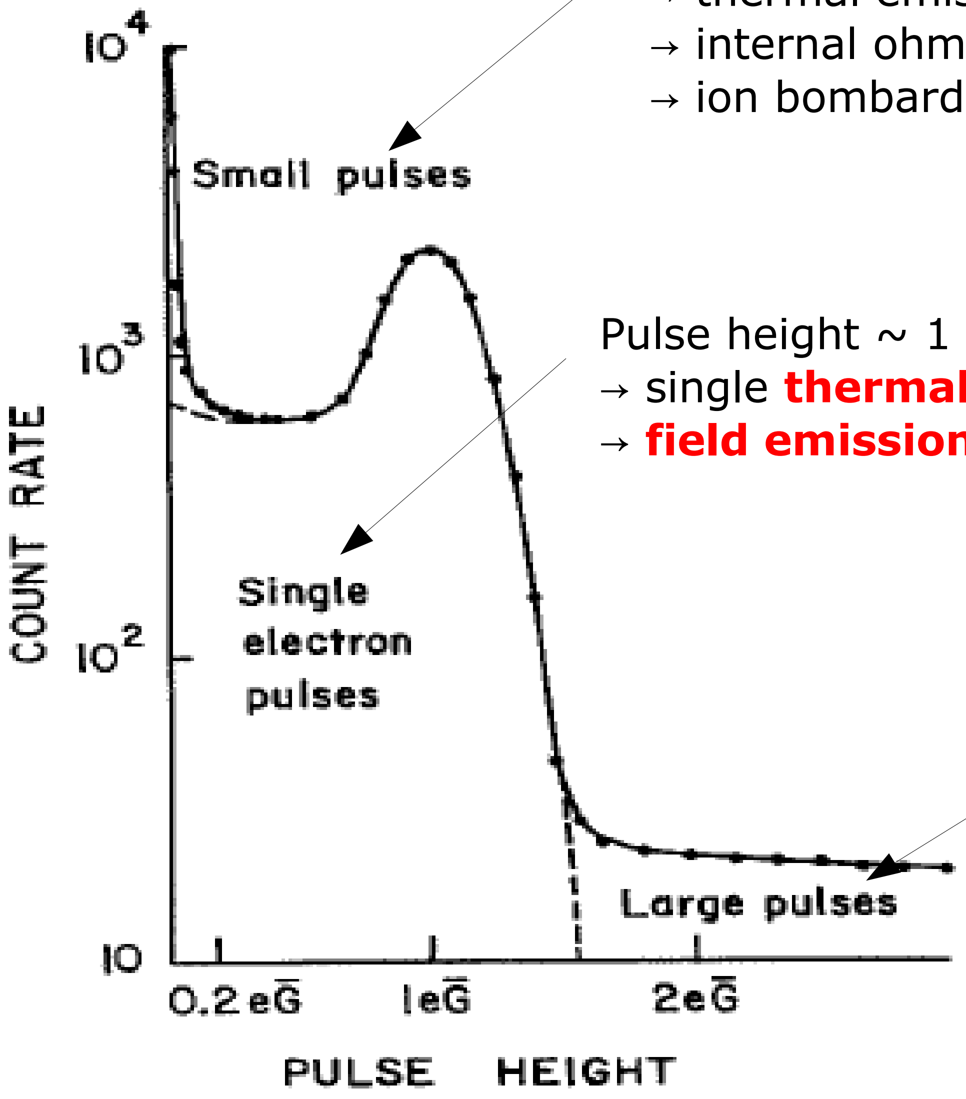

Pulse height < 0.2 ph.e
→ thermal emission from dynodes
→ internal ohmic **leakage current** between dynodes-anode
→ ion bombardment on dynodes (electron emission)

Pulse height ~ 1 ph.e
→ single **thermal electrons** (**shot noise**) from photocathode
→ **field emission** (**1/f noise**) from photocathode

Pulse height > 2 ph.e
→ **ion** bombardment on photocathode
(see afterpulses, **correlated noise**)
→ light **glow** from anode
(see afterpulses, **correlated noise**)
→ **cherenkov** light from cosmic rays
on PMT window (ultrashort pulses)

Dark amplitude spectrum
for high gain PMT (10^7) - K_2CsSb cathode - GaP 1st dynode

Dark Noise (HV and T dependence)

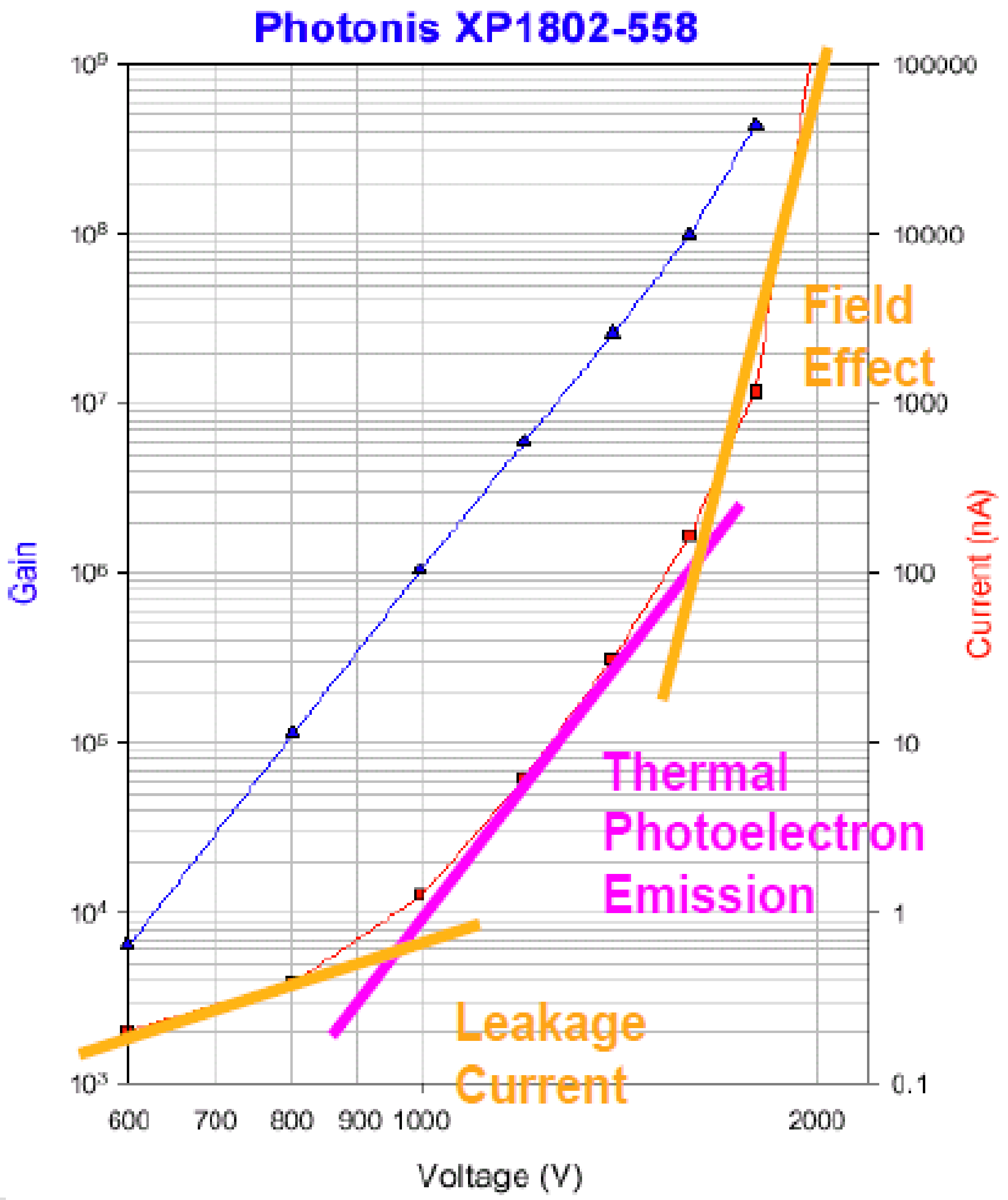

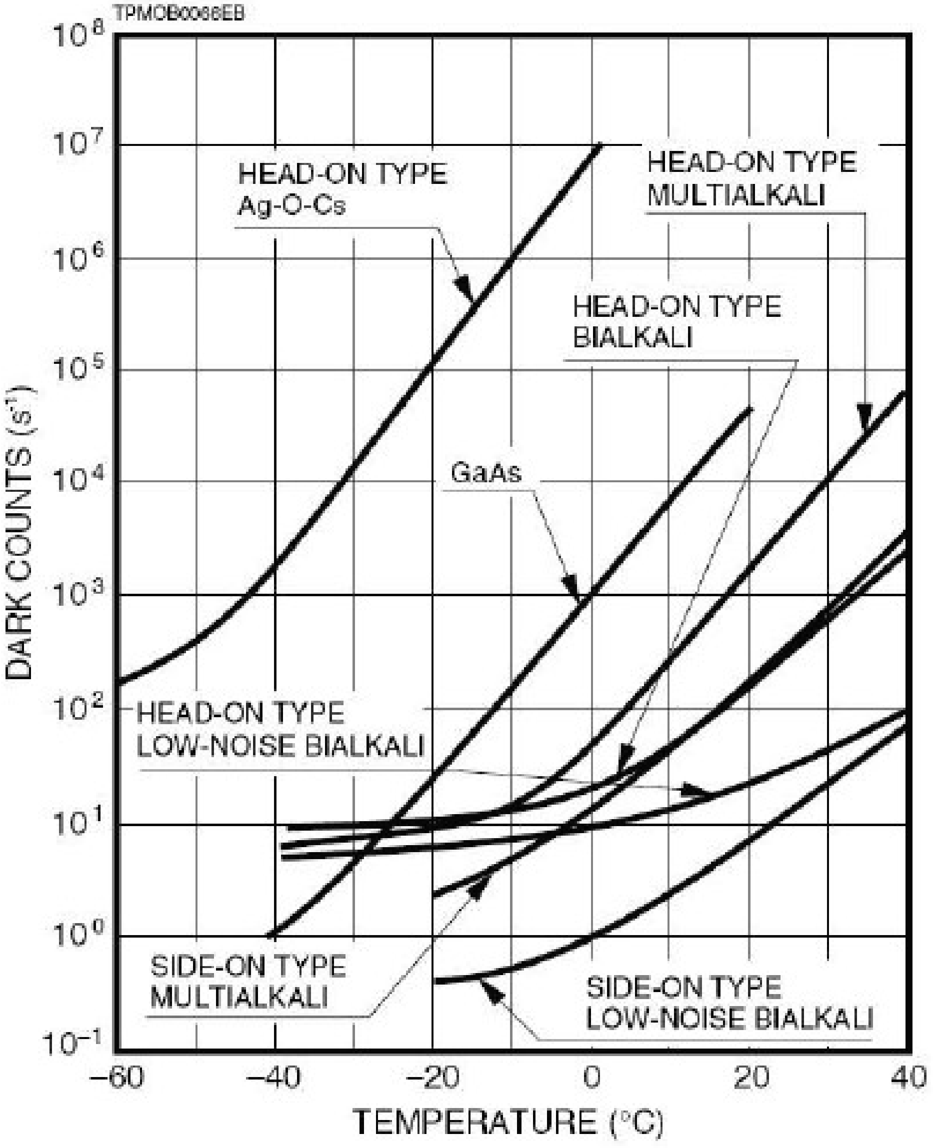

Dark Counts – typical rates

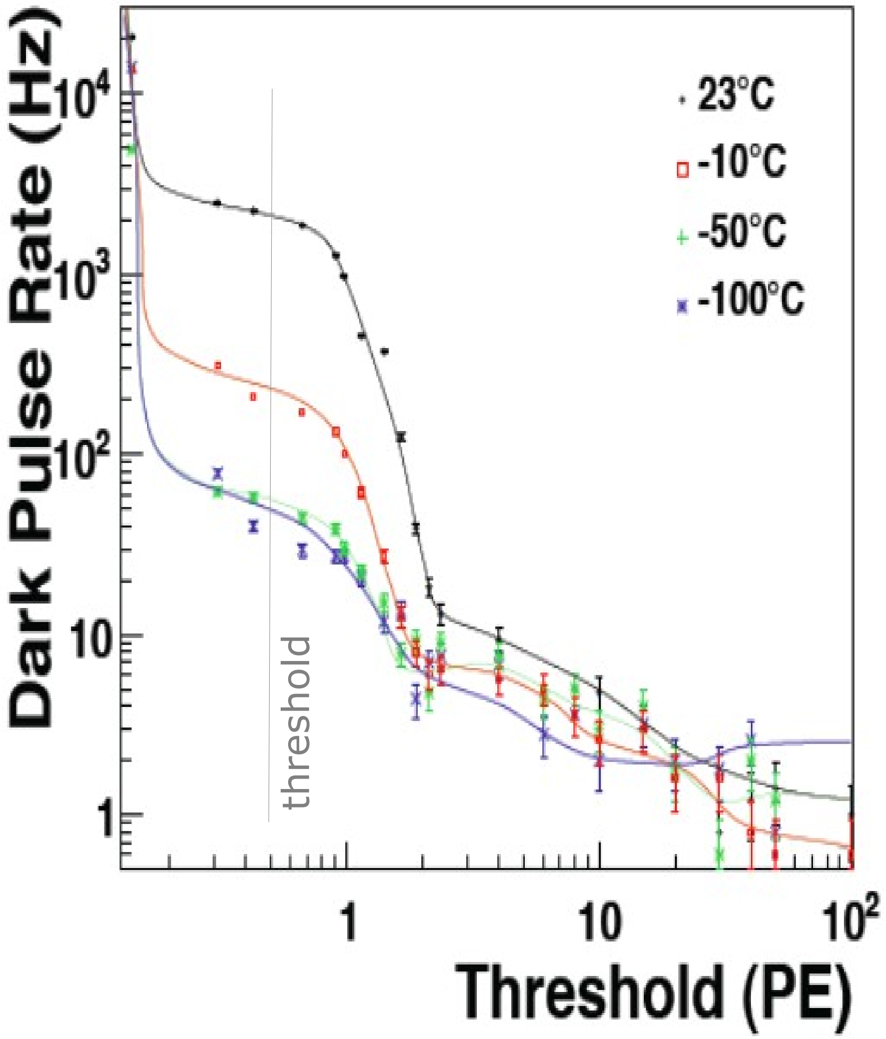

Typical D.C. rates
(T room, 1 ph.e. threshold)

→ PEA cathodes
- S20 < KHz/cm^2
- bialkali < 10Hz/cm^2

→ NEA cahtodes
- S25 ~ 10KHz/cm^2
- III-V < 30KHz/cm^2

Afterpulses – correlated noise

Spurious signals correlated with the photon arrival may appear:

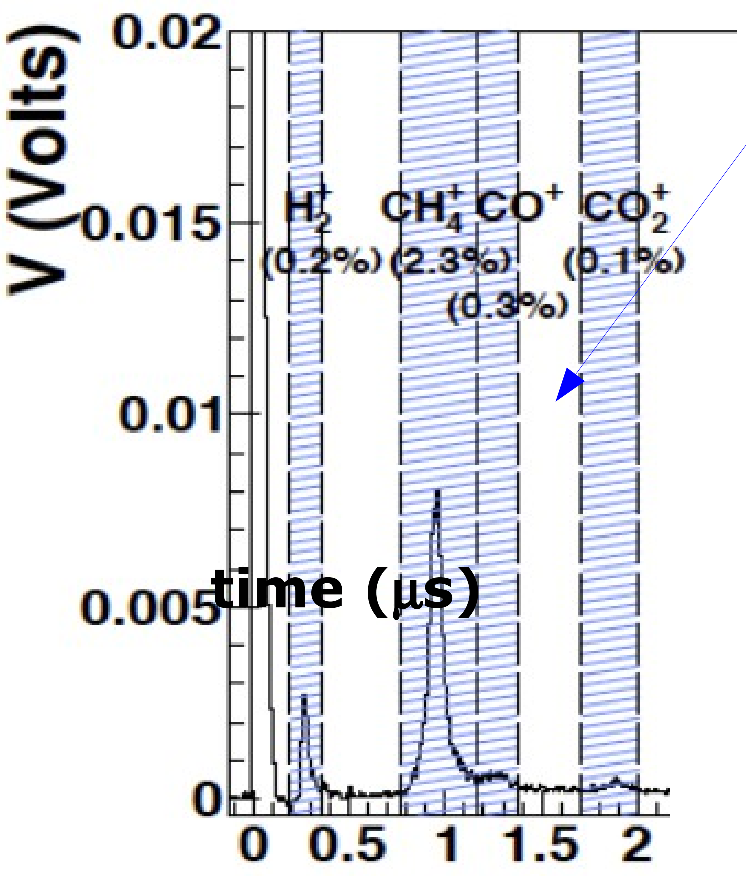

K.Arisaka – IEEE NSS 2012

(1) **Afterpulses** stem from ionisation of the residual gas atoms or those adsorbed by the 1st dynode surface
→ ion feedback delay 100ns – 10µs

Note: afterpulses and anode glow consist in additional delayed signal

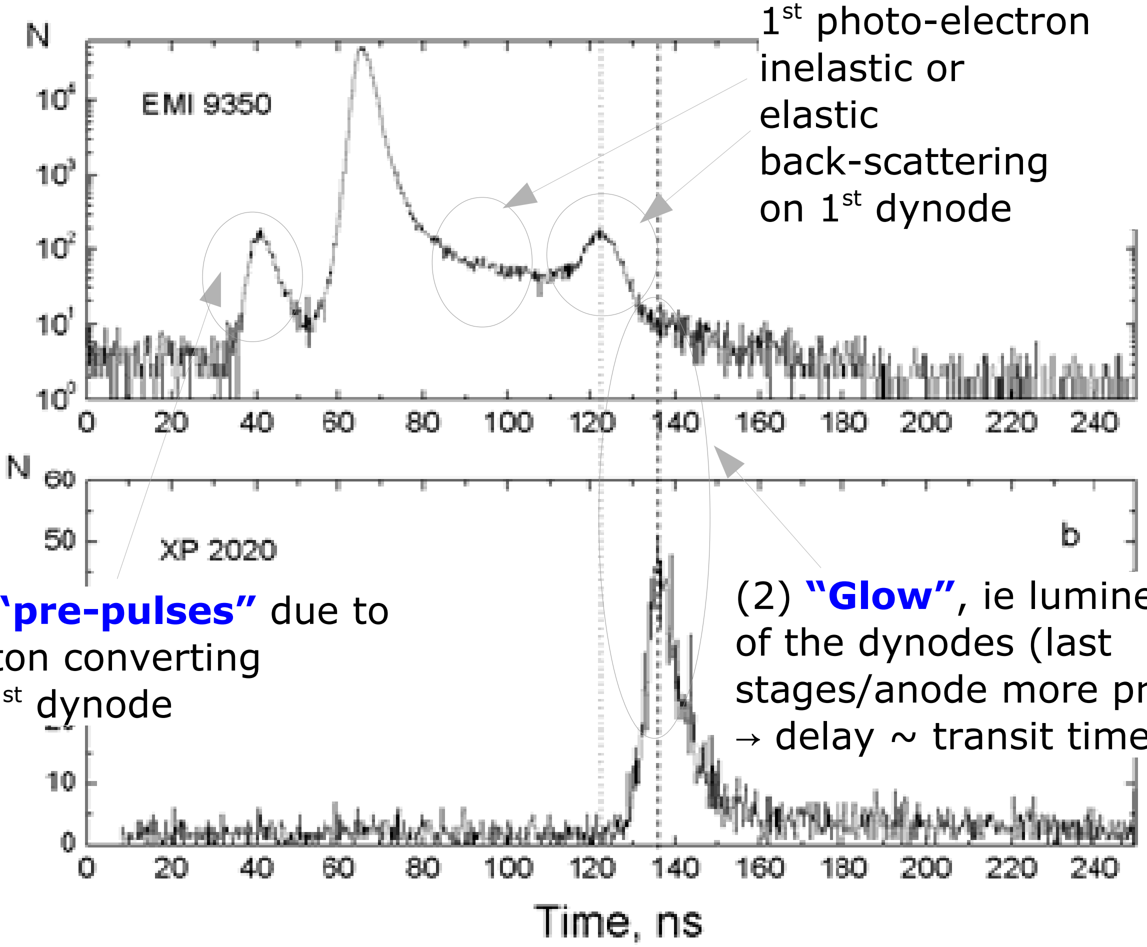

(3) **"late pulses"** due to 1st photo-electron inelastic or elastic back-scattering on 1st dynode

(4) **"pre-pulses"** due to photon converting on 1st dynode

(2) **"Glow"**, ie luminescence of the dynodes (last stages/anode more probable)
→ delay ~ transit time

B.K.Lubsandorzhiev et al "Photoelectron backscattering in vacuum phototubes"

Timing resolution – Single electron response

<Transit Time> = sum of <time of flight> between stages K→Dy_1→...Dy_n→A

TT = $t_{K\text{-}Dy1} + t_{Dy1\text{-}Dy2} + \ldots + t_{Dyn\text{-}A}$ (ignoring charge induction Dy_n→ A)

TT fluctuations → **timing jitter** $\sigma^2_{TT} \sim \sigma^2_{KDy1} + \dfrac{\sigma^2_{Dy1Dy2}}{g_1} + \dfrac{\sigma^2_{DyDy}}{g_1(g-1)}$

main contributions
- cathode → 1st dynode
- 1st → 2nd dynode

Note: time of flight of the following stages are sampled many times (due to multiplication)
→ little contribution

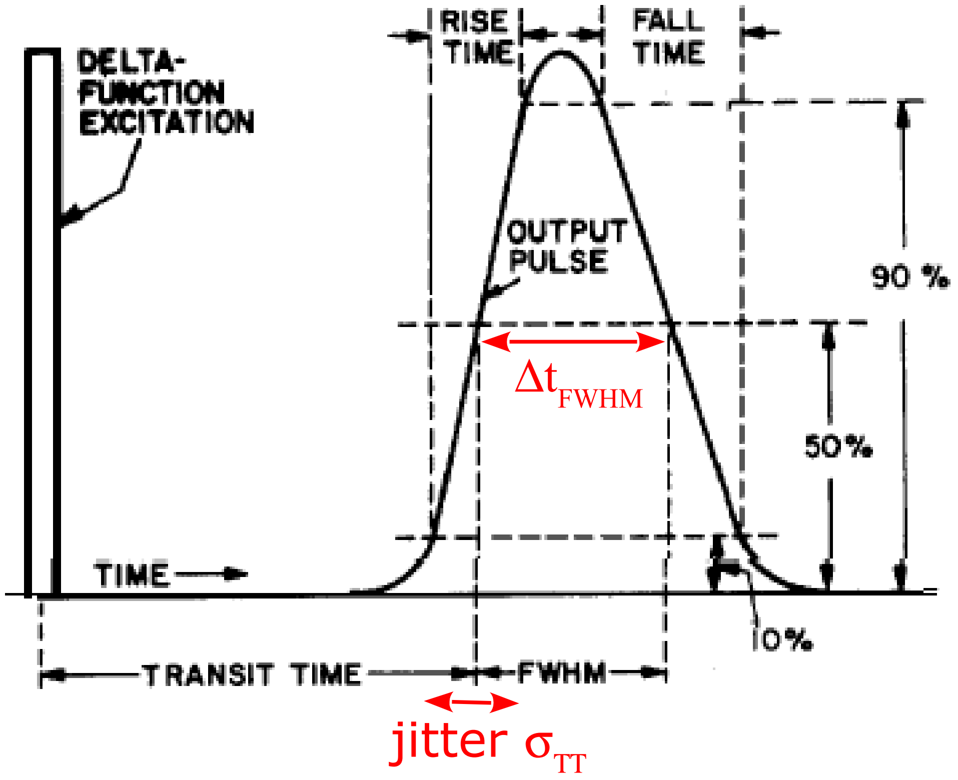

Pulse width → **rate limit**

$$\Delta t_{FWHM} \sim \sqrt{n\,\sigma^2_{DyDy} + \sigma^2_{Dy_n A}}$$

Note: 1) the front stages give little contribution to pulse width
→ time resolution is independent of frequency response of the PMT

2) LC ringing and RC usually affect signal fall front

Single photon timing resolution

S.K.Poultney – "single photon detection and timing"

$$\sigma^2_{TT} \sim \sigma^2_{KDy1} + \frac{\sigma^2_{Dy1Dy2}}{g_1} + \frac{\sigma^2_{DyDy}}{g_1(g-1)}$$

1st high gain dynode
strongly reduce time jitter

main contribution
depends on
1) electrode geometry
2) electric fields
3) process of
photoemission at cathode

Despite time of flight equalization, residual time difference across photocathode area O(100ps)

In PMT for fast timing:
dedicated dynode shapes allow compensation of different time of flight along different paths between adjacent dynodes
(eg linear focus multiplier)

- Small contribution from fluctuations of time lag due to photocathode response (relevant only for NEA cathodes)
- Important contribution from the different velocities of emitted electrons

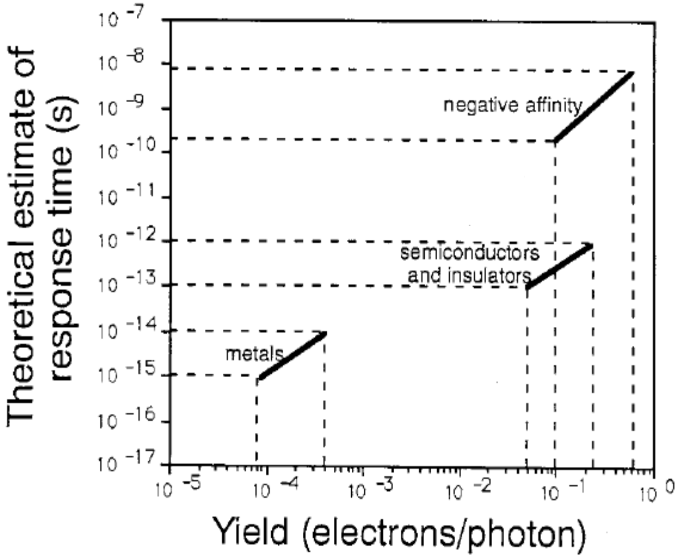

$$\frac{\sigma_{KDy1}}{t_{KDy1}} \approx \sqrt{\frac{W}{q_e V_{KDy1}}}$$

$W = h(\nu_0 - \nu)$
ν_0= freq. of photocathode threshold

ddp between cathode and 1st dynode

single photon time resolution σ_{TT}

1) **depends on wavelength** (improves at long wavelengths)

2) lower limit for $\sigma_{TT} \geq$ **150ps**

Single photon timing resolution

Single ph.e
time spectra
for incident light
at different
wavelengths

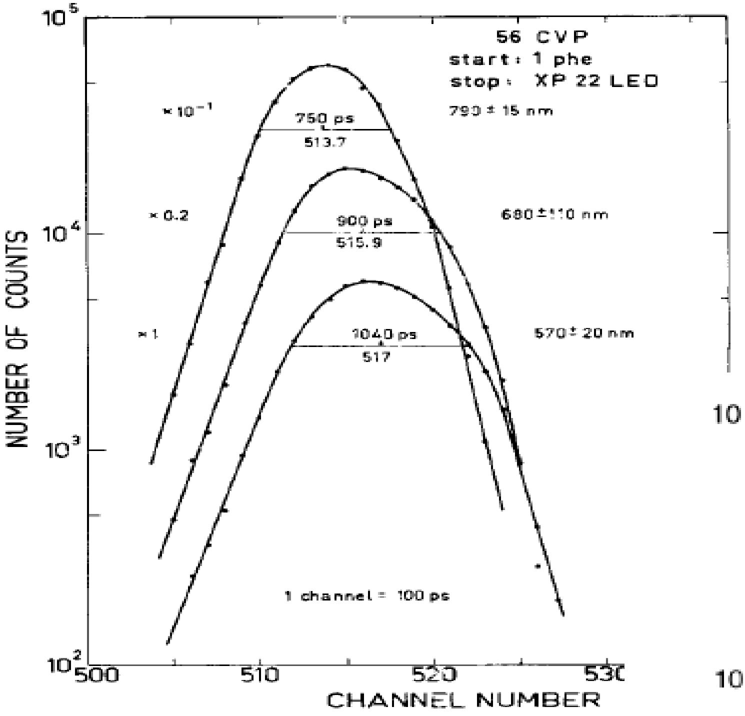

M.Moszynski NIM 141 (1977) 319

TT, $\sigma_{TT} \sim V^{-1}$

dependences

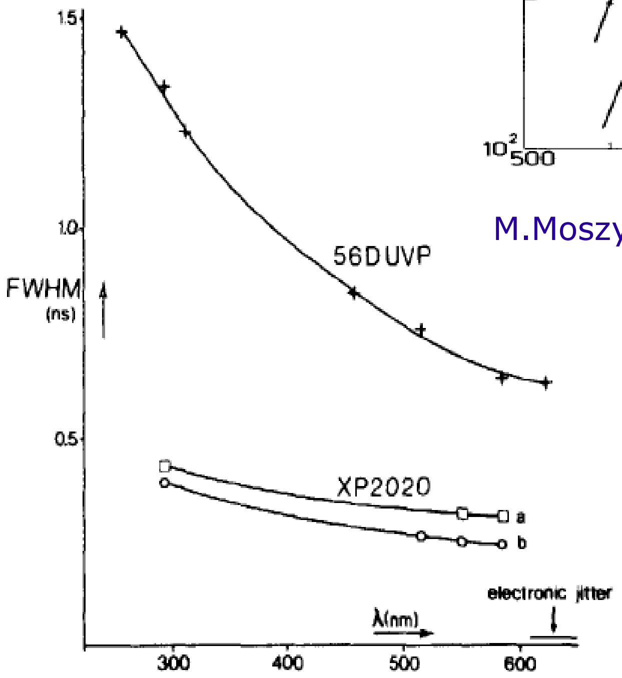

Bebelaar Rev Sci Instr 57 (1986)

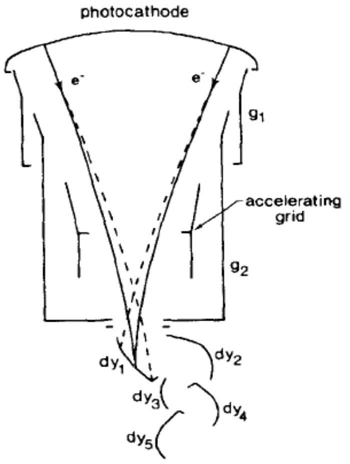

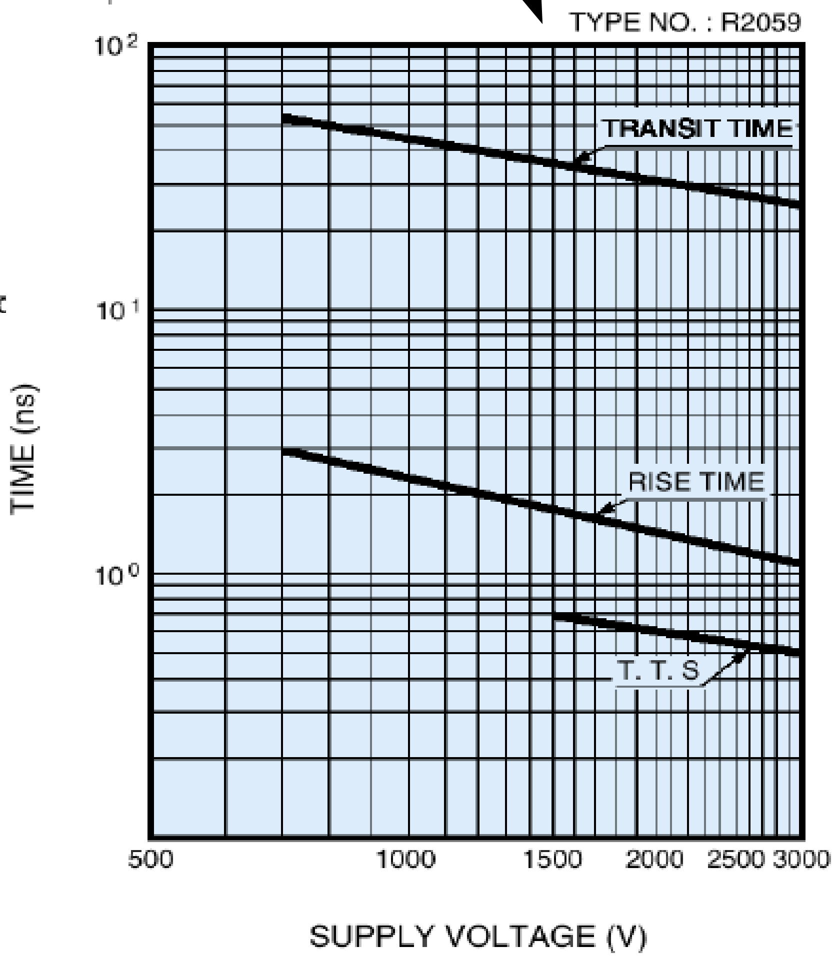

Single photon timing resolution

Slower rise front
without screening
grid at anode

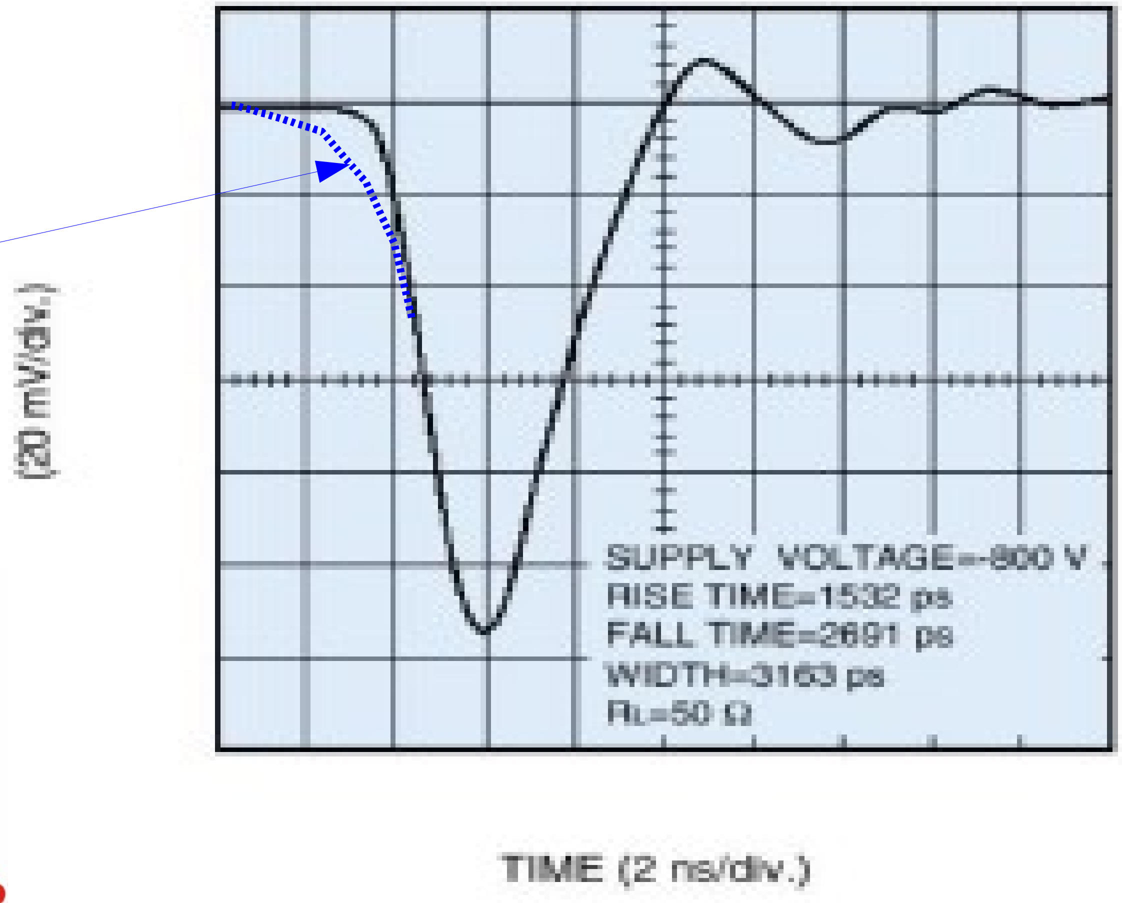

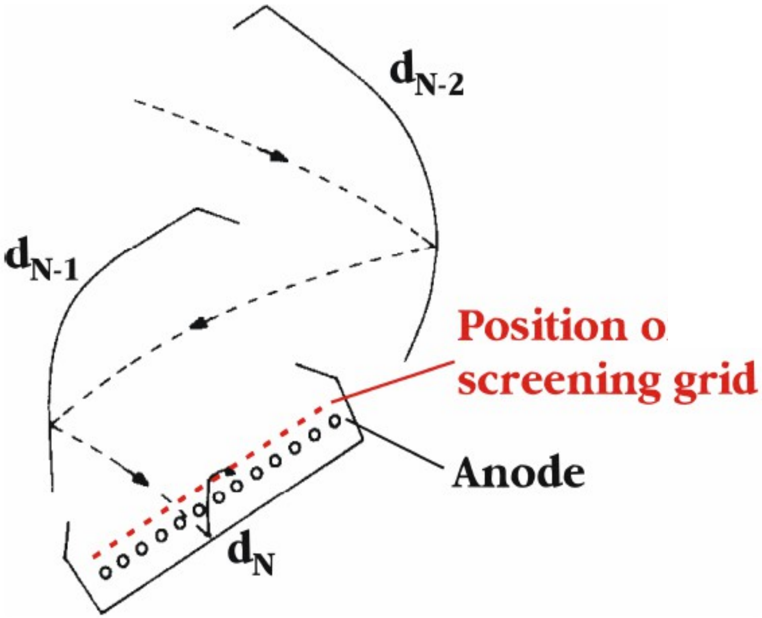

Micro Channel Plates - MCP-PMT

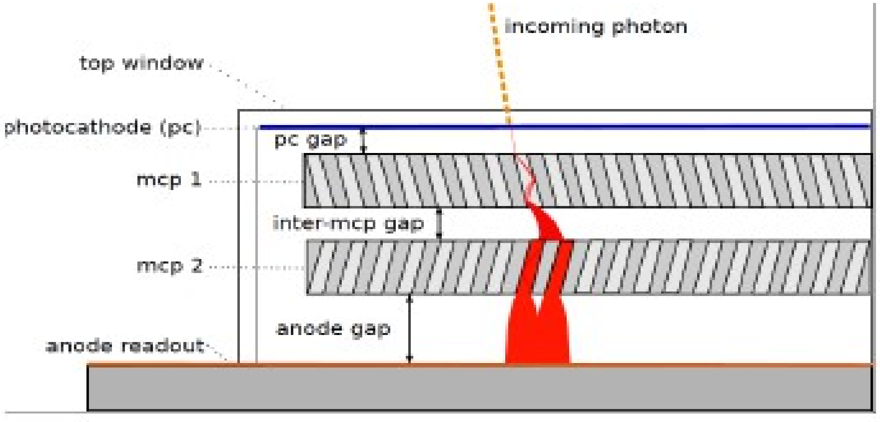

Tiny electron multipliers
Diameter 20μm, 10μm, 6μm, 3μm
Length ~ O(500μm)

High Gain
G ~10^6 for two-stage type

Can operate under
magnetic field

Very Fast time Response
Rise time < 500ps
$\sigma_{TT} < 50$ps

Position measurement
- analog charge division
- Multi-anode readout
- Strip-lines readout
– $\sigma_x \sim$ O(mm), not intrinsic

Large Area
→ recent developments
cheap production: ALD on glass

Noise
quite low noise ~ 0.1 Hz/cm^2
(Rb,K contamination)

Ageing
ion feed-back on cathode
→ recent improvements

MCP – single photon timing resolution

Short channel (500µm) and high E field in the channel (few 10kV/cm)
→ **ultra fast response** limited by
1) TTS in the gaps → short gaps
2) RC and parasitic LC filtering → **RF impedance matching**

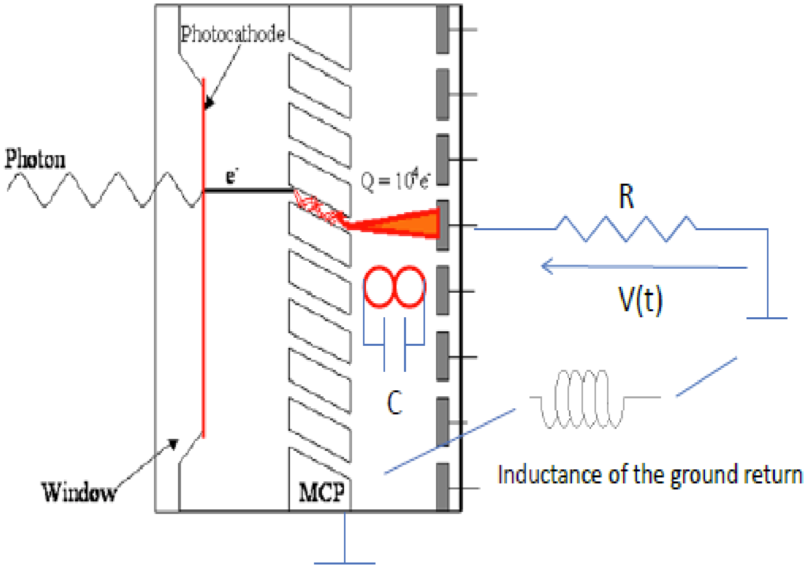

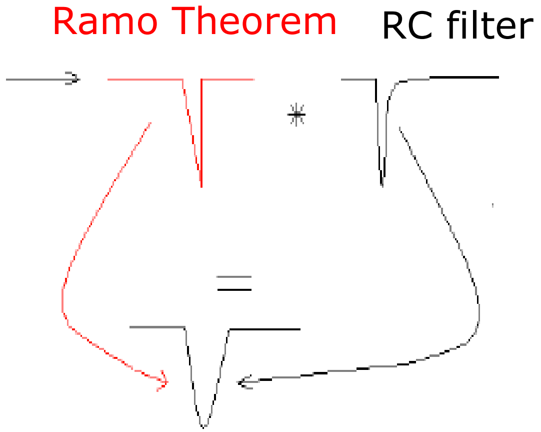

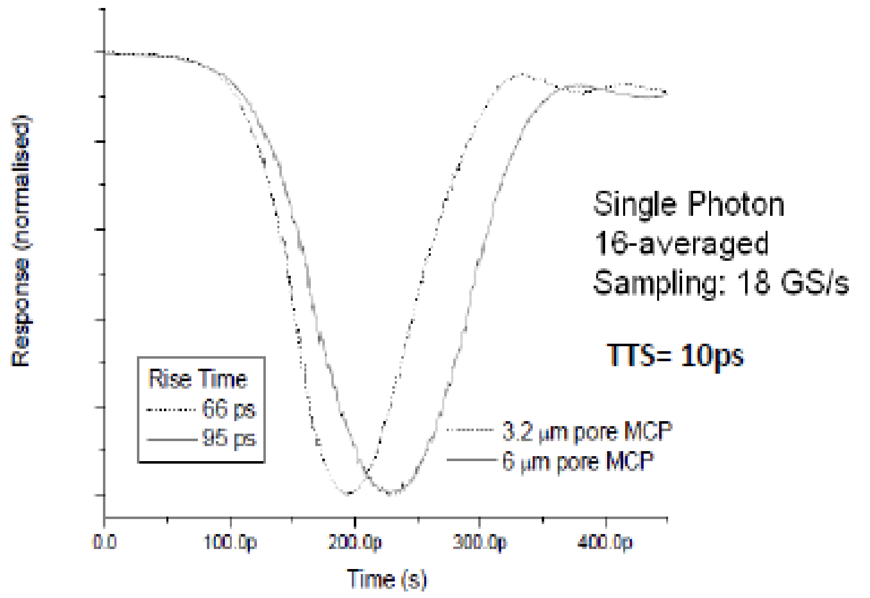

Time response curves for two models of PMT110 with different MCP pore diameters.

From Photek

11 mm diameter Micro-Channel Plate signal
Signal full bandwidth: 10 GHz

Typical Timing resolution:
Single Photoelectron Time Transit Spread: 10ps

MCP – single photon timing resolution

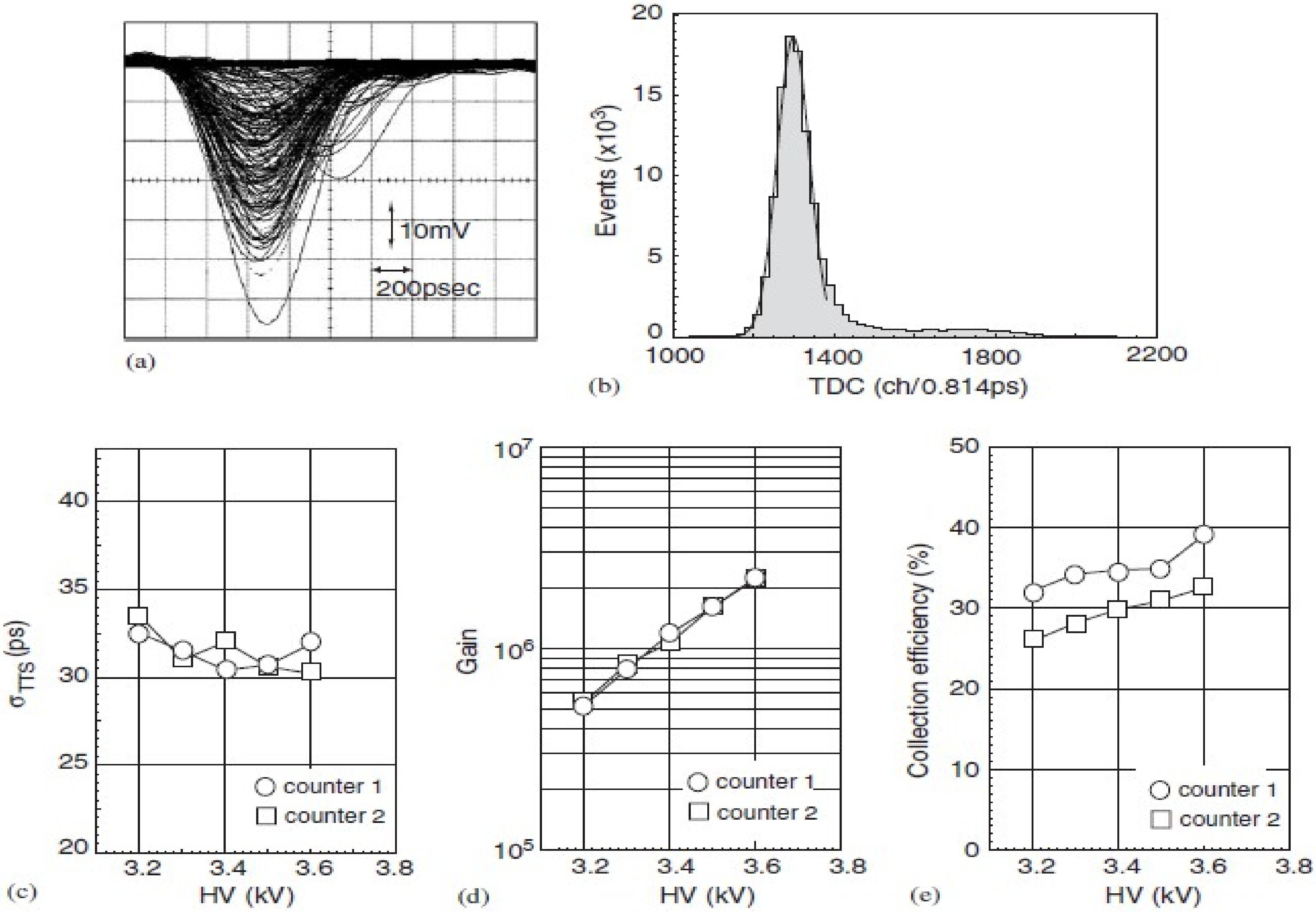

Fig. 3. Performance of the HPK6, measured using single-photons.

Inami et al NIM A 560 (2006) 303

Timing - Imaging devices

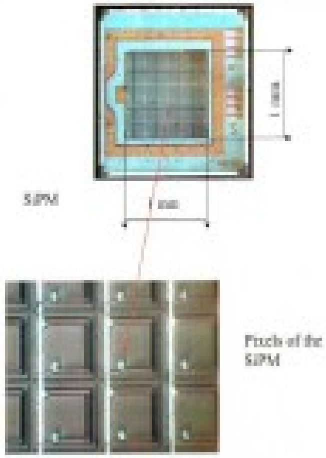

	Multi-anodes PMTs Dynodes	Silicon-PMTs [10] Quenched Geiger in Silicon	Micro-Channel Plates [1] Micro-Pores
Quantum Eff.	30%	90%	30%
Collection Eff.	90%	70%	70%
Rise-time	0.5-1ns	250ps	50-500ps
Timing resolution (1PE)	150ps	100ps	20-30ps
Pixel size	$2x2mm^2$	$50x50\mu m^2$	$1.5x1.5mm^2$
Dark counts	1-10Hz	1-10MHz/pixel	$1Hz-1kHz/cm^2$
Dead time	5ns	100-500ns	1μs
Magnetic field	no	yes	15kG
Radiation hardness		1kRad=noisex10	good (a-Si, Al_2O_3)

Recovery Time

J.F.Genat, LAPPD Electronics Workshop (2012)

Large Area Pico-second Photodetectors

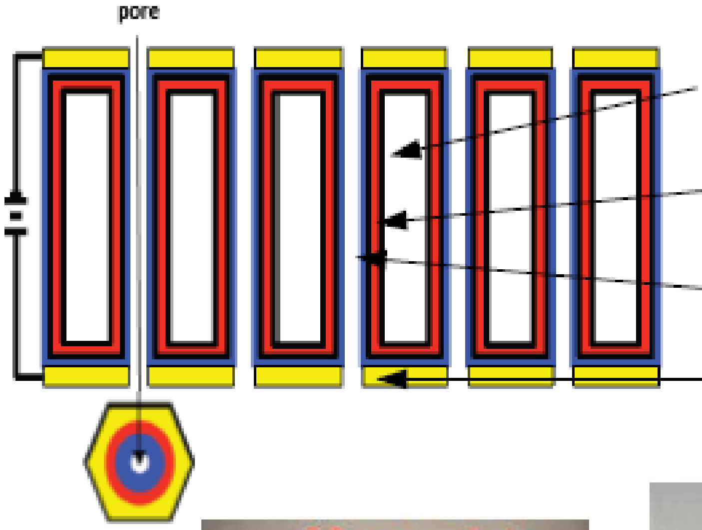

Porous glass

Resistive coating ~100nm (ALD)

Emissive coating ~ 20nm (ALD)

Conductive coating
(thermal evaporation or sputtering

Incom glass substrate

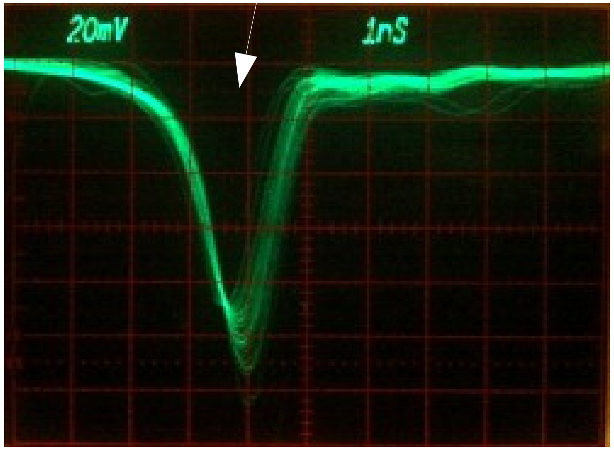

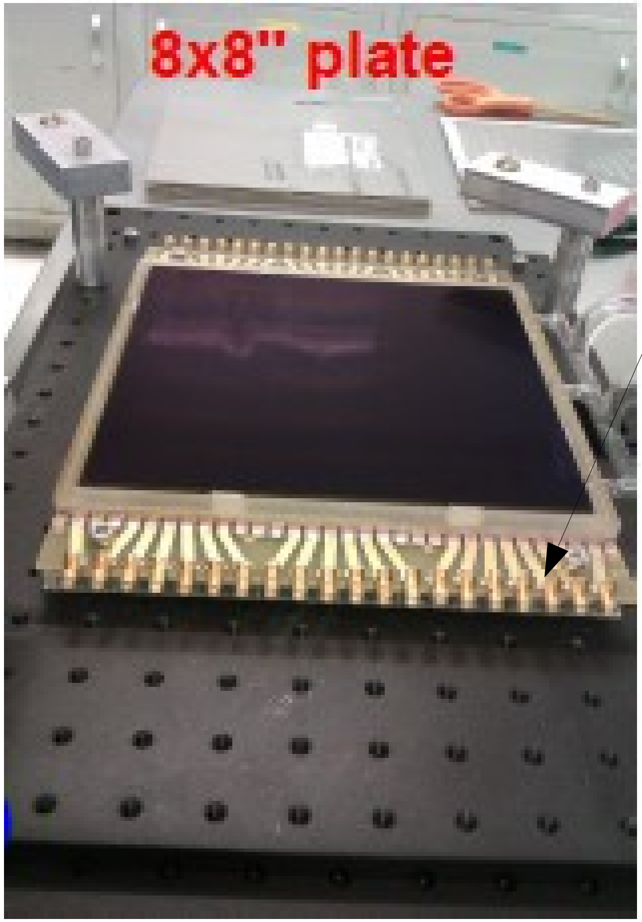

RF strip-line anodes

- 50 Ω impedance
- 1.6-0.4GHz bandwidth

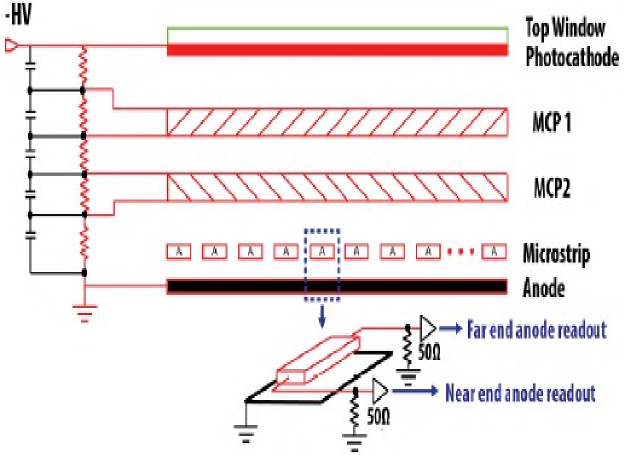

LAPPD
http://psec.uchicago.edu/

Solid state devices – PIN diode

One of the simplest kind of photodiodes is the **p-i-n photodiode**
→ intrinsic piece of semiconductor sandwiched
between two heavily (oppositely) doped regions

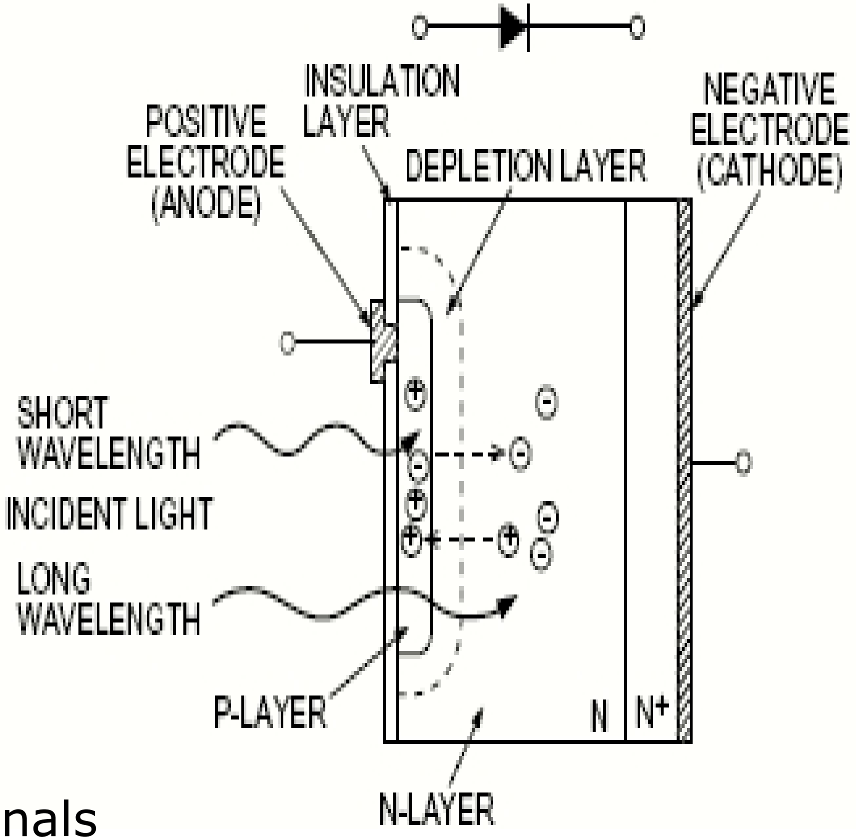

The two charge sheets on the n+ and p+ sides produce an **electric field**

→ separate charges produced in the **depleted region** (even without an external E field)

Charge are separated and swept to terminals
→ can be detected as an (induced) current
provided that they did not **recombine**

Solid state devices

APD: avalanche photo-diode

- Bias BELOW V_{bd} ($V_{APD} < V < V_{bd}$)
- Linear Mode/ AMPLIFIER device
- Multiplication < 10^3 (lim. by fluctuations)
- Sensitivity ~ 5 ph.e
- (1ph.e. at low T with slow electronics...)

Reverse biased junction: internal gain via impact ionization in high E field

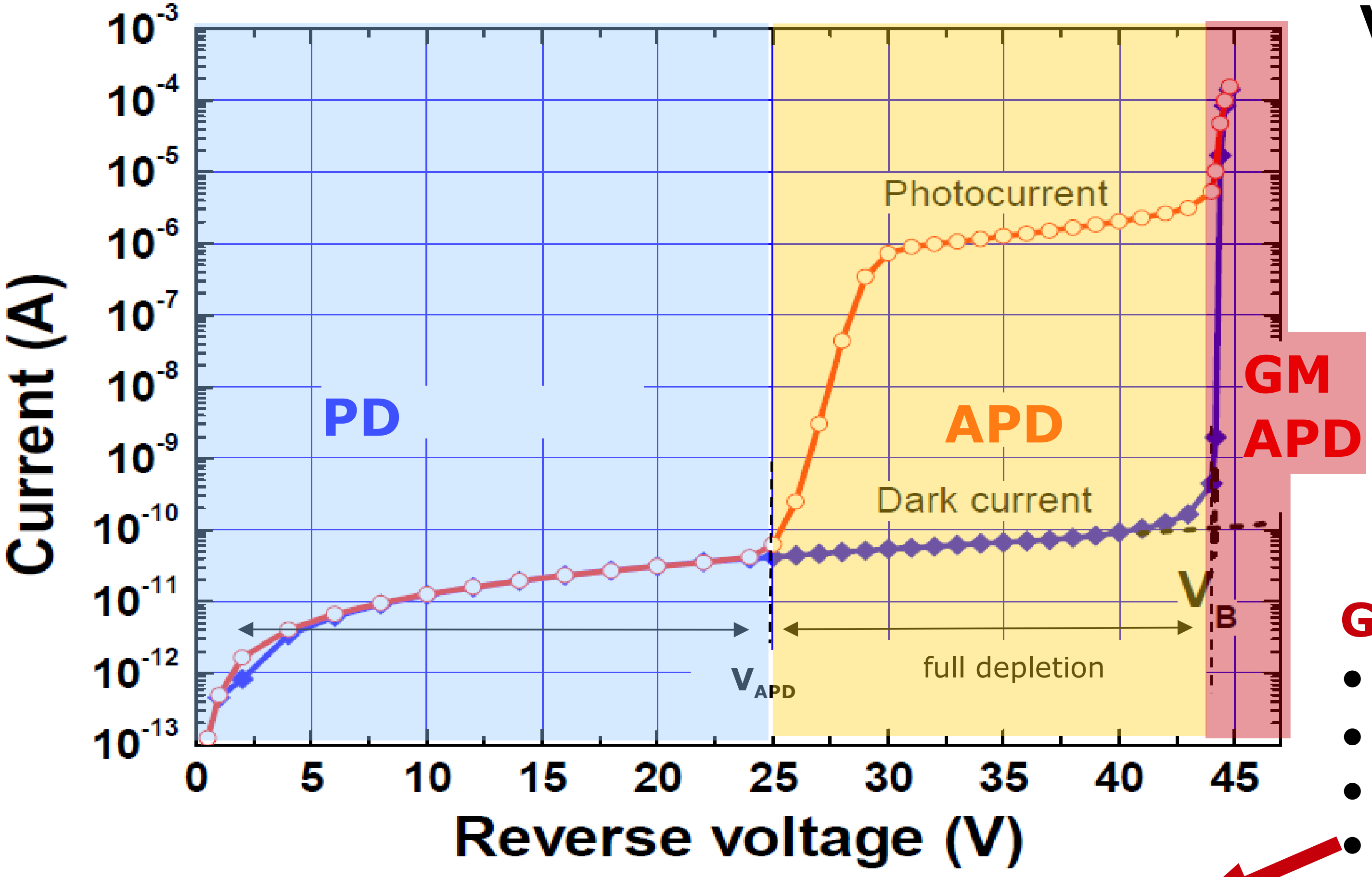

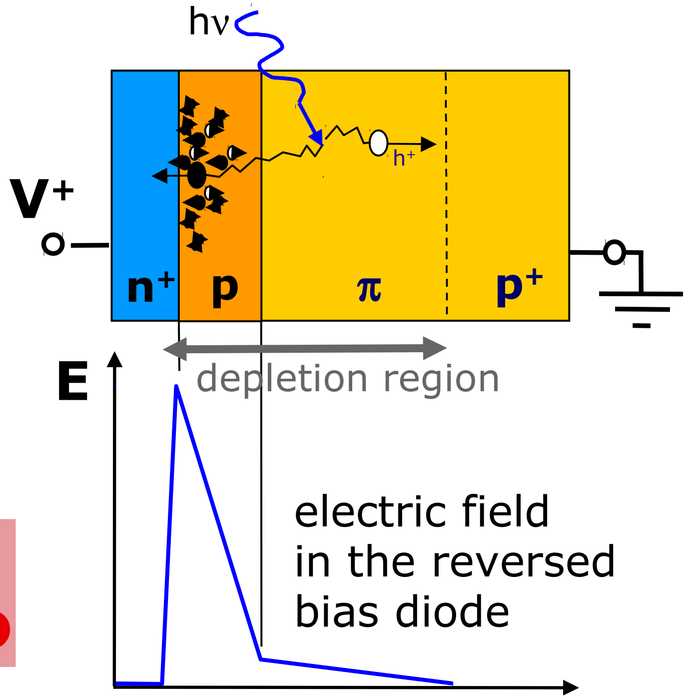

GM-APD: Geiger Mode

- Bias ABOVE V_{bd} (a few V)
- **BINARY** device
- Gain: ~10^6 (lim. by C)
- **Single ph.e. resolution**
- Limited by dark count rate
- Need Reset (Quenching)

basis for building alternative to PMT

The Silicon PM: array of GM-APD

Single GM-APD gives **no information** on light intensity → use array of GM-APDs' first proposed in the late '80-ies by Golovin and Sadygov

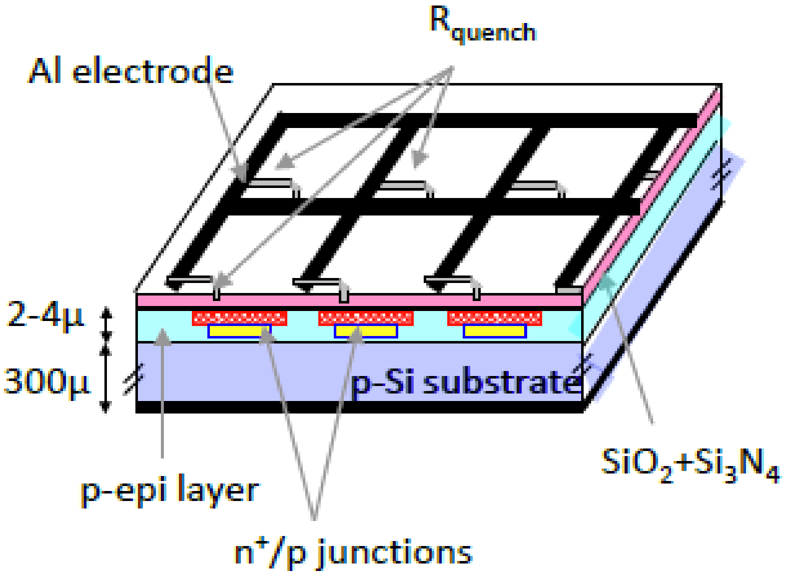

A SiPM is segmented in tiny GM-APD cells and connected in parallel trough a decoupling resistor, which is also used for quenching avalanches in the cells

Each element is independent and gives the same signal when fired by a photon

Σ of binary signals → analog signal

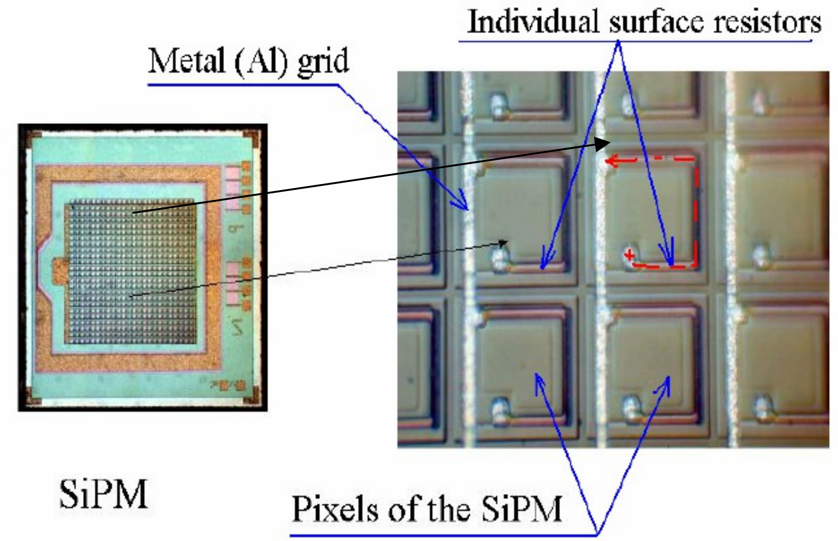

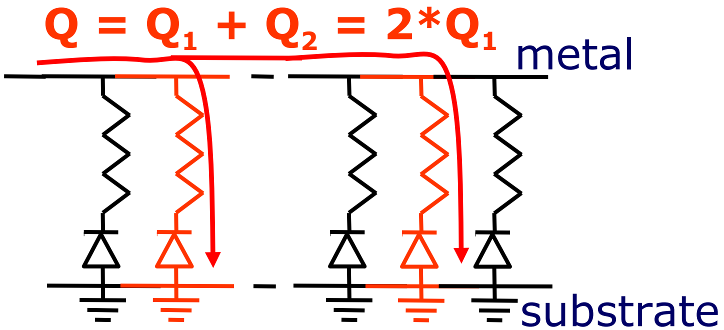

Output ∝ number incident photons

Close up of a cell (custom process)

Shallow-Junction APD

Example of implementation

C.Piemonte NIM A 568 (2006) 224

Optical window → Anti-Reflective Coating (ARC)
note: light absorption in Si, SiO_2

Optically
dead region
(20%-80%)

Optical
isolation
(cross-talk)

Shallow n^+ layer
O(100 nm)
Abrupt junction

(fully) depleted region
O(μm)

Substrate
low resistivity contact
O(500 μm)

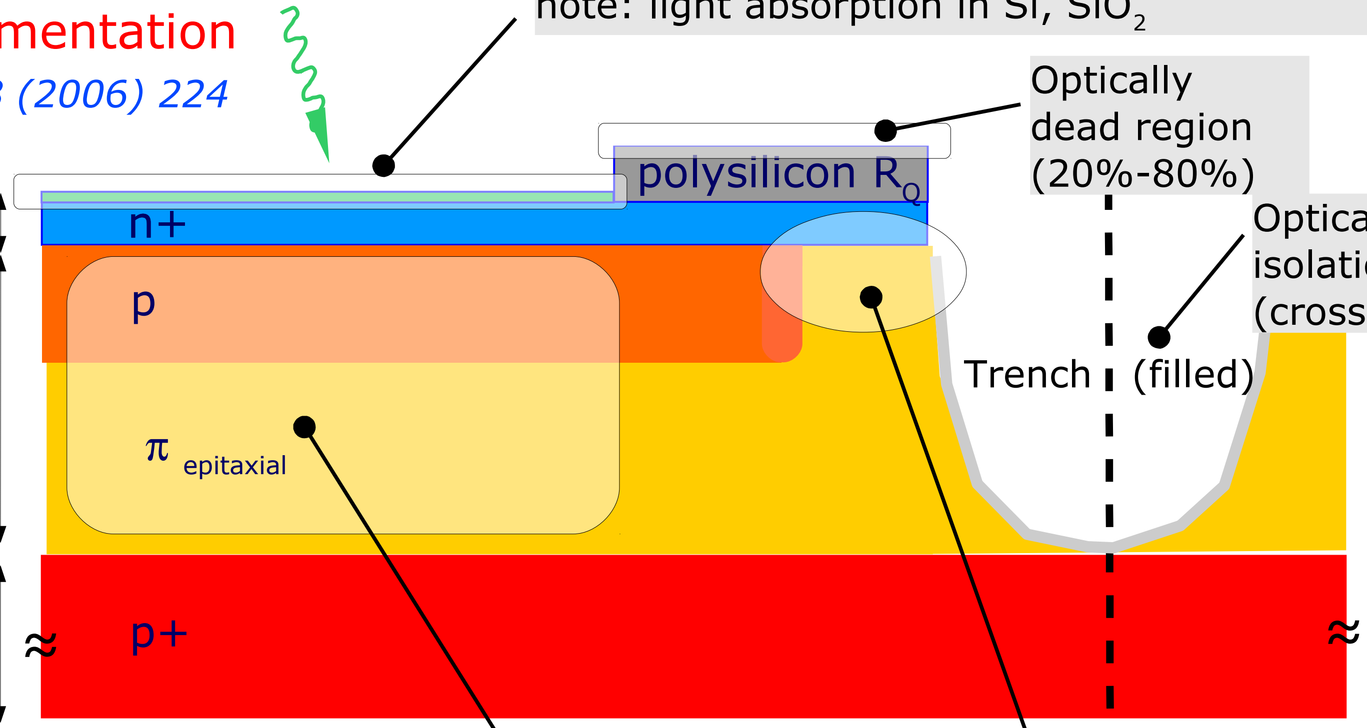

Active volume
- no micro-plasma's high quality epitaxial
- doping / E field profile engineering

Critical region:
- Leakage current
- Surface charges
- Guard Ring for
  - preventing early edge-breakdown
  - isolating cells
  - tuning E field shape

→impact on Fill Factor

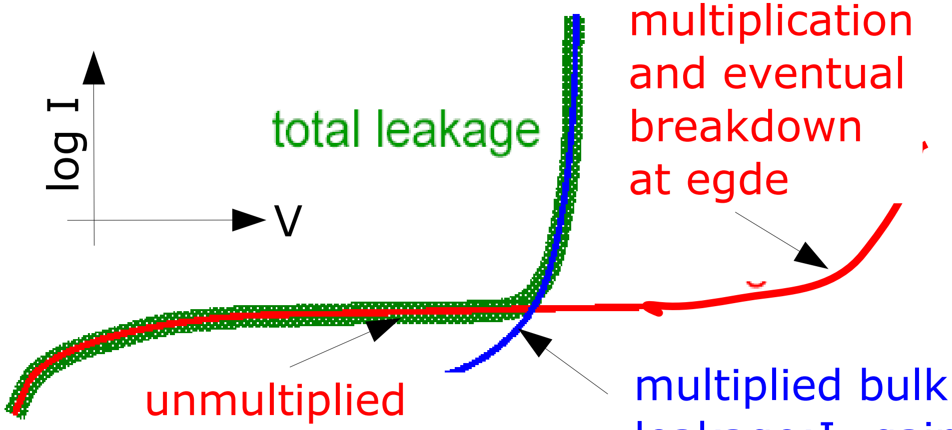

multiplication and eventual breakdown at egde

unmultiplied perimeter leakage: I~ V_{bias}

multiplied bulk leakage: I~gain·DCR ~$(V_{bias} - V_{bias})^2$

Operation principle of a GM-APD

Avalanche processes in semiconductors are studied in detail since the '60 for modeling micro-plasma instabilities

McIntyre JAP 32 (1961), Haitz JAP 35 (1964) and Ruegg IEEE TED 14 (1967)

currents **internal** / **external**

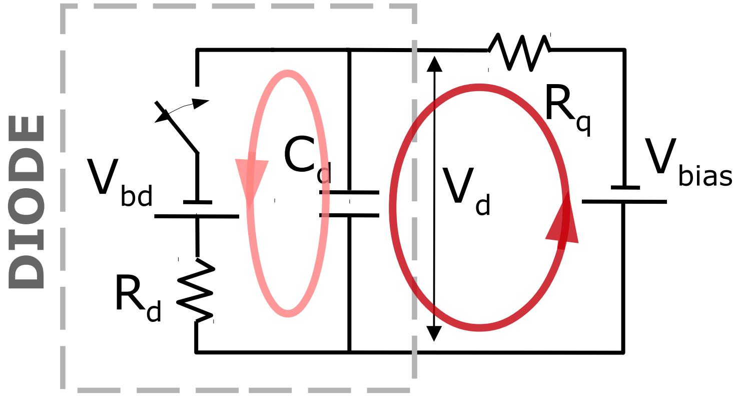

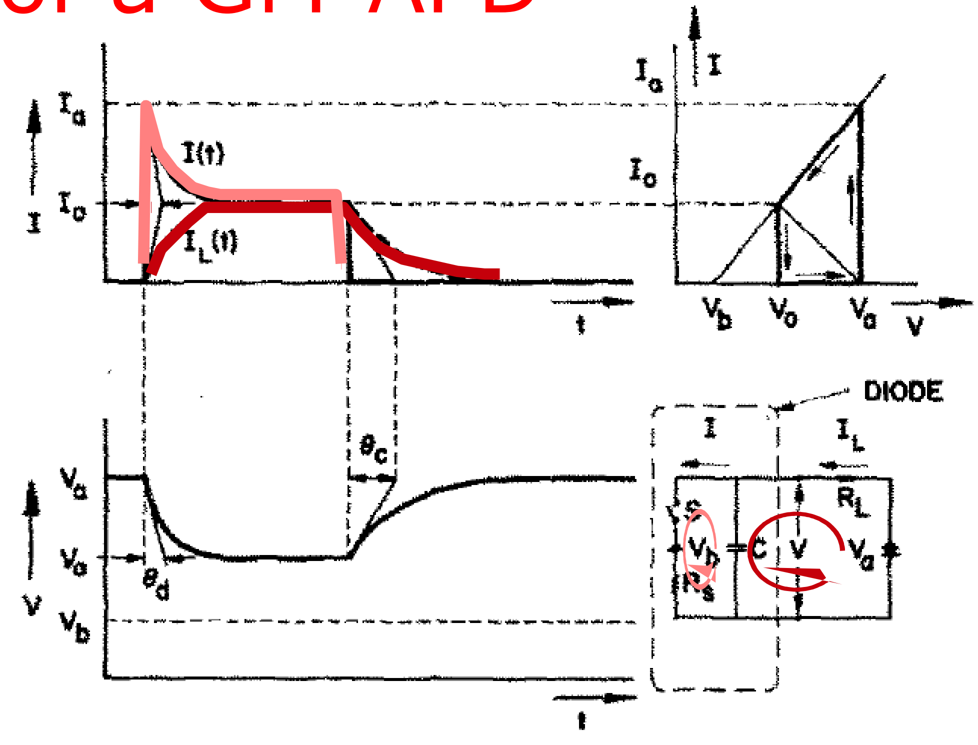

FIG. 3. Shape of current pulse for $\theta_d \ll \tau_1(I_0)$.

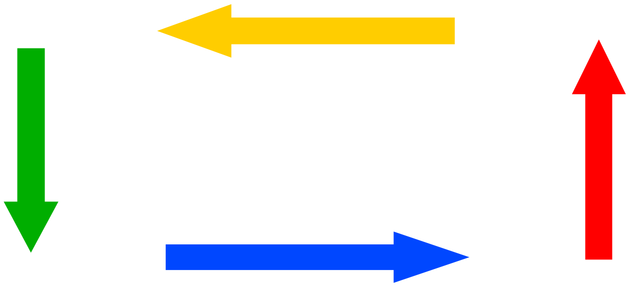

ON condition: avalanche triggered, switch closed C_d discharges to V_{bd} with a time constant $R_dC_d= \tau_{discharge}$ at the same time the external current asymptotic grows to $(V_{bias}-V_{bd})/(R_q+R_d)$

P_{10} = turn-off probability
probability that the number of carriers traversing the high-field region fluctuates to 0

P_{01} = turn-on probability
probability that a carrier traversing the high-field region triggers the avalanche

OFF condition: avalanche quenched, switch open, capacitance charged until no current flowing from V_{bd} to V_{BIAS} with time constant $R_qC_d = \tau_{recovery}$

Operation principle of a GM-APD

Avalanche processes in semiconductors are studied in detail since the '60 for modeling micro-plasma instabilities

McIntyre JAP 32 (1961), Haitz JAP 35 (1964) and Ruegg IEEE TED 14 (1967)

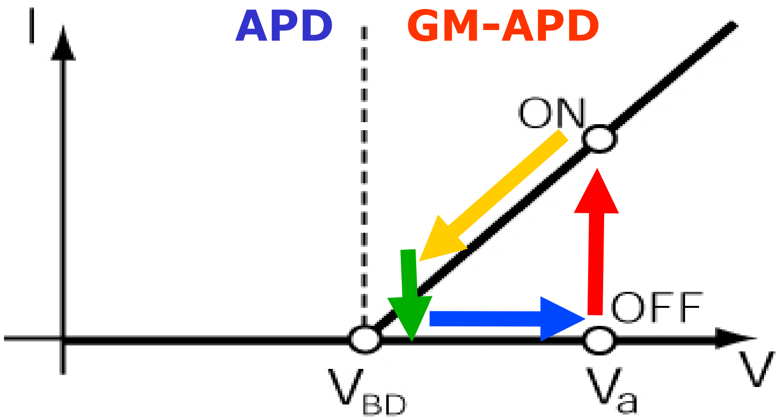

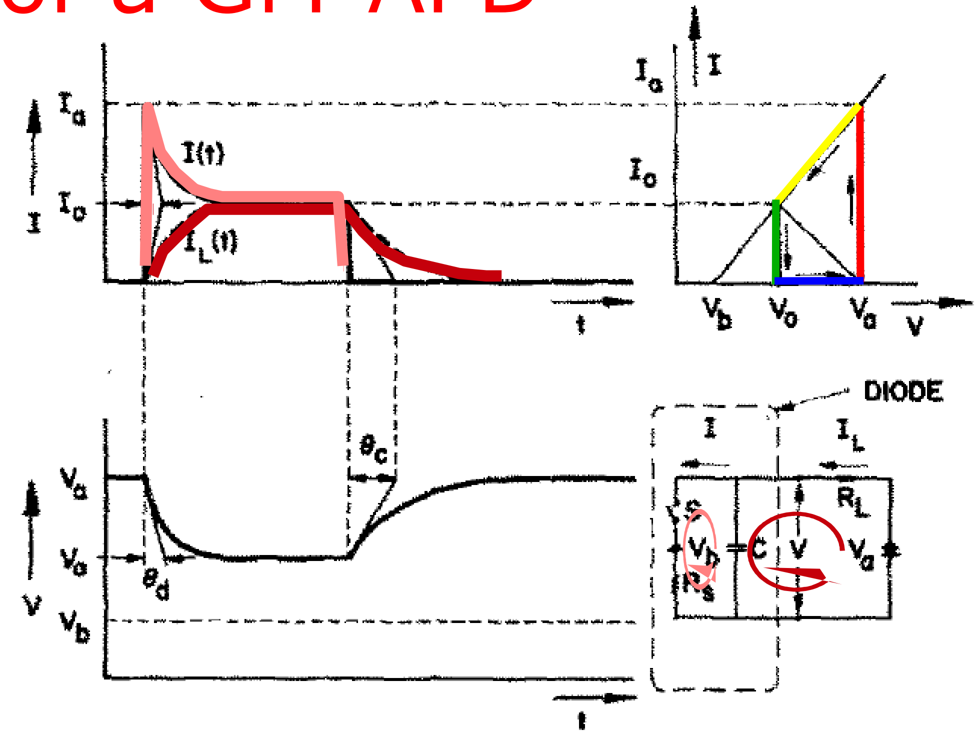

FIG. 3. Shape of current pulse for $\theta_d \ll \tau_1(I_0)$.

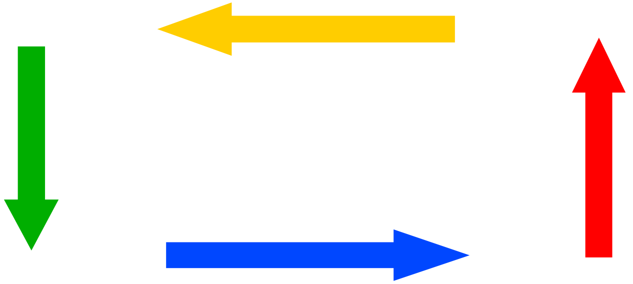

ON condition: avalanche triggered, switch closed C_d discharges to V_{bd} with a time constant $R_dC_d = \tau_{discharge}$ at the same time the external current asymptotic grows to $(V_{bias}-V_{bd})/(R_q+R_d)$

P_{10} = turn-off probability
probability that the number of carriers traversing the high-field region fluctuates to 0

P_{01} = turn-on probability
probability that a carrier traversing the high-field region triggers the avalanche

OFF condition: avalanche quenched, switch open, capacitance charged until no current flowing from V_{bd} to V_{BIAS} with time constant $R_qC_d = \tau_{recovery}$

Passive Quenching: tread-off τ_{quench} vs $\tau_{recovery}$

If R_Q is high enough the internal current is so low that statistical fluctuations may quench the avalanche

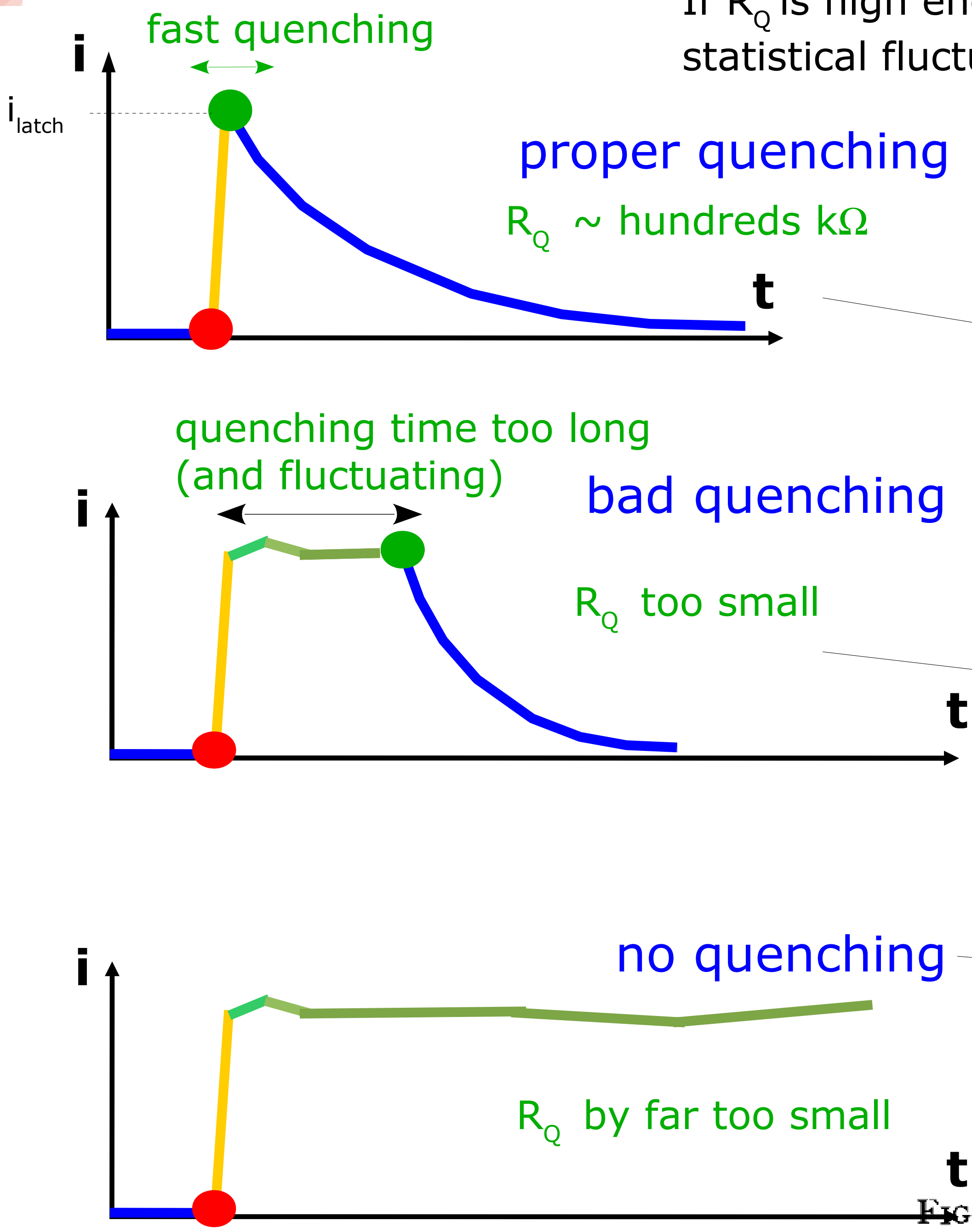

Haitz JAP 35 (1964)

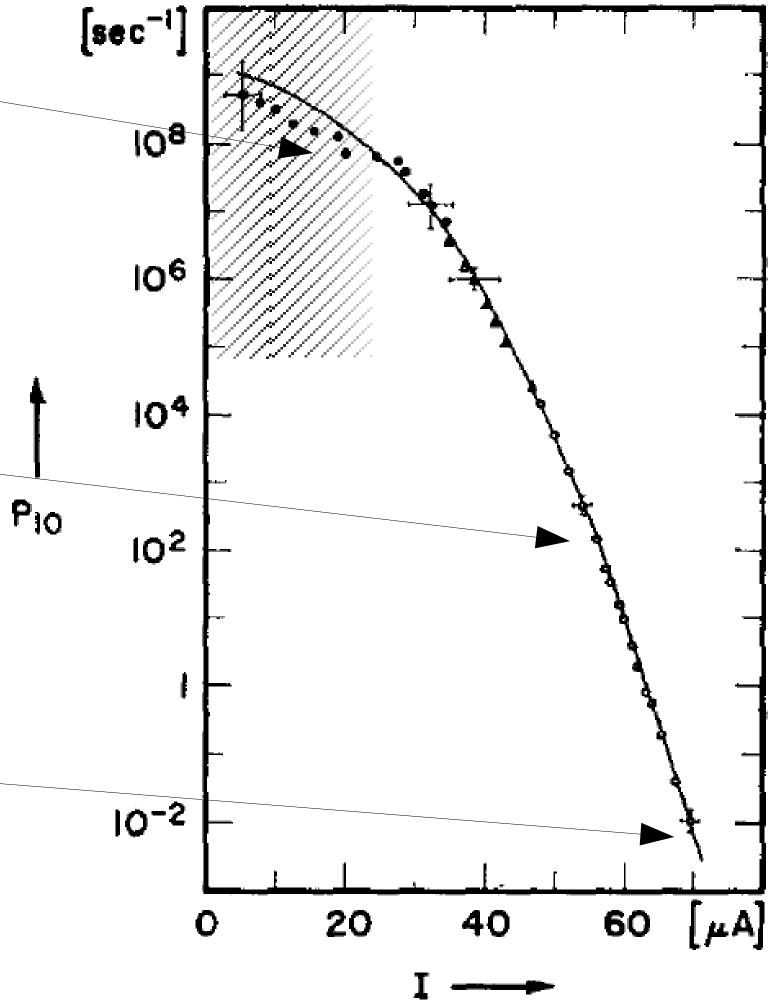

FIG. 2. Turnoff probability per second as function of pulse cu

Basic electrical model and signal shape

Diode (capacitor) fast discharge
and slow recharge

charge stored defines Gain
→ Gain ~ C ΔV
$\Delta V = V_{bias} - V_{bd}$ "Over-Voltage"

currents internal / external

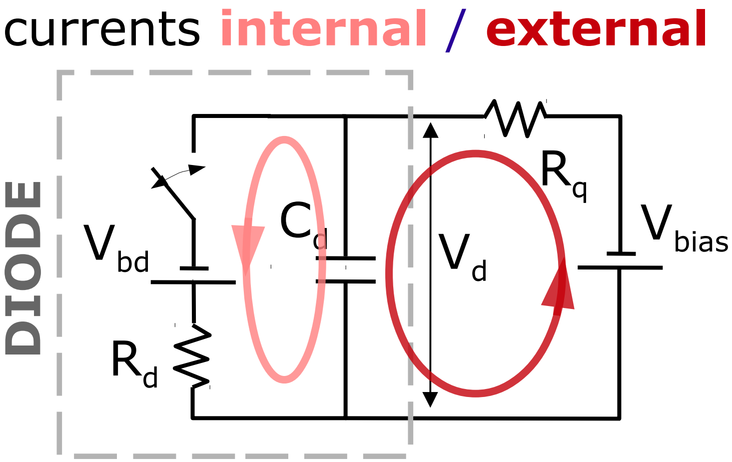

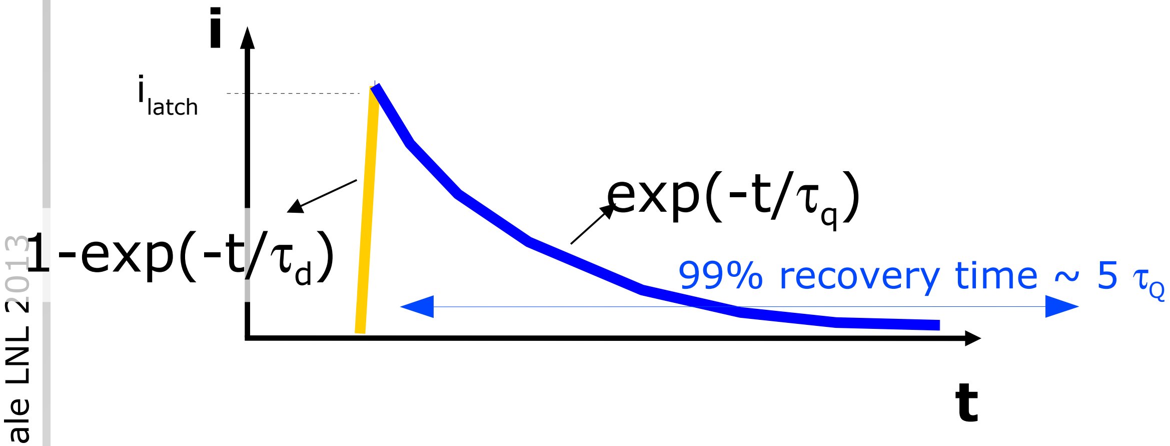

Rise time | Fall time (recovery)

$\tau_d = R_d C_d \ll \tau_q = R_q C_d$

Gain → linear with ΔV (≠ APD)
→ no intrinsic fluctuations !!! (≠ APD)
→ independent of T at fixed ΔV (≠ APD)

Rise time T dependence (weak) due to R_d

Recovery time T dependence (strong) due to R_q
C_d is independent of T

SiPM equivalent circuit and pulse shape

Single cell model → $(R_d||C_d)+(R_q||C_q)$

SiPM + load → $(||Z_{cell})||C_{grid} + Z_{load}$

Signal = slow pulse ($\tau_{d\ (rise)}, \tau_{slow\ (fall)}$) +

+ fast pulse ($\tau_{d\ (rise)}, \tau_{fast\ (fall)}$)

- $\tau_{d\ (rise)} \sim R_d(C_q+C_d)$
- $\tau_{fast\ (fall)} = R_{load}\ C_{tot}$ (fast; parasitic spike)
- $\tau_{slow\ (fall)} = R_q\ (C_q+C_d)$ (slow; cell recovery)

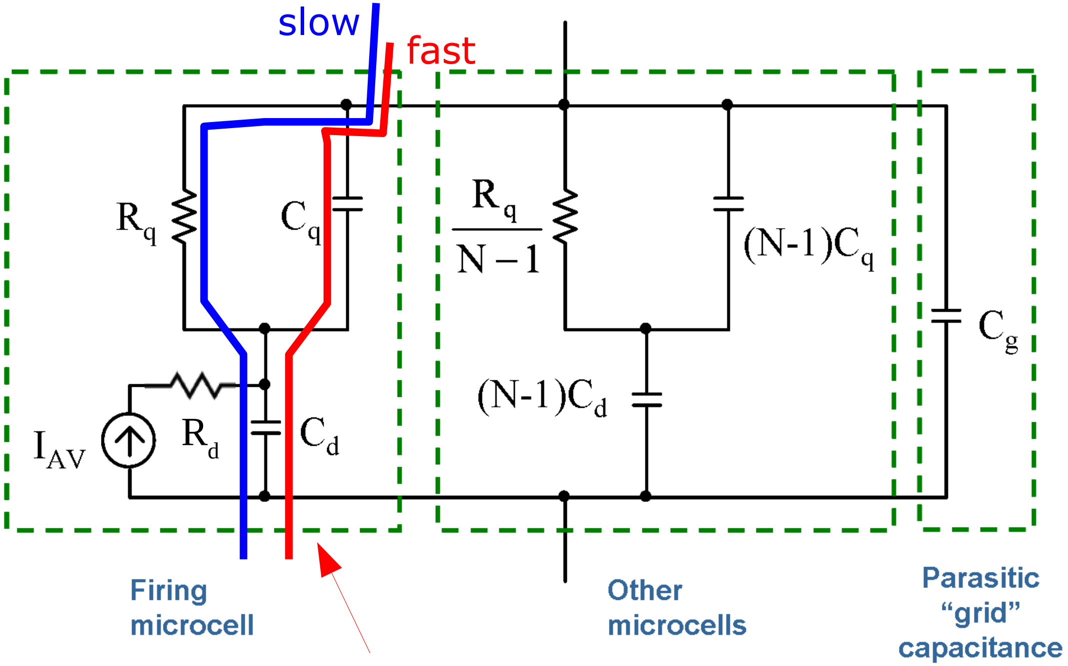

Cq → fast current supply path in the beginning of avalanche

- Rise: Exponential
- Fall: Sum of 2 exponentials: transient + recovery

Sp.Charge Rd x Cd,q filtered by parasitic inductance, stray C, ... (Low Pass)

$$V(t) \simeq \frac{Q}{C_q+C_d}\left(\frac{C_q}{C_{tot}} e^{\frac{-t}{\tau_{FAST}}} + \frac{R_{load}}{R_q}\frac{C_d}{C_q+C_d} e^{\frac{-t}{\tau_{SLOW}}}\right) \text{ for } R_{load} << Rq$$

where $Q = \Delta V\ (C_q+C_d)$ is the total charge released by the cell

→ 'prompt' charge on C_{tot} is $Q_{fast} = Q\ C_q/(C_q+C_d)$

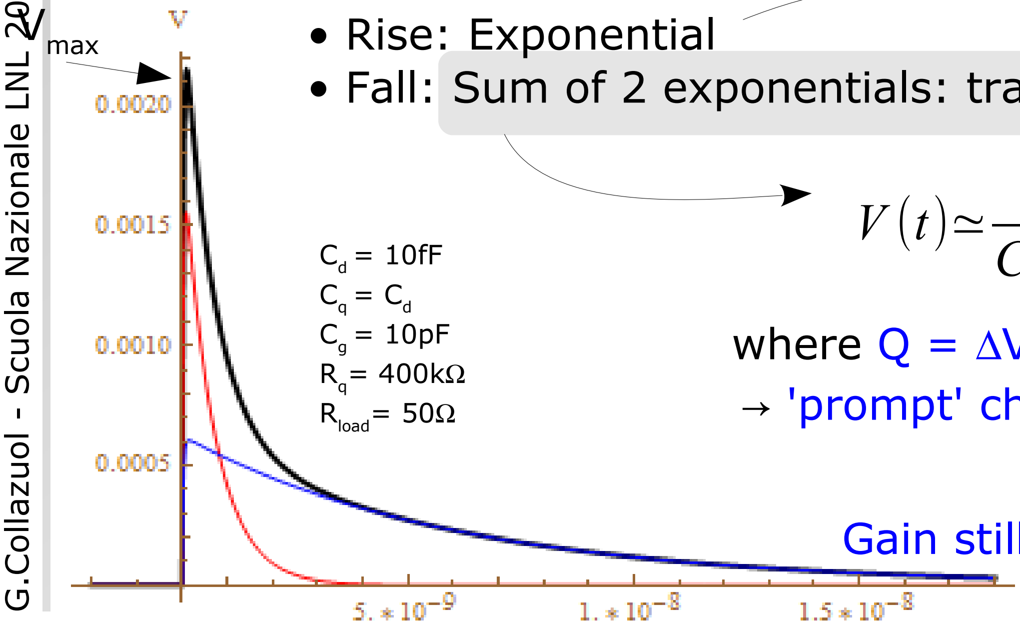

C_d = 10fF
C_q = C_d
C_g = 10pF
R_q = 400kΩ
R_{load} = 50Ω

Gain still well defined:

$$G = \int dt \frac{V(t)}{q_e R_{load}} = Q/q_e = \frac{\Delta V(C_d+C_q)}{q_e}$$

Pulse shape: dependence on Temperature

The two current components behave differently with Temperature

→ fast component is independent of T because C_{tot} couples to external R_{load}

→ slow component is dependent on T because $C_{d,q}$ couple to $R_q(T)$

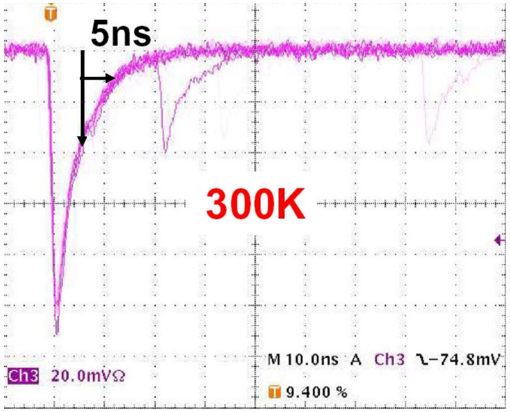

HPK MPPC

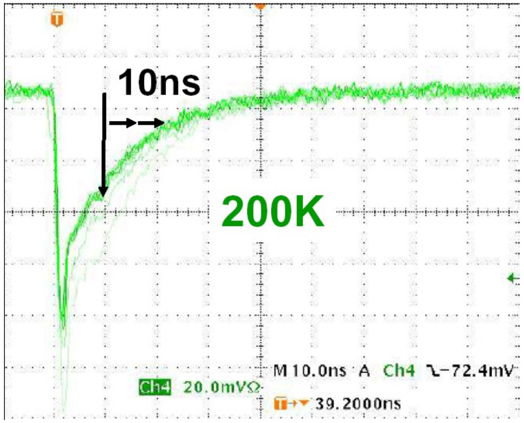

H.Otono, et al. PD07

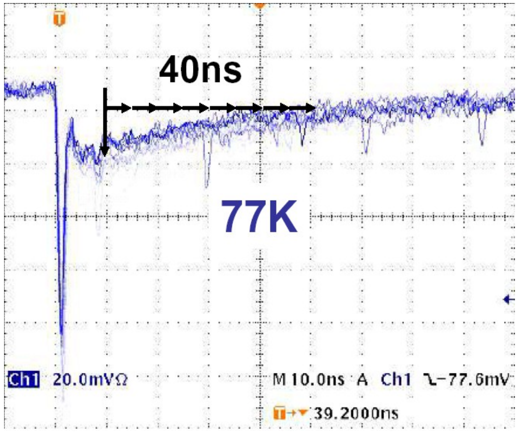

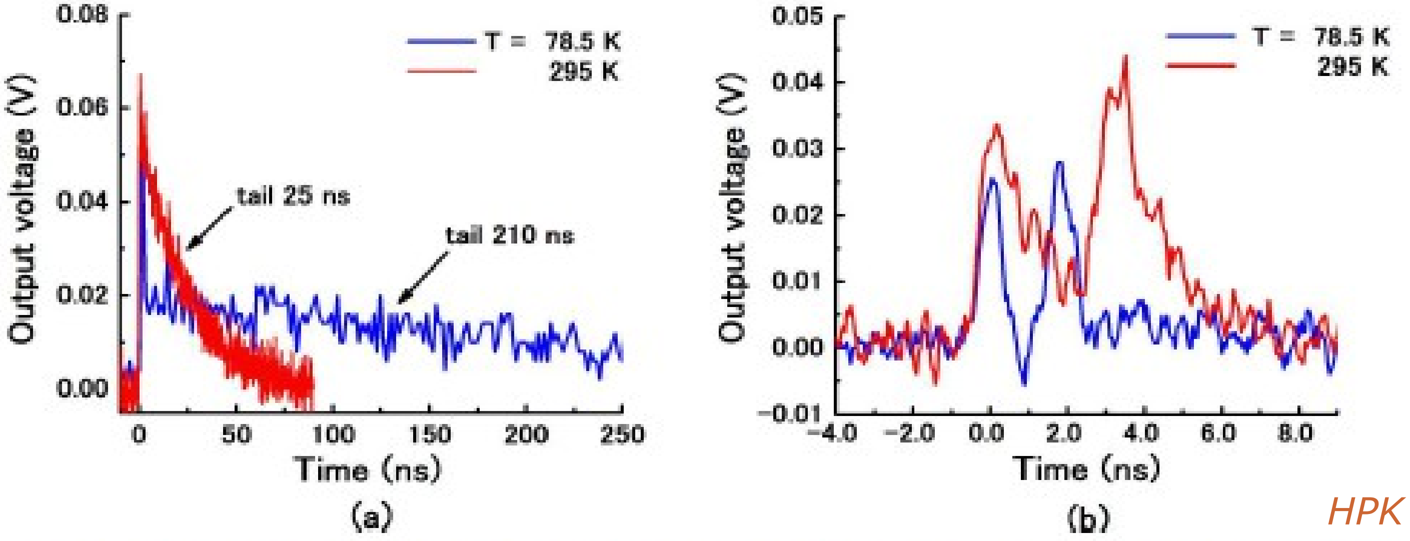

high pass filter / shaping
→ recover fast signals

HPK MPPC

Fig. 2. (a) Output signals from the MPPC when no high-pass filter is used, and (b) output signals from the high-pass filter when two pulses were generated successively.

Akiba et al Optics Express 17 (2009) 16885

Close up of a CMOS cell

Key elements for CMOS SiPMs
- **APD cell isolation** from CMOS circuitry
- **guard ring** (again)

APD integration into CMOS

Example of implementation *T.Frach in US patent 2010/0127314*

Note
- extended CMOS processes exploited
- careful design of cell isolation and guard ring

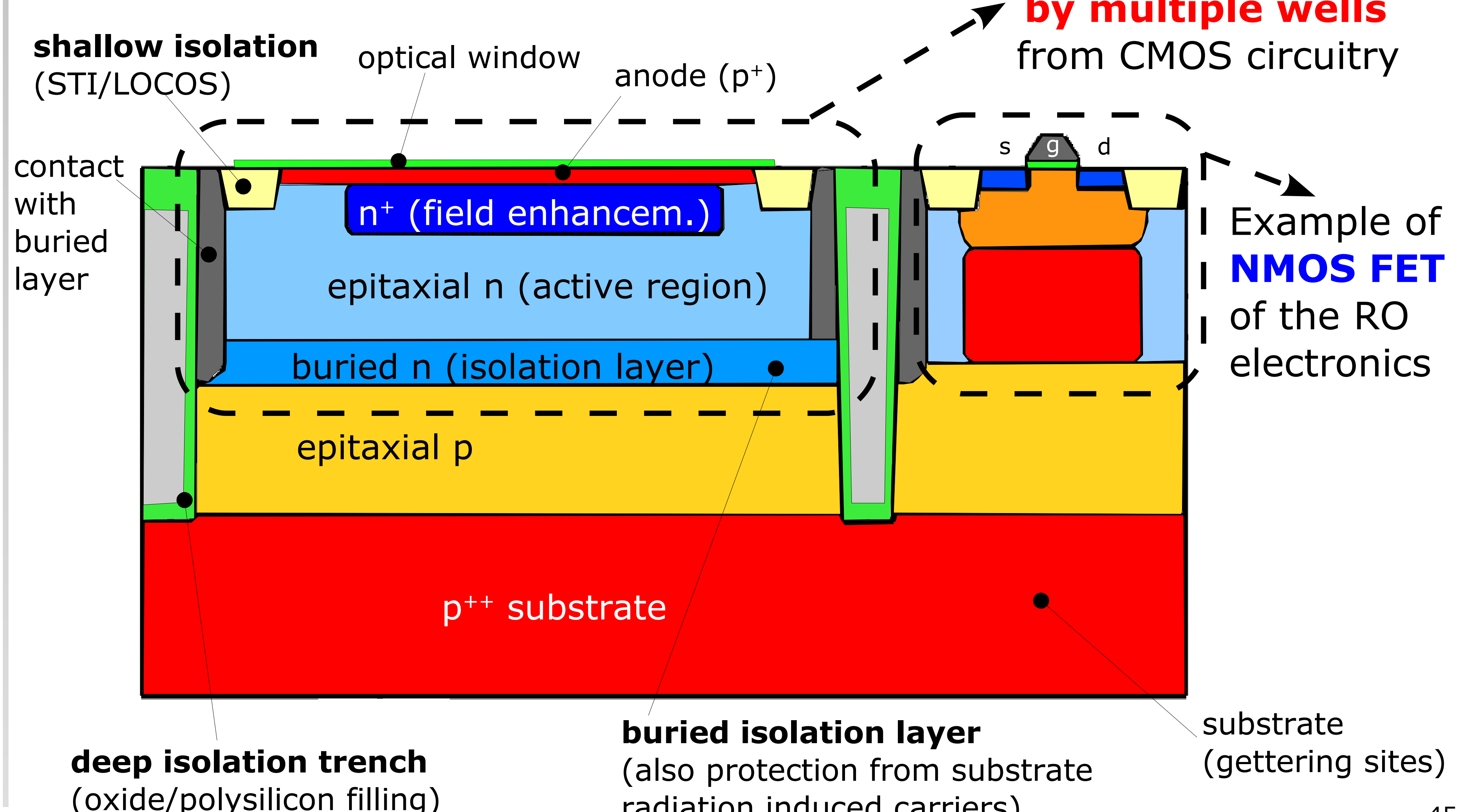

APD cell isolated by multiple wells from CMOS circuitry

Example of **NMOS FET** of the RO electronics

deep isolation trench (oxide/polysilicon filling)

buried isolation layer (also protection from substrate radiation induced carriers)

substrate (gettering sites)

Active Quenching (CMOS process)

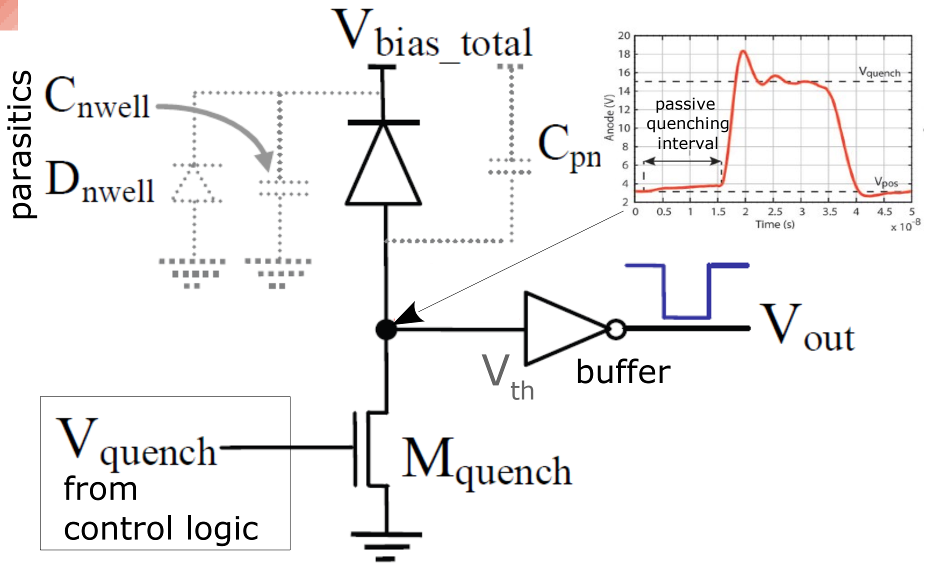

Basic circuit elements:

1) quench circuit to detect and stop the avalanche and restore bias conditions

2) buffer (low capacitive load) for isolating the APD from the external electronics capacitance

Configuration with anode to ground potential is best: only C_{det} is involved → minimum RC load

→ minimum quenching dead-time

→ minimum charge flow in APD (less after-pulses)

(in addition n-well regions (cathode) can be shared among many cells)

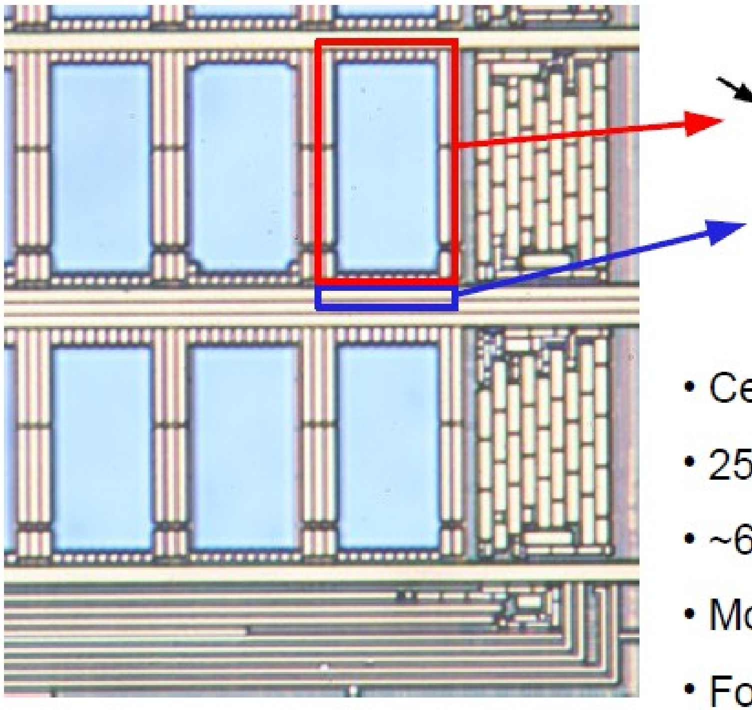

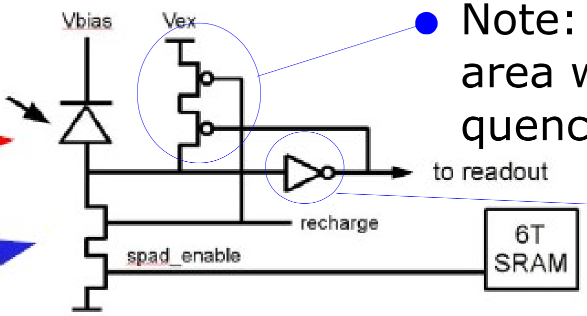

- Note: use of PMOS to minimize the area wrt NMOS for the same target quenching resistance
- buffer → simple inverter as input signal is already digital

dSiPM cell electronics

- Cell electronics area: 120μm²
- 25 transistors including 6T SRAM
- ~6% of total cell area
- Modified 0.18μm 5M CMOS
- Foundry: NXP Nijmegen

- Cell area ~ 30x50μm^2
- Fill Factor ~ 50%

T.Frach at LIGHT 2011

Analog vs Digital SiPM

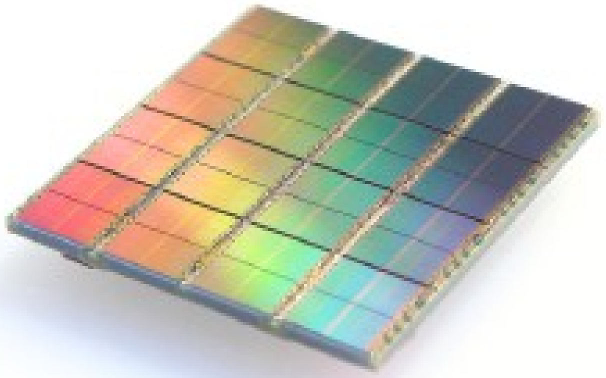

Analog Silicon Photomultiplier

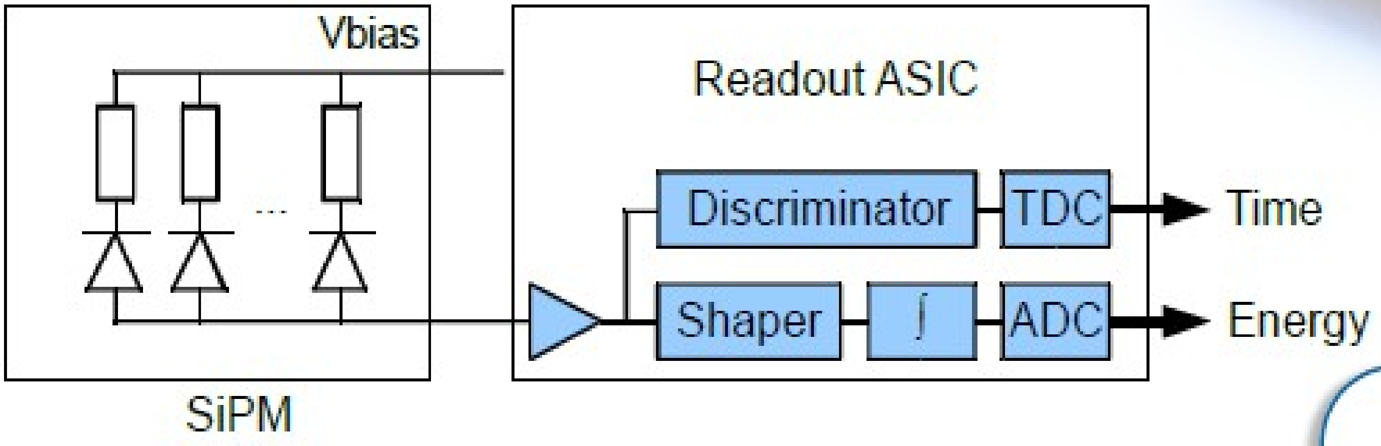

Digital Silicon Photomultiplier

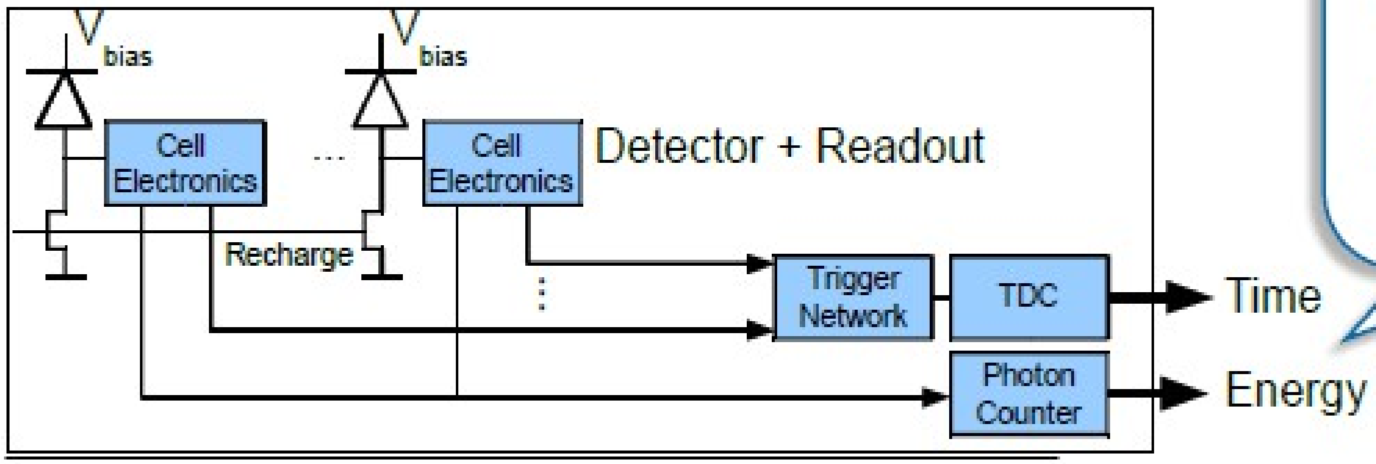

dSiPM provides a digital timestamp and the photon count for each light pulse, without the need of any analog front-end electronics

Fundamental SiPM parameters

Gain, Signal formation and Dynamic Range - Linearity

related to the recharge of the diode capacitance from V_{bd} to V_{bias} during the avalanche quenching time after I_{latch} is reached

Noise: dark count

pulses triggered by non-photo-generated carriers (thermal / tunneling generation in the bulk or in the surface depleted region around the junction)

afterpulses

carriers can be trapped during an avalanche and then released triggering another avalanche

optical cross-talk

photo-generation during the avalanche discharge. Some of the photons can be absorbed in the adjacent cell possibly triggering new discharges

Photo-detection efficiency

$PDE = QE * P_{01} * \varepsilon$

QE = quantum efficiency

P_{01} = avalanche triggering prob.

ε = geometrical fill factor

Time resolution

Related to the photo-generation and to the avalanche propagation

Pulse shape, Gain and Noise

Pulse shape

1. fast component
(parasitic transient)

2. slow component due to
(99% recovery time ~100ns)

Waveform (Dark noise)

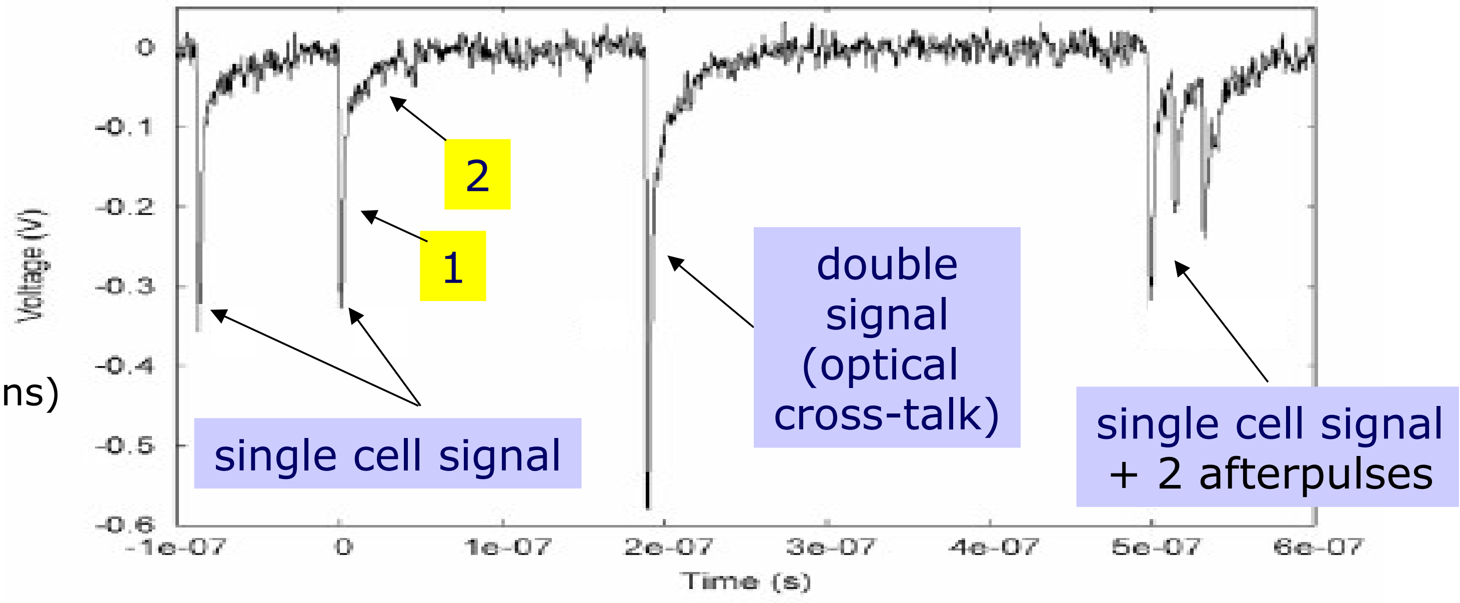

single cell signal

double signal (optical cross-talk)

single cell signal + 2 afterpulses

Charge spectrum

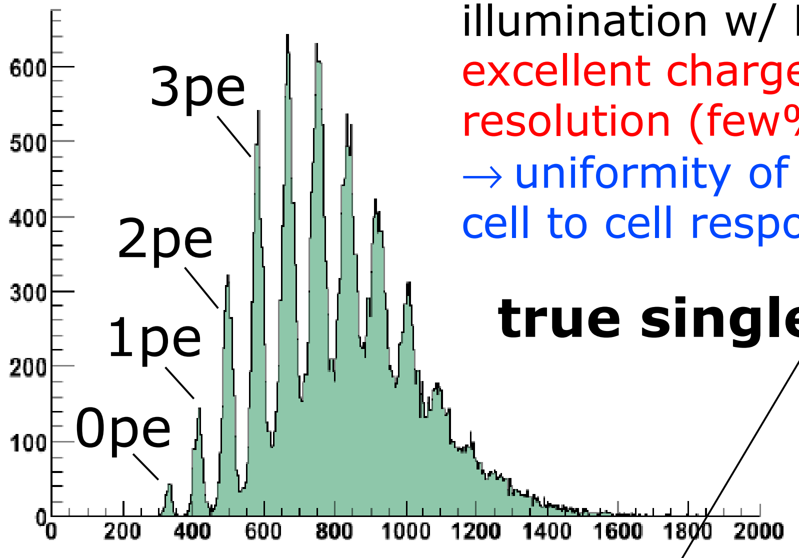

illumination w/ LED
excellent charge resolution (few%)
→ uniformity of cell to cell response

true single ph.e

NOTE: gain easily measured

Gain

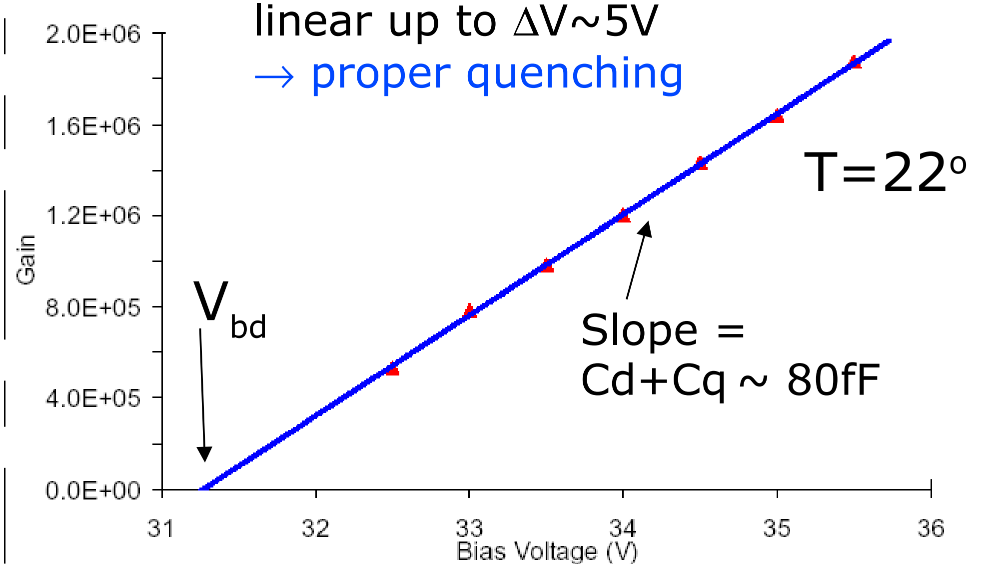

linear up to ΔV~5V
→ proper quenching

T=22°

Slope = Cd+Cq ~ 80fF

Gain and fluctuations

$$G = \Delta V \left(C_q + C_d\right)/q_e$$

→ Gain is linear if ΔV in quenching regime

but

there are many sources for non-linearity of response (non proportionality)

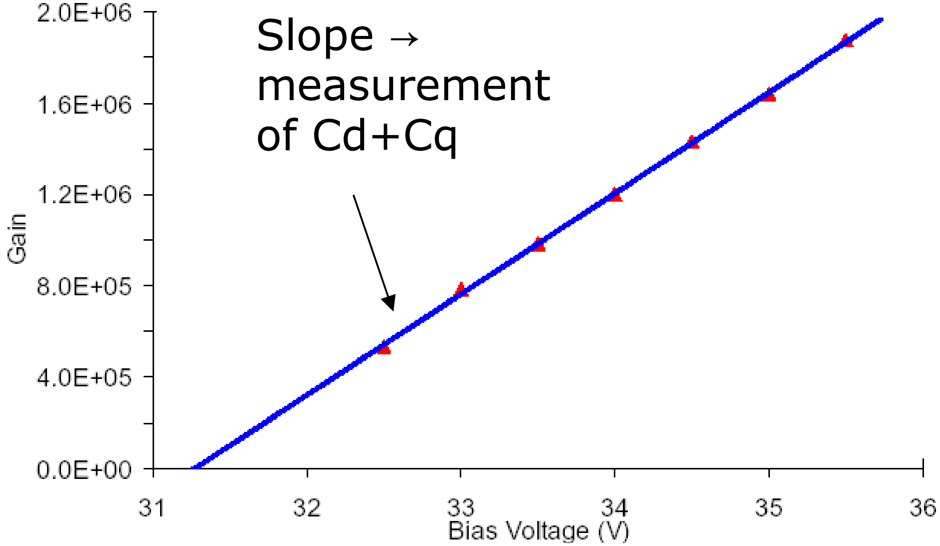

Slope → measurement of Cd+Cq

SiPM gain fluctuations (intrinsic) differ in nature compared to APD where the statistical process of internal amplification shows a characteristic fluctuations

$$\frac{\delta G}{G} = \frac{\delta V_{bd}}{V_{bd}} \oplus \frac{\delta C_{dq}}{C_{dq}}$$

cell to cell uniformity (active area and volume) control at % level

- doping densities (Poisson): $\delta V_{bd} \geq 0.3\text{V}$
  Shockley, Sol. State Ele. 2 (1961) 35
- doping, epitaxial, oxide (processing): $\delta V_{bd} \sim O(0.1\text{V})$

SES MEPhI/PULSAR APD, U=57.5V, T=-28 C

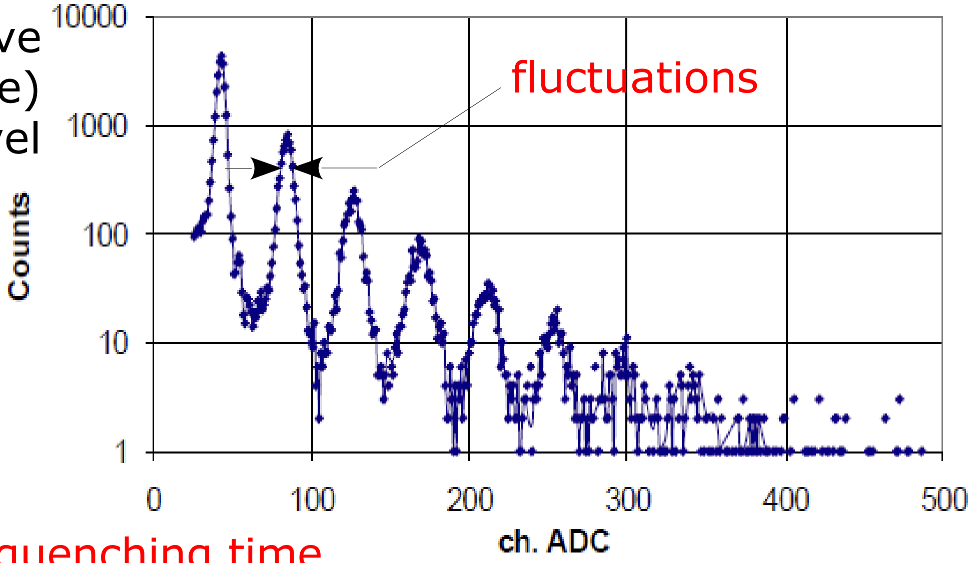

fluctuations

In addition δG might be due to fluctuations in quenching time

… and of course after-pulses contribute too (not intrinsic → might be corrected)

Dynamic range and non-linearity

analog SiPM output =
sum of binary cell's output

- Due to **finite number of cells** → signal **saturation**

- Correction possible BUT
→ **degraded resolution**

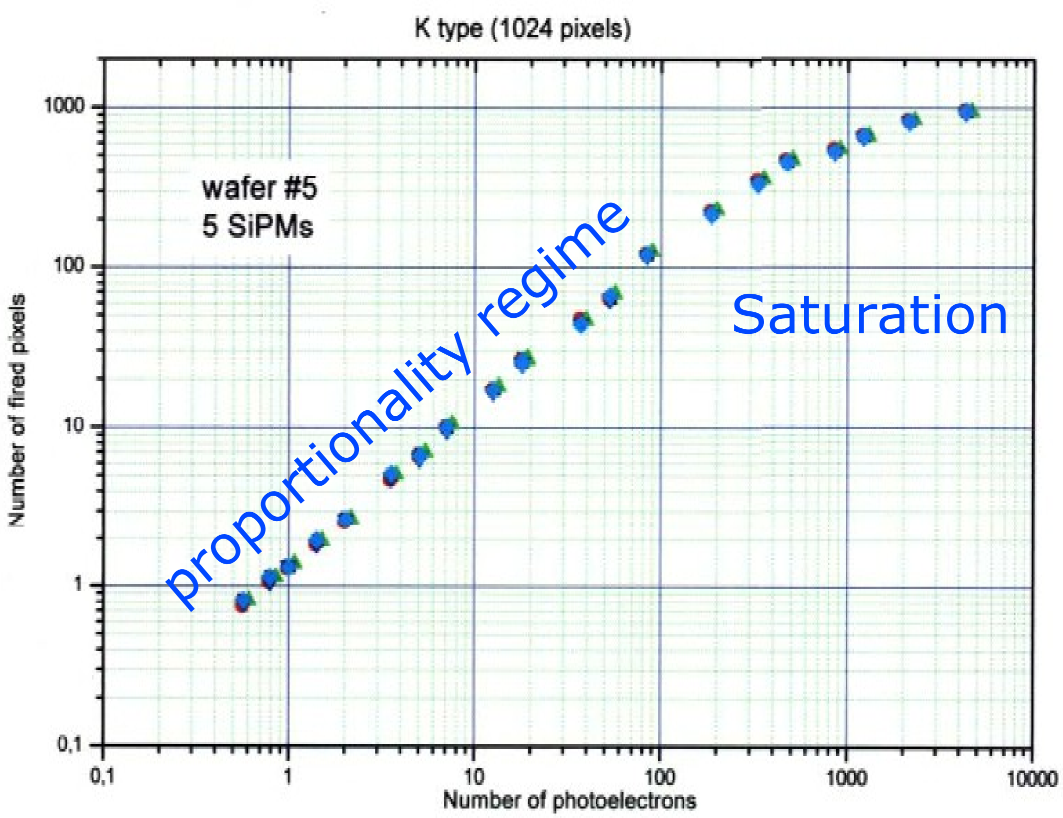

$$A \approx N_{firedcells} = N_{total} \cdot \left(1 - e^{-\frac{N_{photon} \cdot PDE}{N_{total}}}\right)$$

eg: 20% deviation from linearity
if 50% of cells respond

→ Best working conditions: $N_{\text{photo-electrons}} < N_{\text{SiPM cells}}$

Additional complications:
1) need correction to $N_{\text{fired-cells}}$ due to cross-talk and after-pulse
2) effective dynamic range depends on recovery time and time scale of signal burst

High dynamic range new SiPMs

Different types available or in preparation:

- tiny cells
  → HPK, FBK, NDL, MPI-LL
- micro cells
  → Zecotek, AmplititationTech

Latest MPPC tiny cell by Hamamatsu

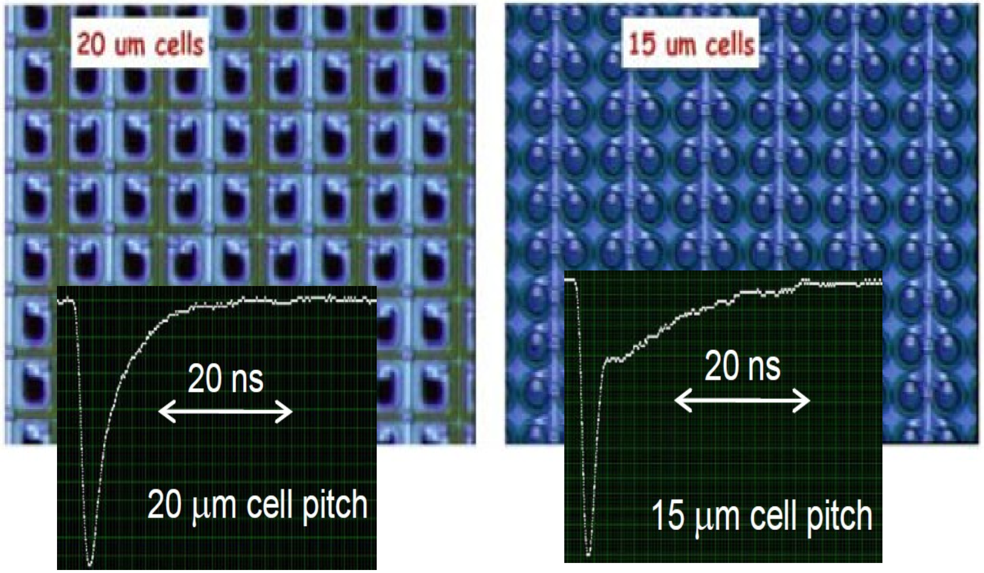

SiPMs NDL (Bejiing)

Zhang et al NIM A621 (2010) 116
Han at NDIP 2011

- type: n-on-p, Bulk Rq
- high cell density (10000/mm^2)
- fast recovery (5ns)
- low gain

→ dynamic range

→ radiation hardness

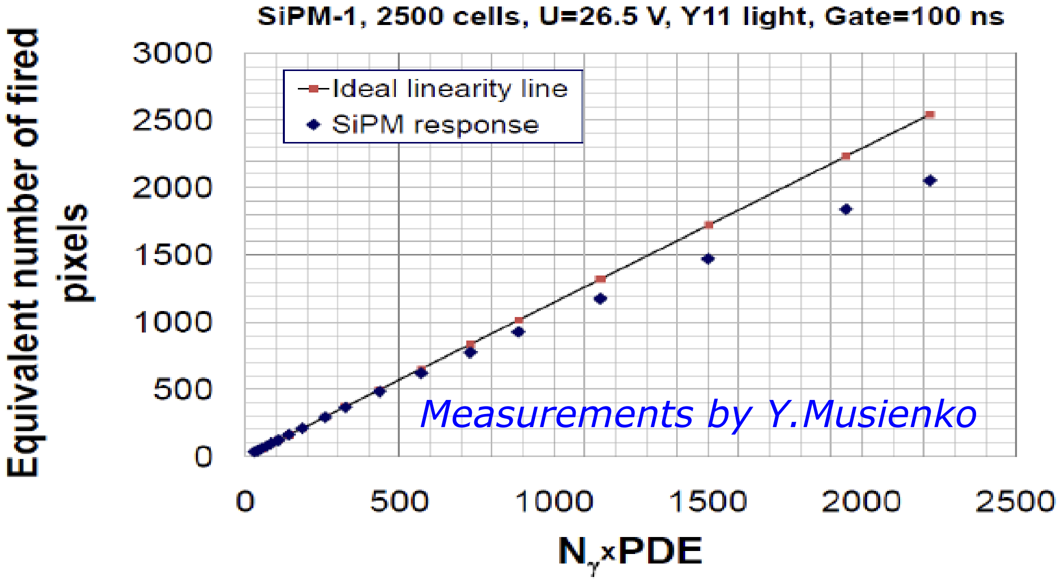

Measurements by Y.Musienko

Reverse I-V → Dark Current and V_{bd}

Reverse I-V characteristics at fixed T

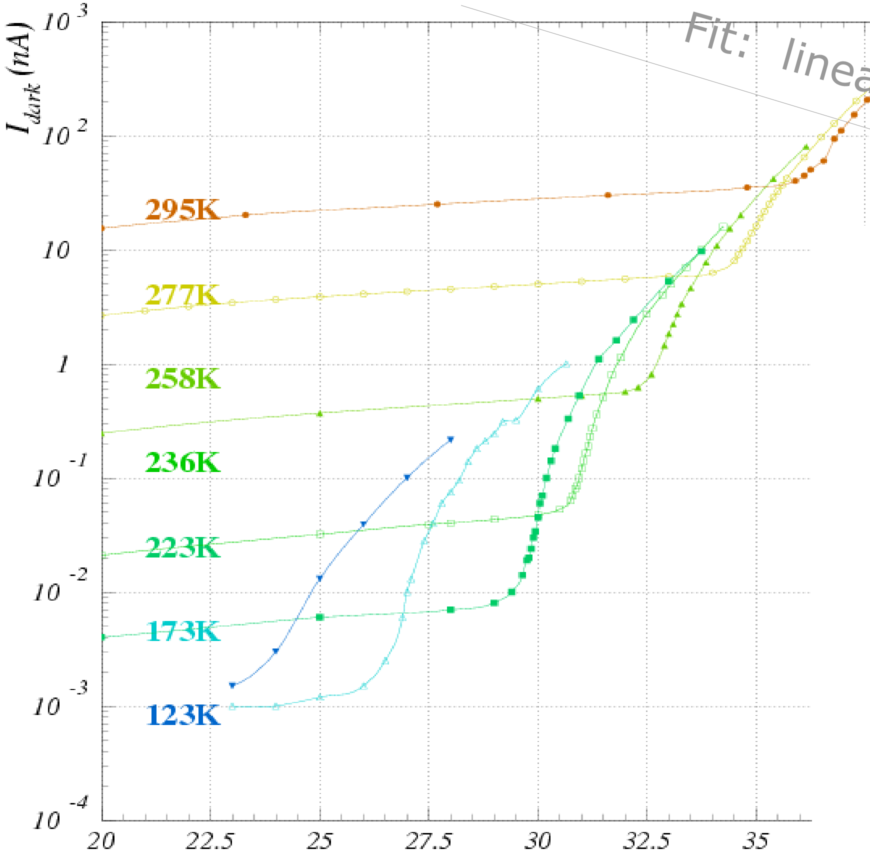

Fit: linear + quadratic ($V > V_{breakdown}$)

Dark current decreases rapidly with T at rate ~ x2 / 10K

Breakdown Voltage vs T

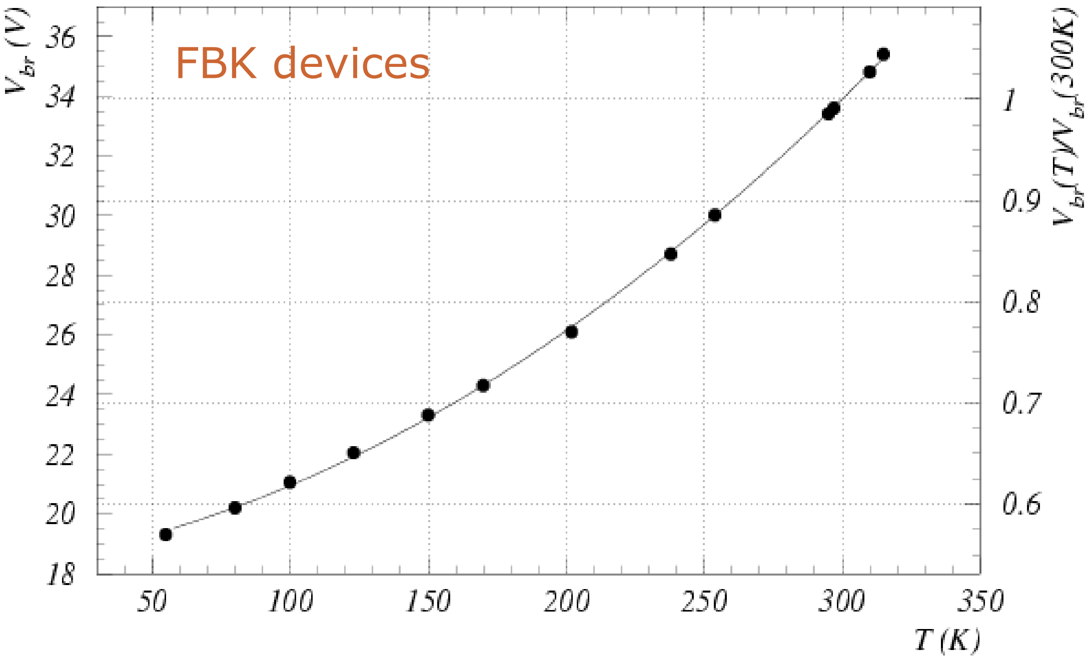

Breakdown voltage decreases
at low T due to larger carriers mobility
→ larger ionization rate (electric E field fixed)

G.C. et al NIM A628 (2011) 389

Dark current vs T   sources of DCR

contribution to DCR from diffusion of minority carriers negligible below 350K

Noise mainly comes from the high E Field region (no whole depletion region)

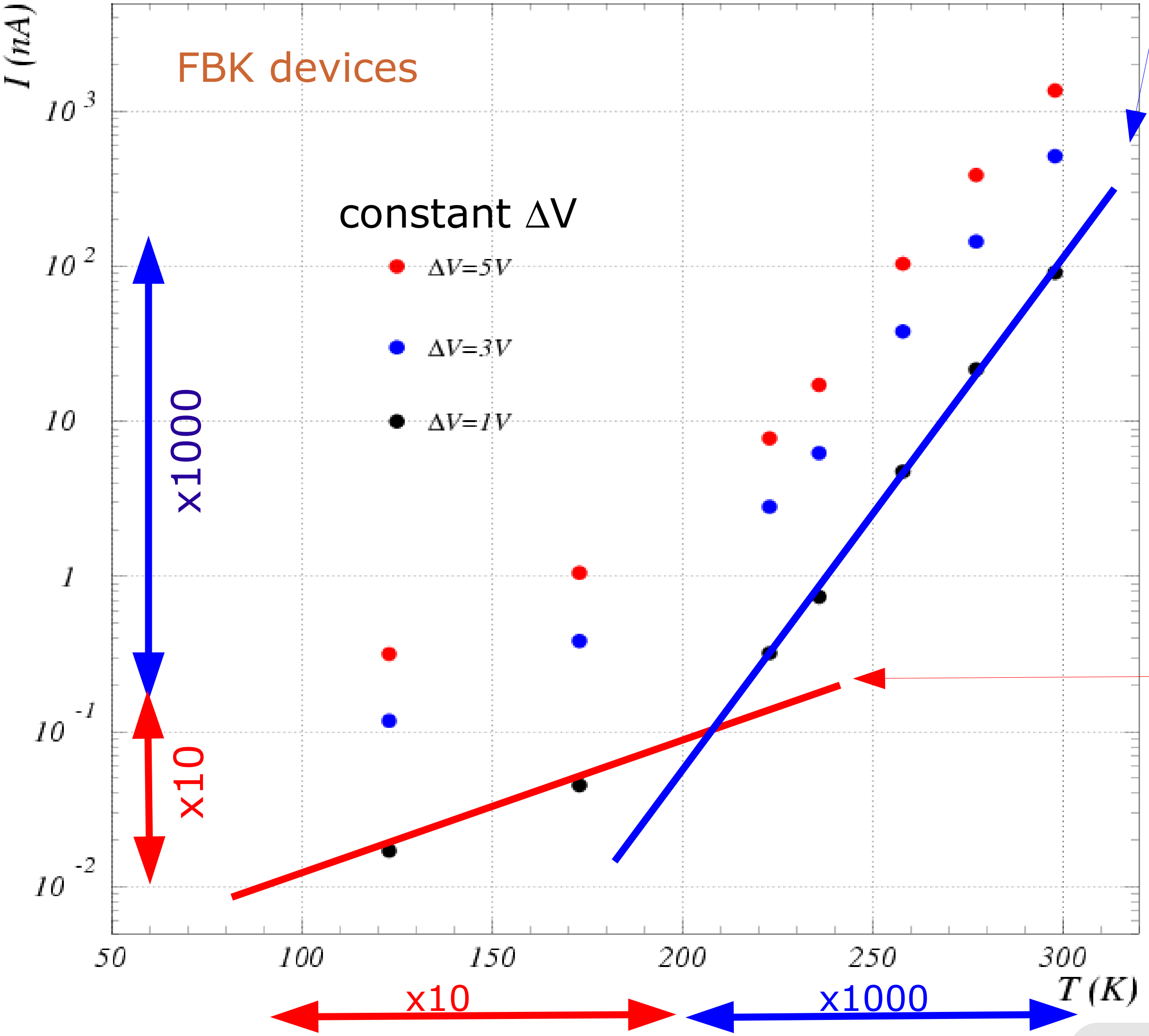

1) Generation/Recombination SRH noise (enhanced by trap assisted tunneling)

$$I_{reverse} \sim T^{1.5} \exp \frac{-E_{act}}{K_B T}$$

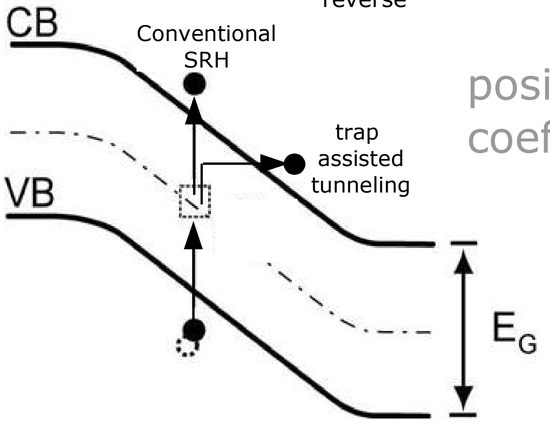

positive T coefficient

2) Band-to-band Tunneling noise (strong dependence on the Electric field profile)

negative T coefficient

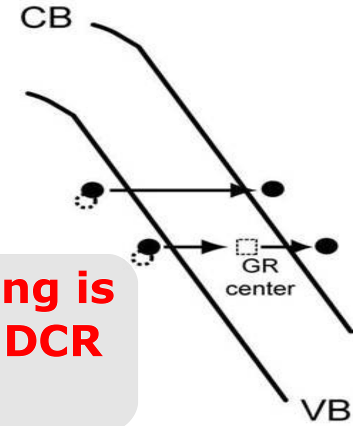

Tunneling noise dominating for T<200K
(sharp high E field region → higher noise)

Efield engineering is crucial for min. DCR (esp. at low T)

Dark Count Rate

- DCR → linear dependence due to $P_{01} \propto \Delta V$ (→ same as PDE vs ΔV)
  → non-linear at high ΔV due to cross-talk and after-pulsing → $\propto \Delta V^2$
- DCR scales with active surface (not with volume: high field region)

KETEK PM 3350 (p^+-on-n, shallow junction)
3x3mm² active area pixel size 50x50 μm²

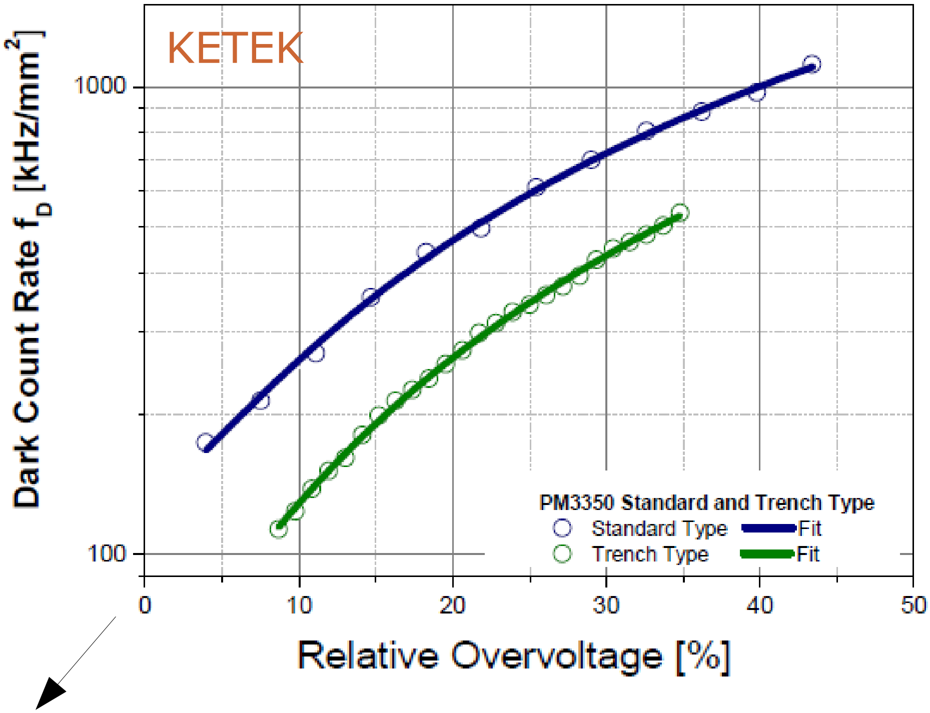

V_{bd} ~ 25V

F.Wiest – AIDA 2012 at DESY

Critical issues:
- quality of epitaxial layer
- gettering techniques
- Electric field engineering

Exelitas 1st generation SiPM 2011
(p^+-on-n) 1x1mm²

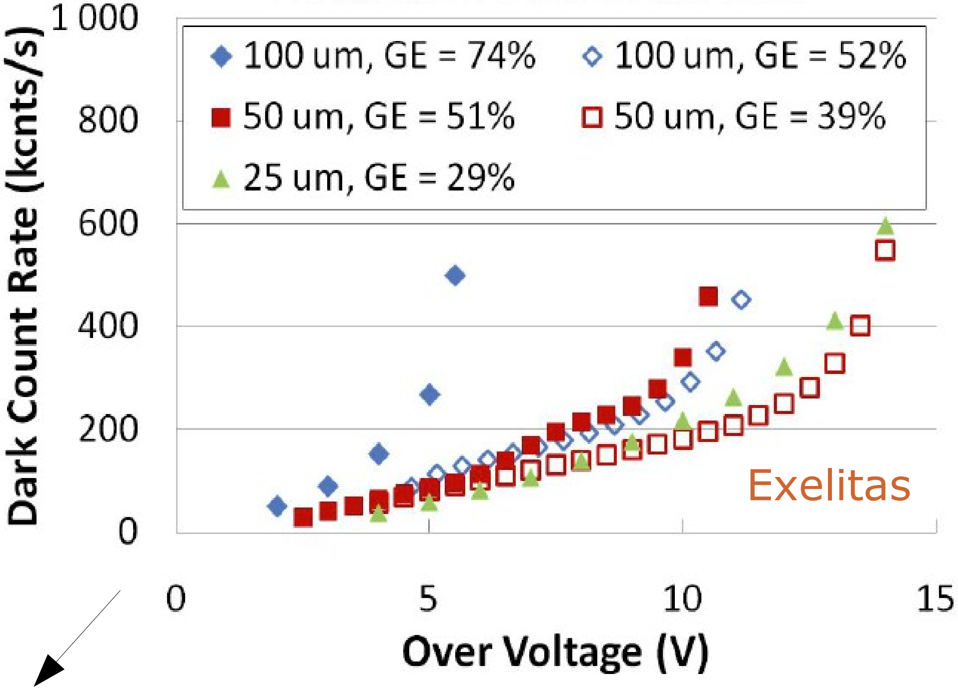

V_{bd} ~ 140V

P.Berard – NDIP 2011

Latest Hamamatsu devices reached ~80kHz/mm²

HPK claiming for additional improvements coming (*HPK at LIGHT 2011*)

After-Pulsing Carrier trapping and delayed release

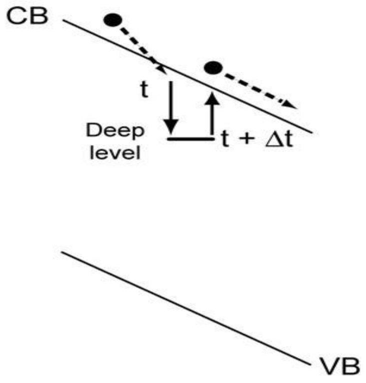

$$P_{afterpulsing}(t) = P_c \cdot \frac{\exp(-t/\tau)}{\tau} \cdot P_{01} \quad \boxed{\propto \Delta V^2}$$

~Few % level at 300K

avalanche triggering probability
$\propto \Delta V(t)$

τ : trap lifetime
depends on trap level position

P_c : trap capture probability
$\propto$ carrier flux (current) during avalanche $\propto \Delta V$
$\propto$ N traps

quadratic dependence on ΔV

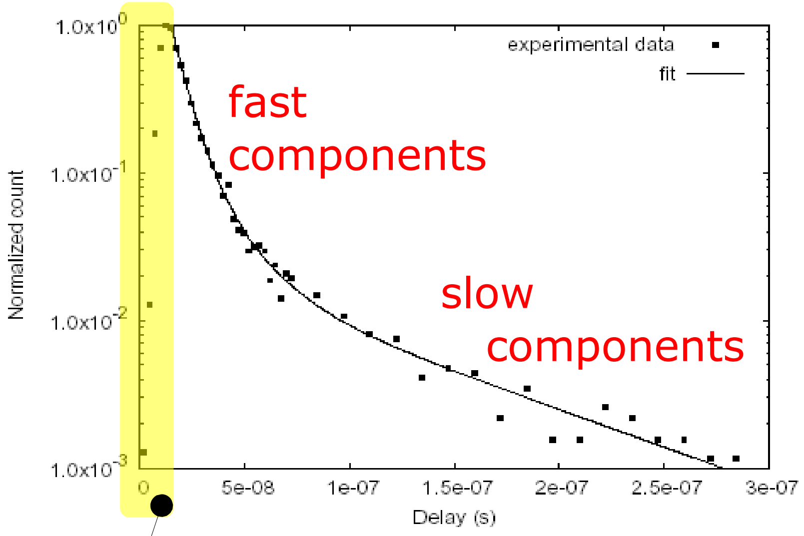

Fig. 10. Spectrum of the delay time from the primary pulse to the after-pulse.

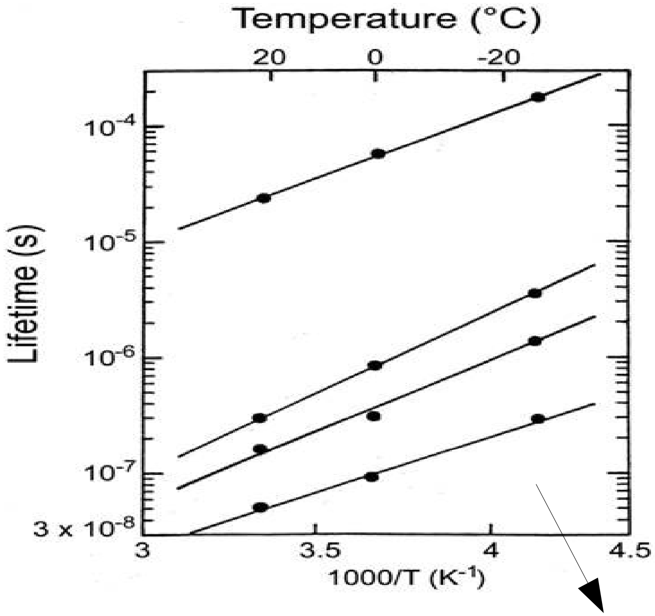

S.Cova, A.Lacaita, G.Ripamonti, IEEE EDL (1991)

not trivial dependence on T

Only partially sensitive to after-pulsing during recovery
ie recovery hides After-pulses (does not cancel them)

Radiation damage effects on SiPM

→ increase of **dark count** rate due to introduction of generation centers
→ increase of **after-pulse** rate due to introduction of trapping centers
→ may change VBD, leakage current, noise, PDE…

HPK devices
T Matsumura – PD07

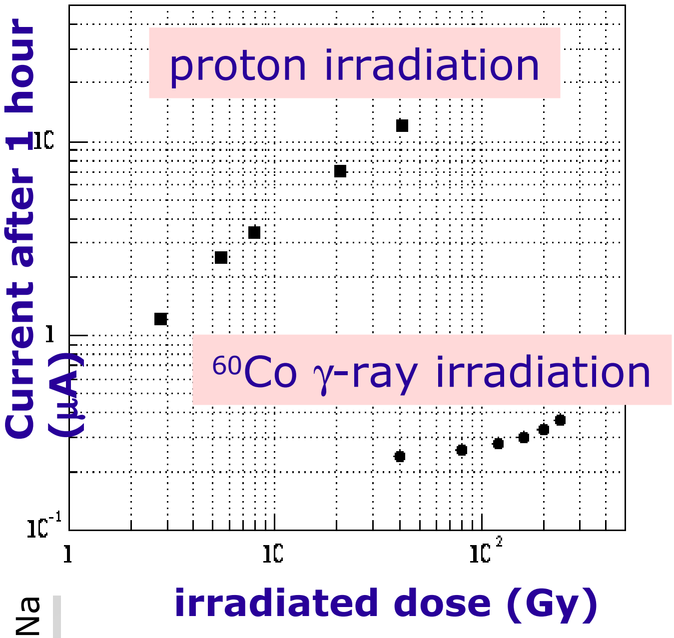

4.2×10^5 n/mm^2/s
I_{leak} @ (V_{op}, 1.0x10^8 n/mm^2) = 8.5 µA

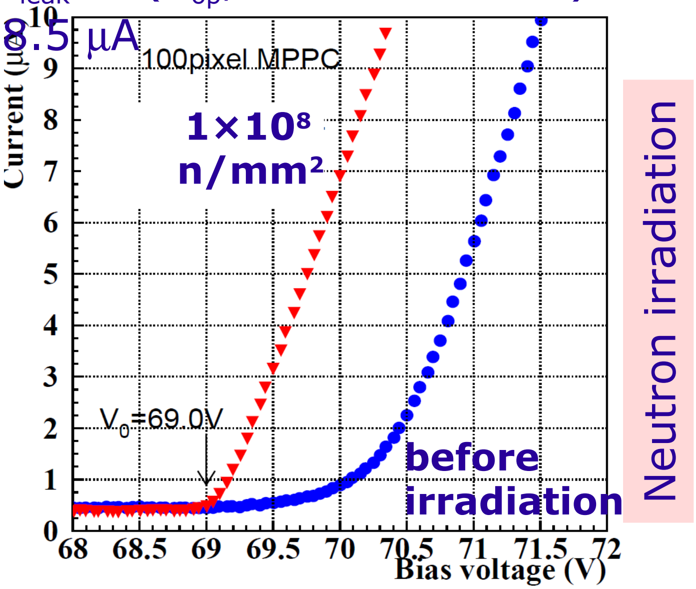

2.3×10^5 p/mm^2/s (130 Gy/h)
I_{leak} @ (V_{op}, 1.4x10^8 p/mm^2) = 6.7 µA

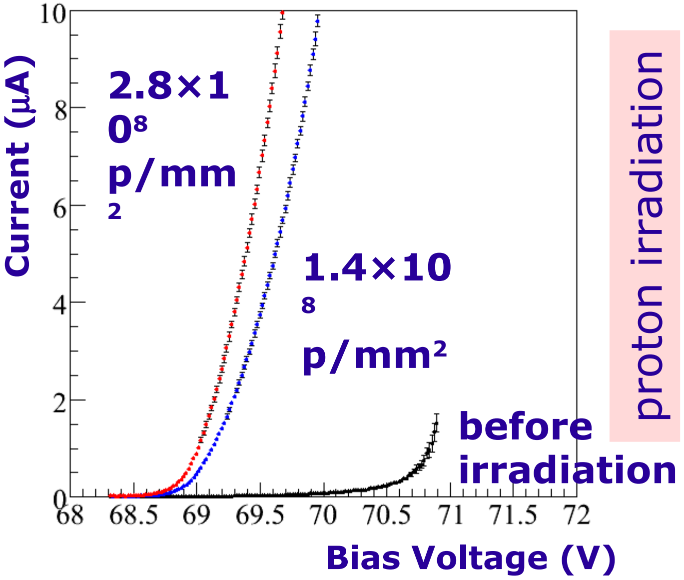

→ almost the same for protons and neutrons

Effects reduced by
→ **small cells** → smaller charge flow (small gain, high dynamic range)
→ thin epi-layer

Optical cross-talk:reflections from the bottom

Avalanche luminescence (NIR)

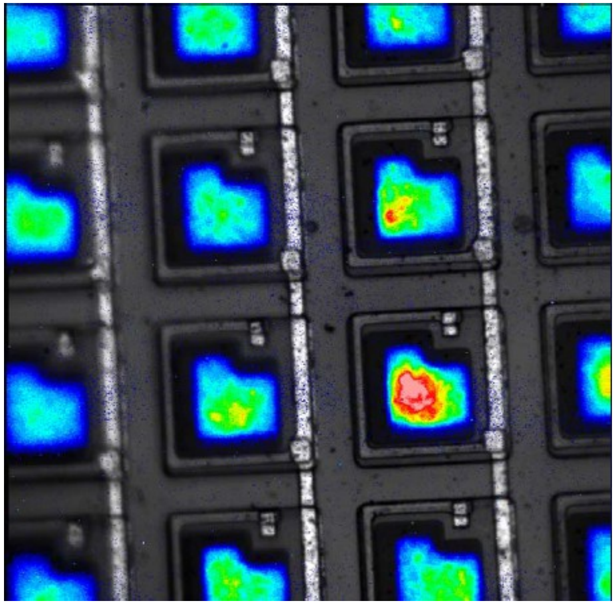

N.Otte, SNIC 2006

Carriers' luminescence (spontaneous direct relaxation in the conduction band) during the avalanche: probability 3.10^{-5} per carrier to emit photons with E> 1.14 eV

A.Lacaita et al. IEEE TED (1993)

Photons can induce avalanches in neighboring cells. Depends on distance between high-field regions

ΔV^2 dependence on over-voltage:

- carrier flux (current) during avalanche $\propto \Delta V$
- gain $\propto \Delta V$

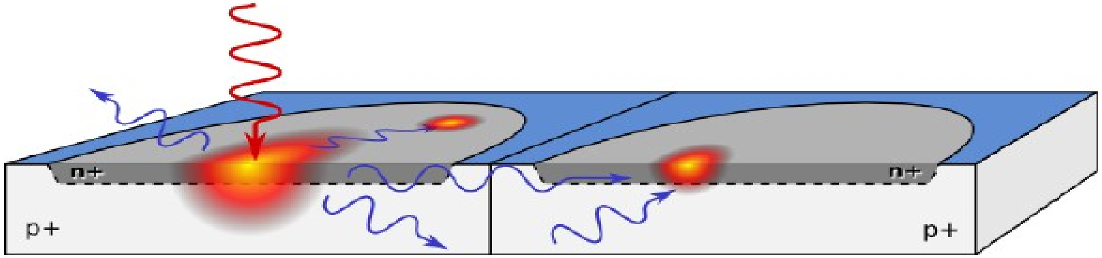

Counteract:

- optical isolation between cells

by trenches filled with opaque material

- low over-voltage operation helps

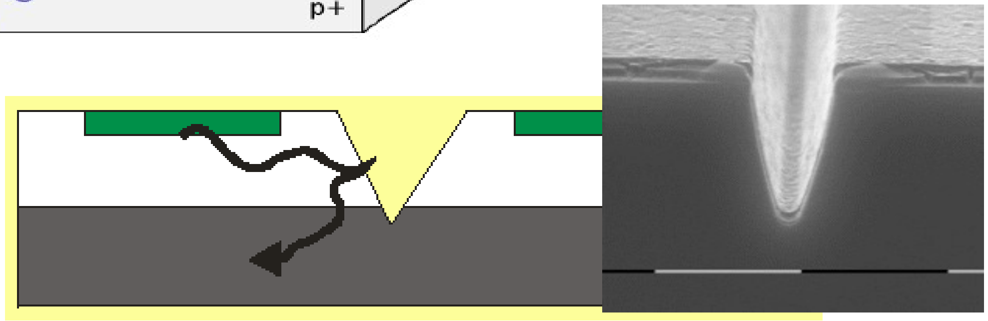

It can be reduced to a level below % in a wide ΔV range

$PDE = QE \cdot P_{01} \cdot FF$

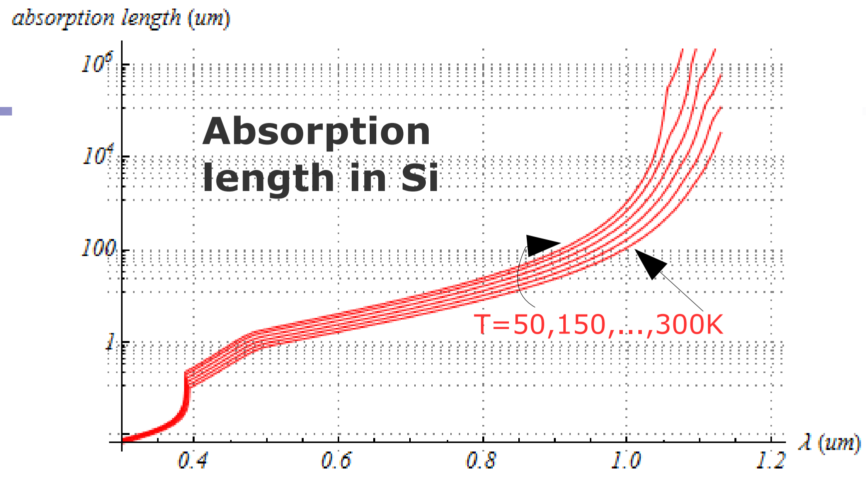

QE: carrier Photo-generation

probability for a photon to generate a carrier that reaches the high field region

→λ and T dependent

→ ΔV independent if full depletion at V_{bd}

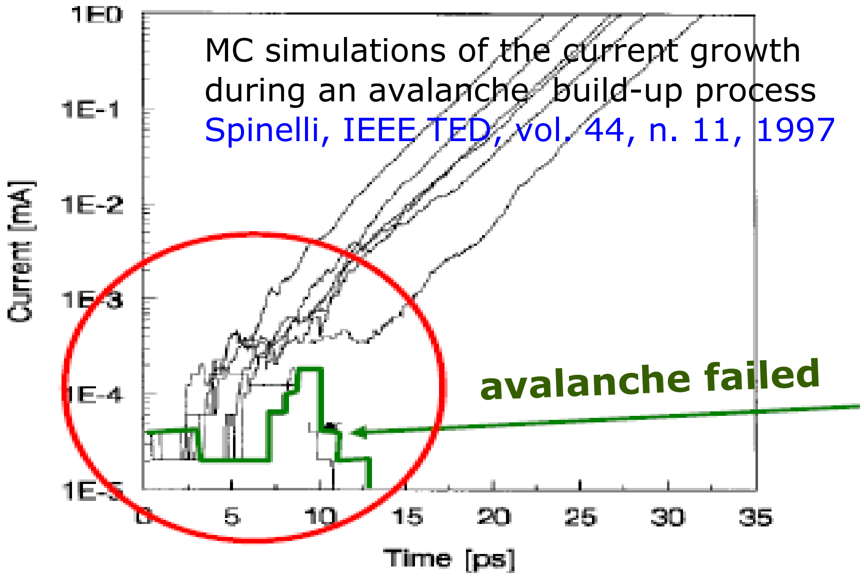

MC simulations of the current growth during an avalanche build-up process

Spinelli, IEEE TED, vol. 44, n. 11, 1997

P_{01} : avalanche triggering probability

probability for a carrier traversing the high-field to generate the avalanche

→λ, T and ΔV dependent

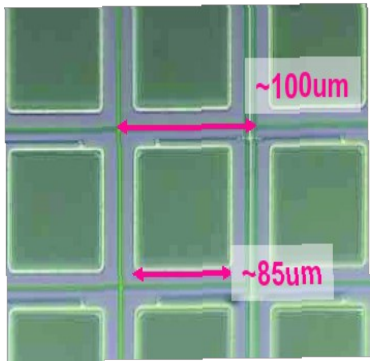

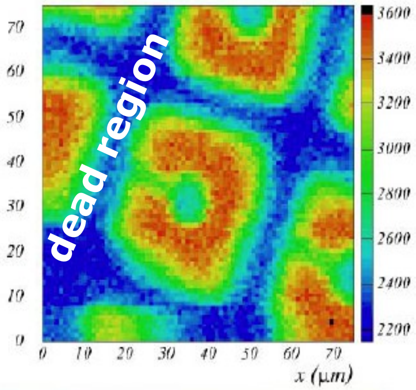

FF: geometrical Fill Factor

fraction of dead area due to structures between the cells, eg. guard rings, trenches

→ moderate ΔV dependence (cell edges)

QE factors

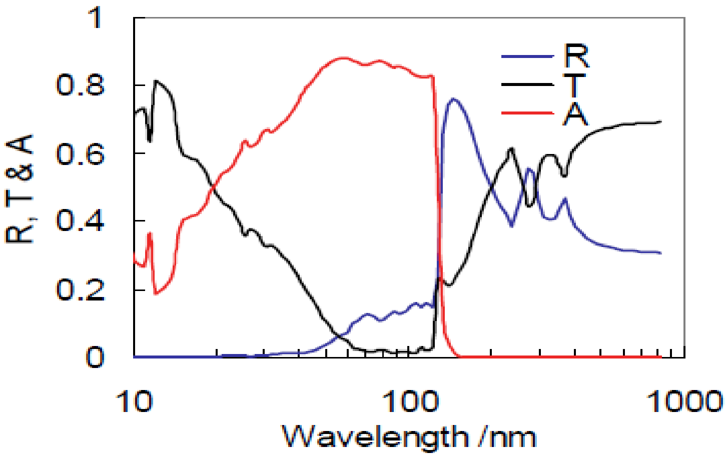

R,T,A coeff. in SiO_2 (example: 30nm SiO_2 on Si layer)

optical T,A,R of the entrance window (SiO_2/Si_3N_4 dielectric on top of Si)

→ angular and polarization dependence

carrier recombination loss: collection efficiency front, depl. region, back

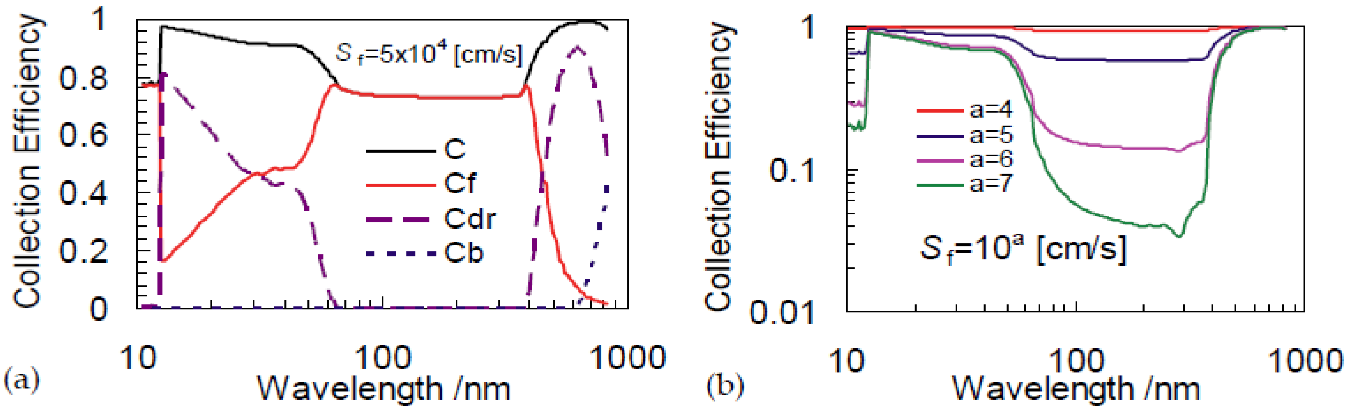

→ front region critical for 60nm < λ < 400nm

→ C eff. depends on surface recombination velocity S_f

→ freeze-out at low T

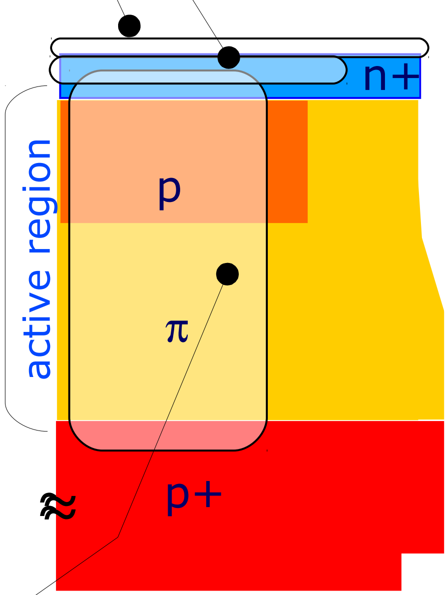

internal quantum efficiency: prob. to photo-generate an e-h pair ~ E_{phoron} (above threshold)

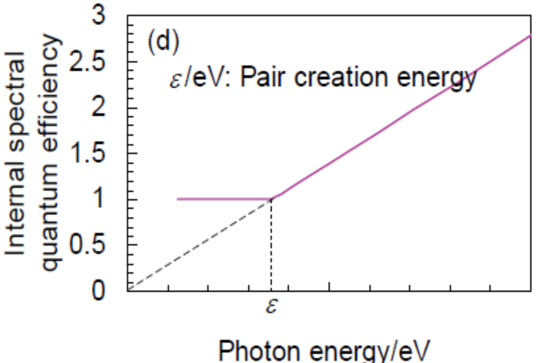

Commercial devices PDE → 0 in VUV due to:

1) protection coating (epoxy resin/silicon rubber)
2) reflectivity of Oxide/Nitride layers
3) insensitive top layer (p+ layer with ~0 E_{field})
5) high reflectivity for VUV on Si surface
4) absorption length in Si VUV photon: a few nm

QE → PDE dependence on wavelength λ

FBK single diode (2006) photo-voltaic regime (V_{bias}~ 0 V)

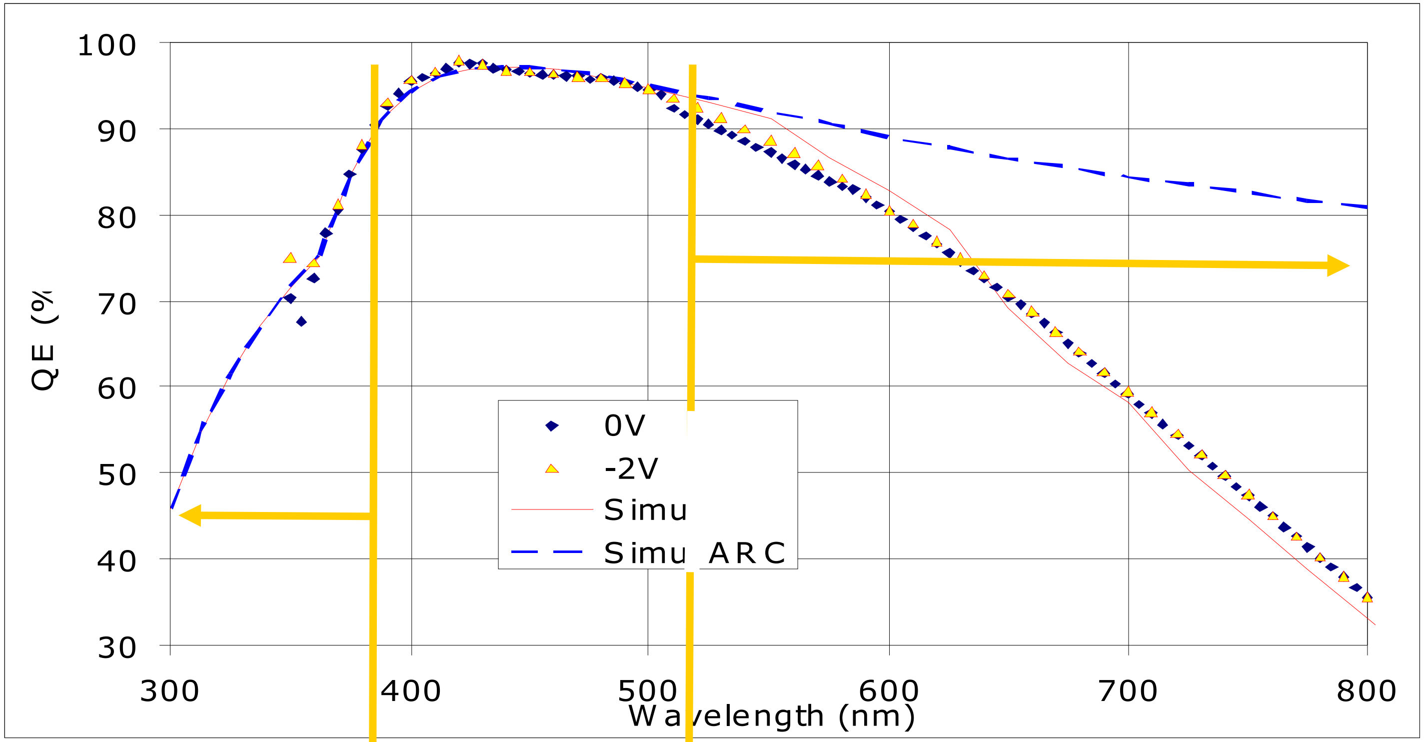

limited by
ARC Transmittance
&
Superficial
Recombination

limited by the
small π layer thickness

Most critical issue for **Deep UV SiPM**
note: reduced superficial recombination
in n-on-p wrt p-on-n

Trigger prob. P_{01} → PDE depends on λ and ΔV

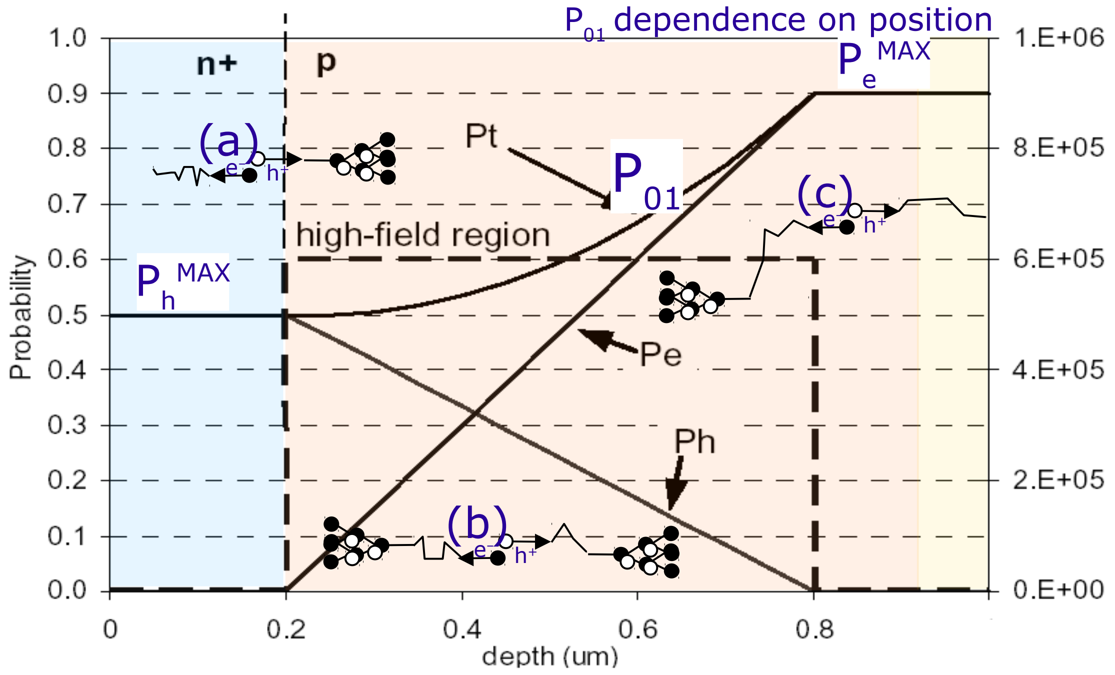

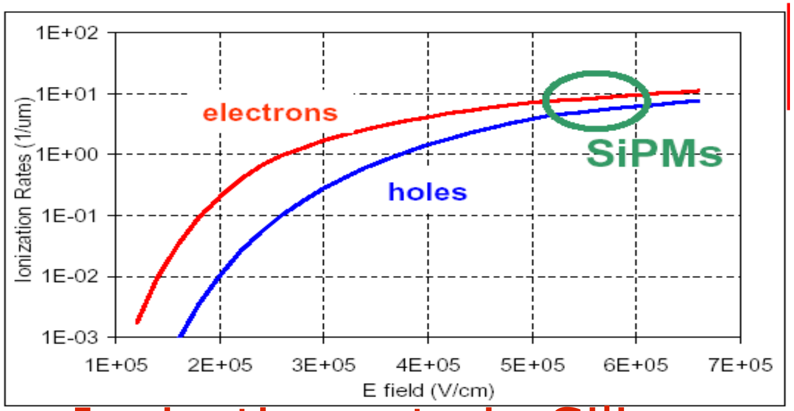

Ionization rate in Silicon

Example with constant high-field:
(a) only holes trigger the avalanche
(b) both electrons and holes trigger
(c) only electrons trigger

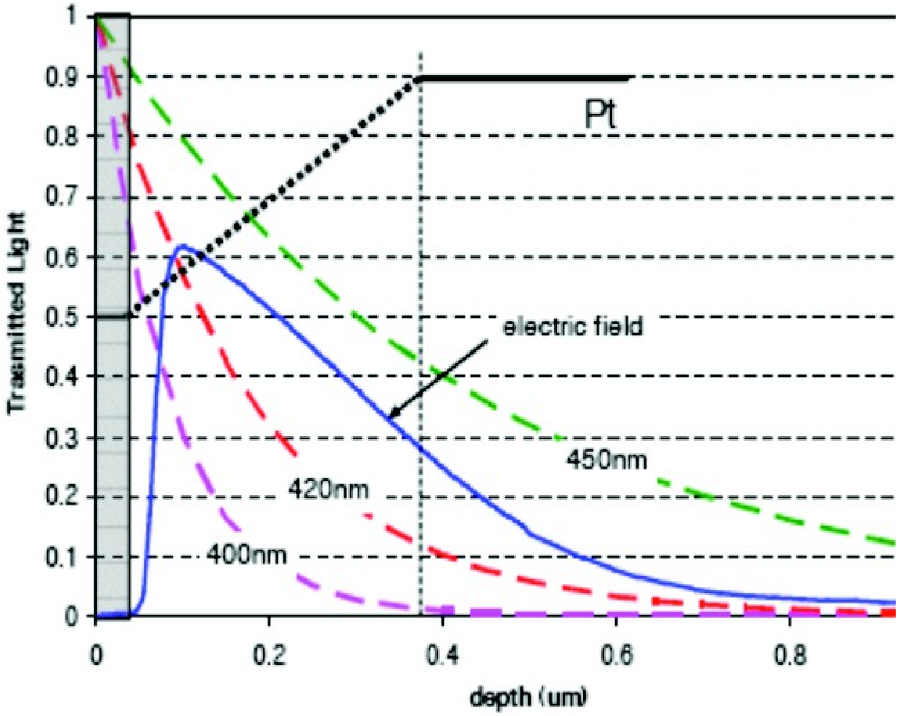

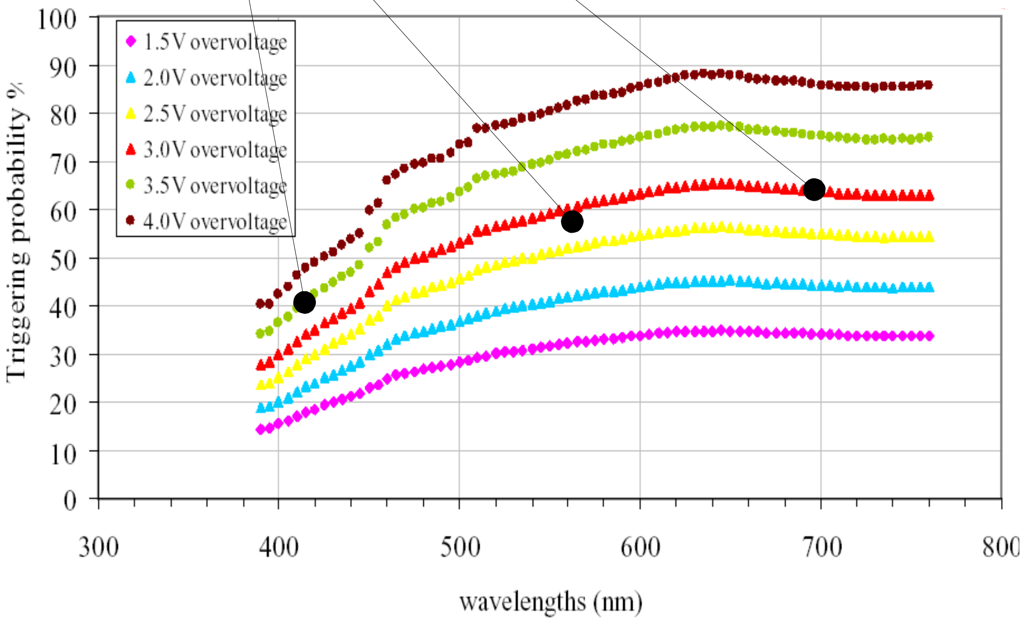

PDE VS λ (shape)

N.Dinu et al. NIM A (2008)

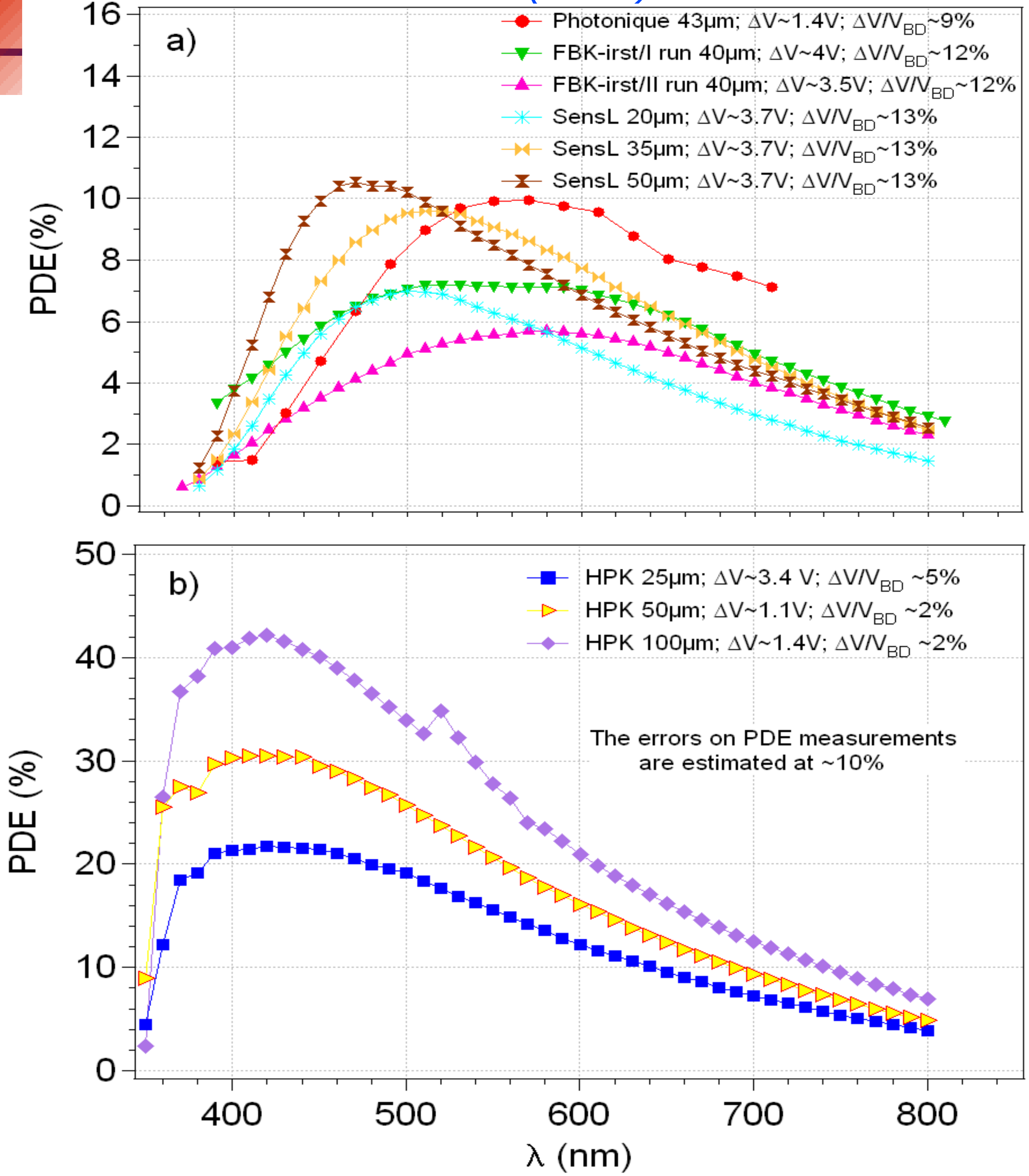

Fig. 5a) The PDE vs. λ of the Photonique, FBK-irst and SensL devices and b) HPK

n-on-p structures

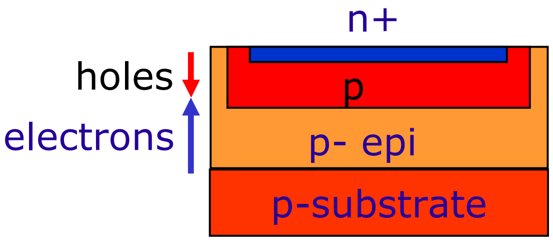

p-on-n structure

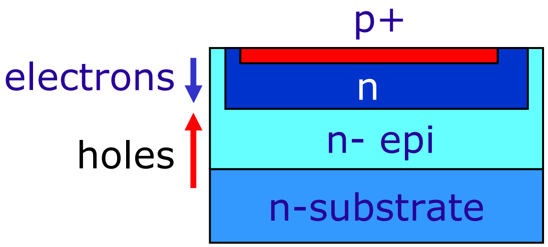

Note: geometrical fill factor included

Improving PDE

→ PDE peak constantly improving for many devices
→ every manufacturer shape PDE for matching target applications
→ UV SiPM eg from MePhi/Excelitas (see *E.Popova at NDIP 2011*)
→ VUV SiPMs in development too

Barlow – LIGHT 2011

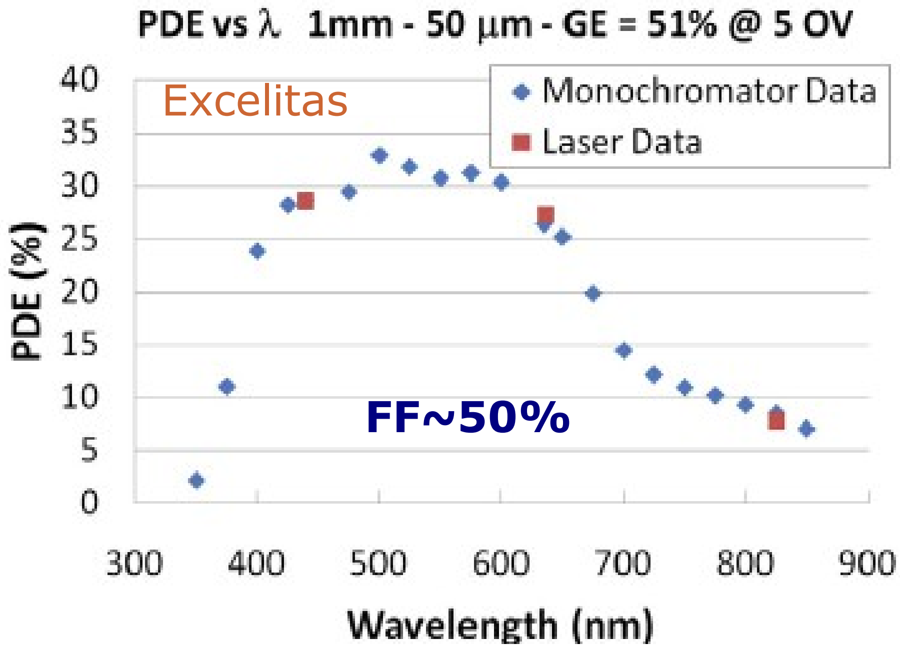

F.Wiest – AIDA 2012 at DESY

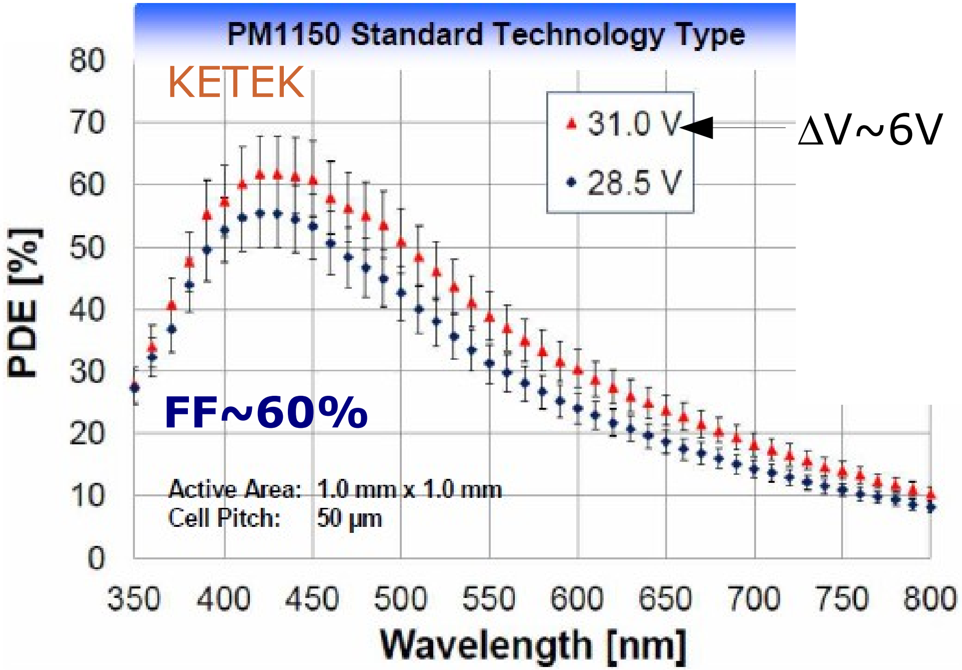

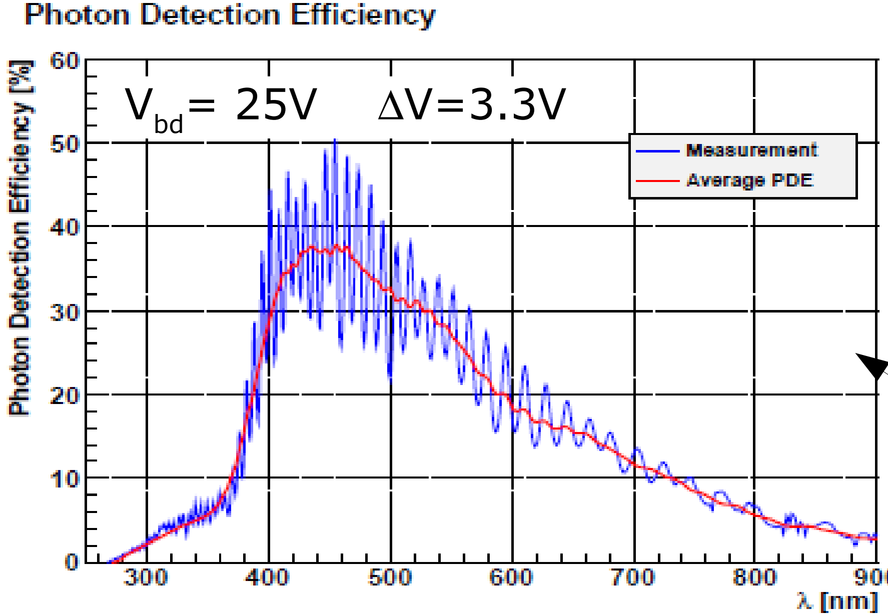

T.Frach 2012 JINST 7 C01112

dSiPM (latest sensor 2011)
→ up to now no optical stack optimization
→ no anti-reflecting coating
→ potential improvement up to 60% peak PDE (*Y.Haemish at AIDA 2012*)

PDE dependence on T

1) silicon E_{gap} increasing
→ larger attenuation length
→ lower QE (for larger λ)

2) mobility increasing
→ larger impact ionization
→ larger trigg. avalanche P_{01}

3) carriers freeze-out
onset below 120K
→ loss of carriers

PDE vs λ (ΔV constant)

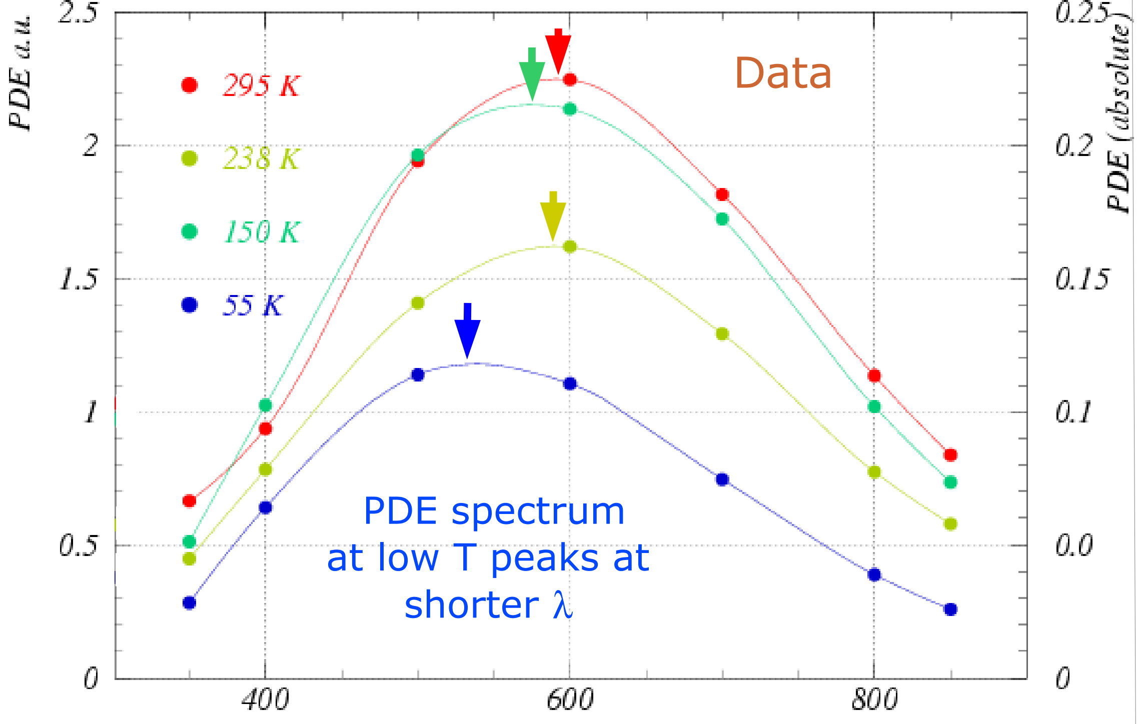

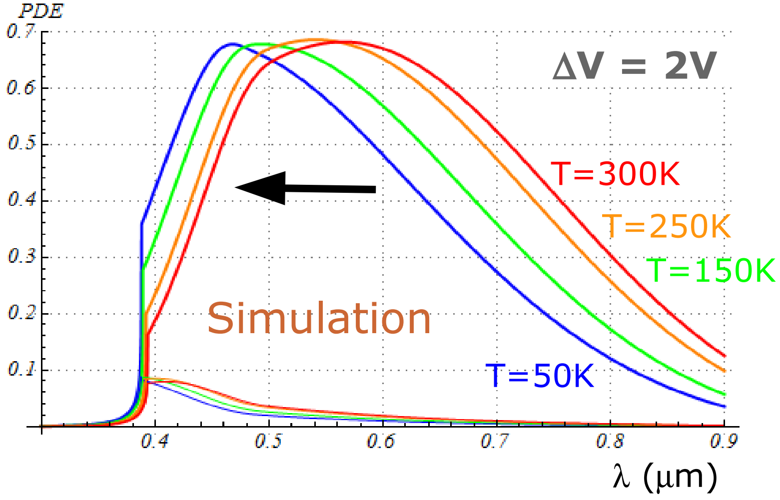

PDE vs ΔV (λ constant)

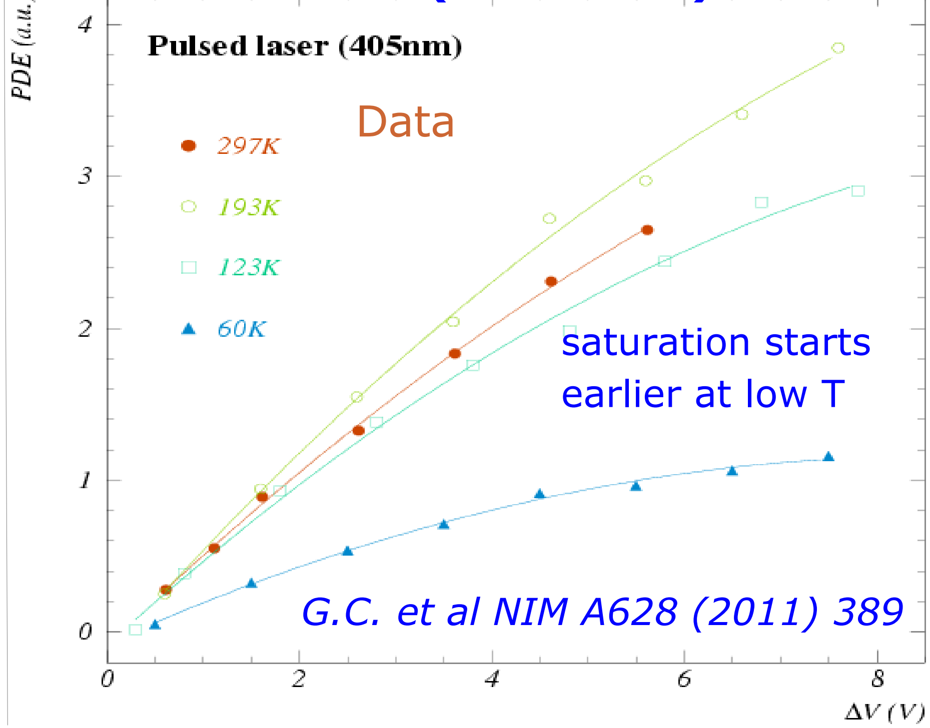

saturation starts earlier at low T

G.C. et al NIM A628 (2011) 389

Timing resolution

SiPM are intrinsically very fast

Two timing components, related to
photo-generation and avalanche developement

1) prompt → gaussian time jitter well below **100ps** (depending on ΔV, and λ)

2) delayed → non-gaussian tails up to **few ns** (depending on λ)

GM-APD avalanche development

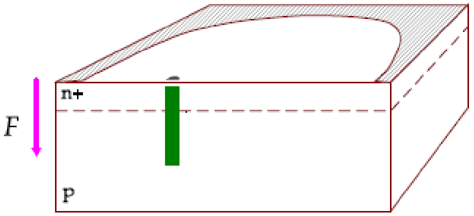

Longitudinal multiplication

Duration ~ few **ps**

Internal current up to ~ few **μA**

(1) Avalanche “seed”: free-carrier concentration rises exponentially by **"longitudinal" multiplication**

(1') Electric field locally lowered (by **space charge R effect**) towards breakdown level

Multiplication is self-sustaining
Avalanche current steady until new multiplication triggered in near regions

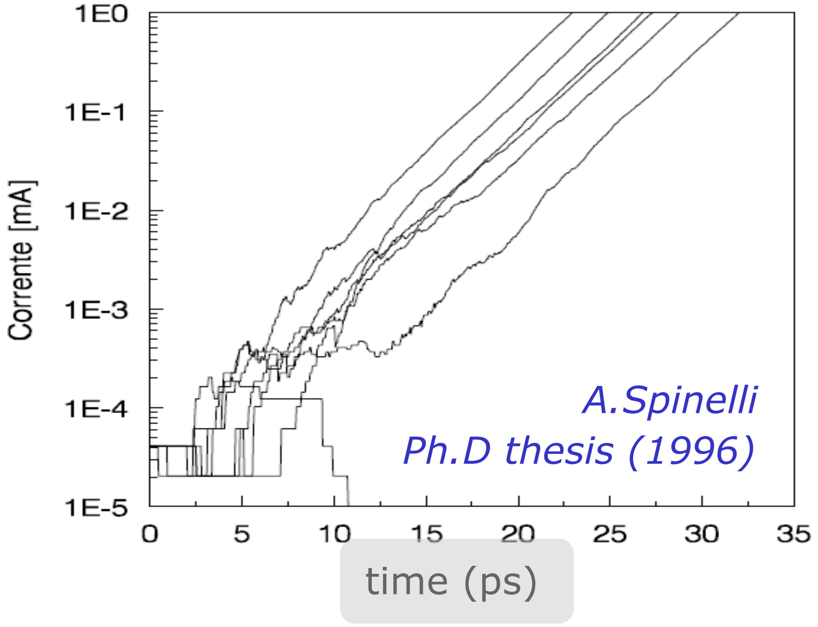

A.Spinelli Ph.D thesis (1996)

×100

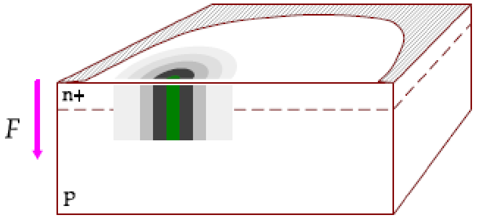

Transverse multiplication

Duration ~ few **100ps**

Internal current up to ~ several **10μA**

(2) Avalanche spreads "transversally" across the junction

(**diffusion speed ~up to 50μm/ns** enhanced by multiplication)

(2') Passive quenching mechanism effective after transverse **avalanche size ~10μm**

(if no quench, avalanche spreads over the whole active depletion volume → avalanche current reaches a final saturation steady state value)

Simulation w/o quenching:
→ steady current reached

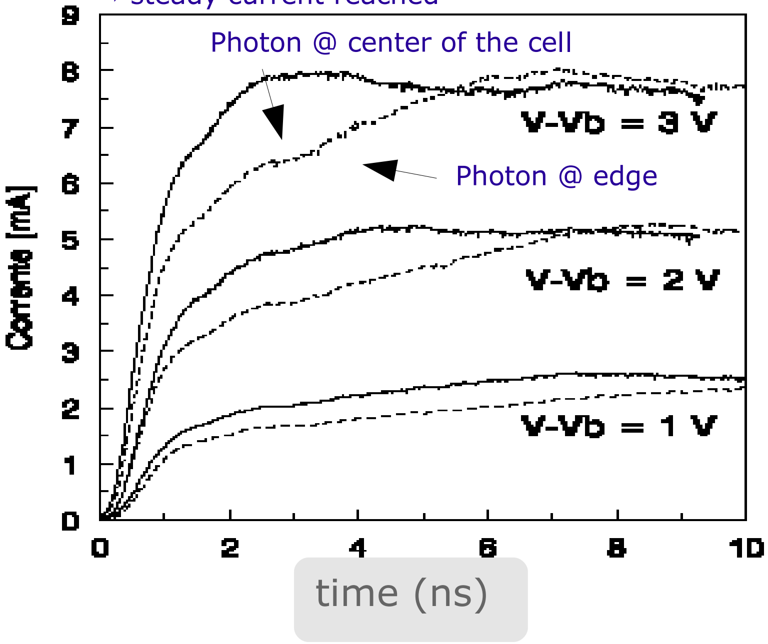

Timing jitter: prompt and delayed components

1) Prompt component: gaussian with time scale O(100ps)

Statistical fluctuations in the avalanche:

- **Longitudinal** build-up (minor contribution)
- **Transversal** propagation (main contribution)
    - - via multiplication assisted diffusion (dominating in few μm thin devices)
      A.Lacaita et al. APL and El.Lett. 1990
    - - via photon assisted propagation (dominating in thick devices – O(100μm))
      PP.Webb, R.J. McIntyre RCA Eng. 1982
      A.Lacaita et al. APL 1992

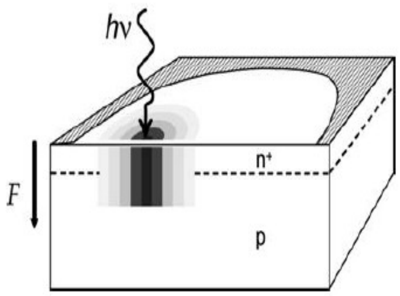

Multiplication assisted diffusion

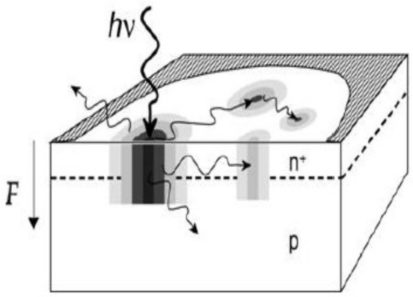

Photon assisted propagation

Fluctuations due to

a) impact ionization statistics

b) variance of longitudinal position of photo-generation: finite drift time even at saturated velocity
note: saturated ve ~ 3 vh
(n-on-p are faster in general)

→ Jitter at minimum → **O(10ps)**
(very low threshold → not easy)

Fluctuations in shock-wave due to

c) variance of the transverse diffusion speed v_{diff}

d) variance of transverse position of photo-generation: slope of current rising front depends on transverse position

→ Jitter → **O(100ps)**
(usually threshold set high)

Timing jitter: prompt and delayed components

2) delayed component: non-gaussian tails with time scale O(ns)

Carriers photo-generated in the neutral regions above/beneath the junction and reaching the electric field region by diffusion

G.Ripamonti, S.Cova Sol.State Electronics (1985)

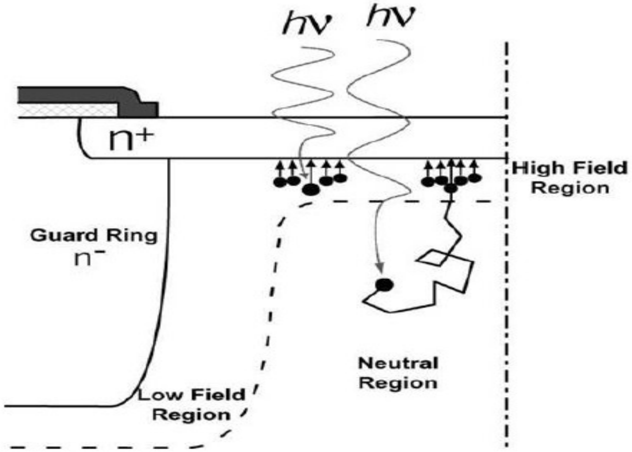

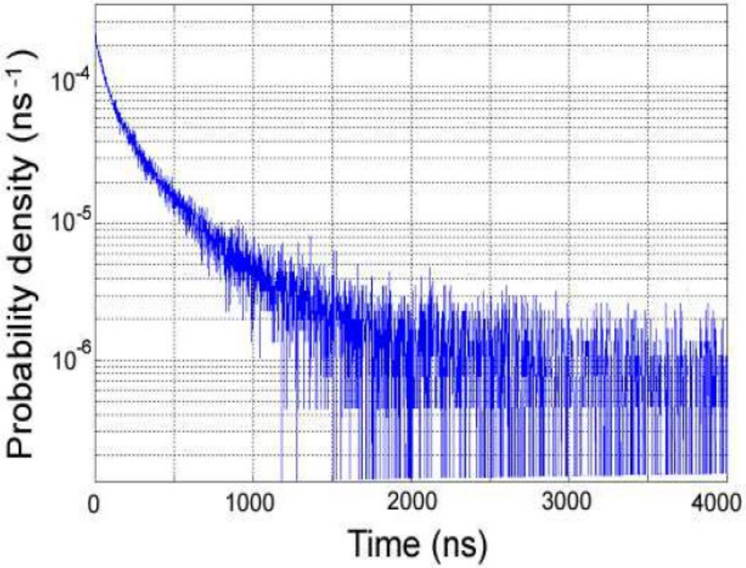

tail lifetime: $\tau \sim L^2 / \pi^2 D$ ~ up to some ns

L = effective neutral layer thickness

D = diffusion coefficient

S.Cova et al. NIST Workshop on SPD (2003)

→ **Neutral regions** underneath the junction : timing tails for long wavelengths

→ **Neutral regions** in APD entrance: timing tails for short wavelengths

GM-APD avalanche transverse propagation

Avalanche transverse propagation by a kind of shock wave: the wavefront carries a high density of carriers and high E field gradients (inside: carriers' density lower and E field decreasing toward breakdown level)

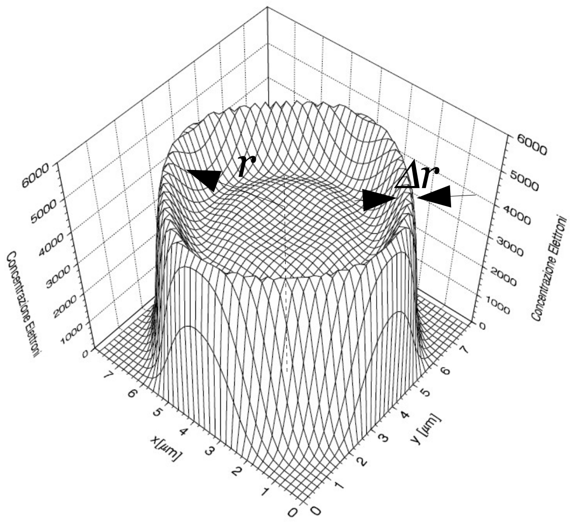

$$\frac{dS}{dt}=\frac{d}{dt}2\pi r(t)\Delta r=2\pi v_{diff}\Delta r=4\pi\Delta r\sqrt{\frac{D}{\tau}}$$

Rate of current production: $\frac{dI}{dt}=\frac{dI}{dS}\frac{dS}{dt}\sim\frac{\sqrt{D}}{R_{sp}\sqrt{\tau}}$

$$\frac{dI}{dS}=J=\frac{V_{bias}}{R_{sp}(S)}$$

S = surface of wavefront (ring of area $2\pi r\Delta r$)

$R_{sp}(S)$ = space charge resistance $\sim w^2/2\varepsilon v \sim O(50\ k\Omega\ \mu m^2)$

$v_{diff} \sim$ O(some $10\mu m$/ns)

D = transverse diffusion coefficient ~ O(μm^2/ns)

τ = longitudinal (exponential) buildup time ~ O(few ps)

Internal current rising front:
the faster it grows, the lower the jitter
dI/dt → understand/engineer timing features of SiPM cells

$$\tau\sim\frac{1}{1-(E_{max}/E_{breakdown})^n}$$

→ timing resolution improves at high V_{bias}

→ E field profile affects τ and R_{sp} (wider E field profile → smaller R) (should be engineered when aiming at ultra-fast timing)

→ T dependence of timing through τ and D

→ slower growth at GAPD cell edges → higher jitter at edges
reduced length of the propagation front

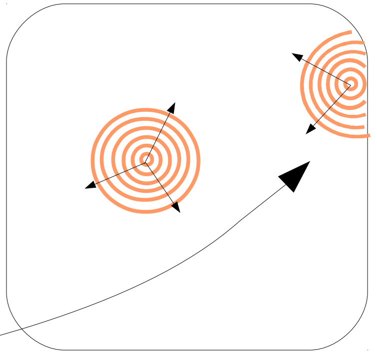

SiPM cell

Avalanche transverse propagation

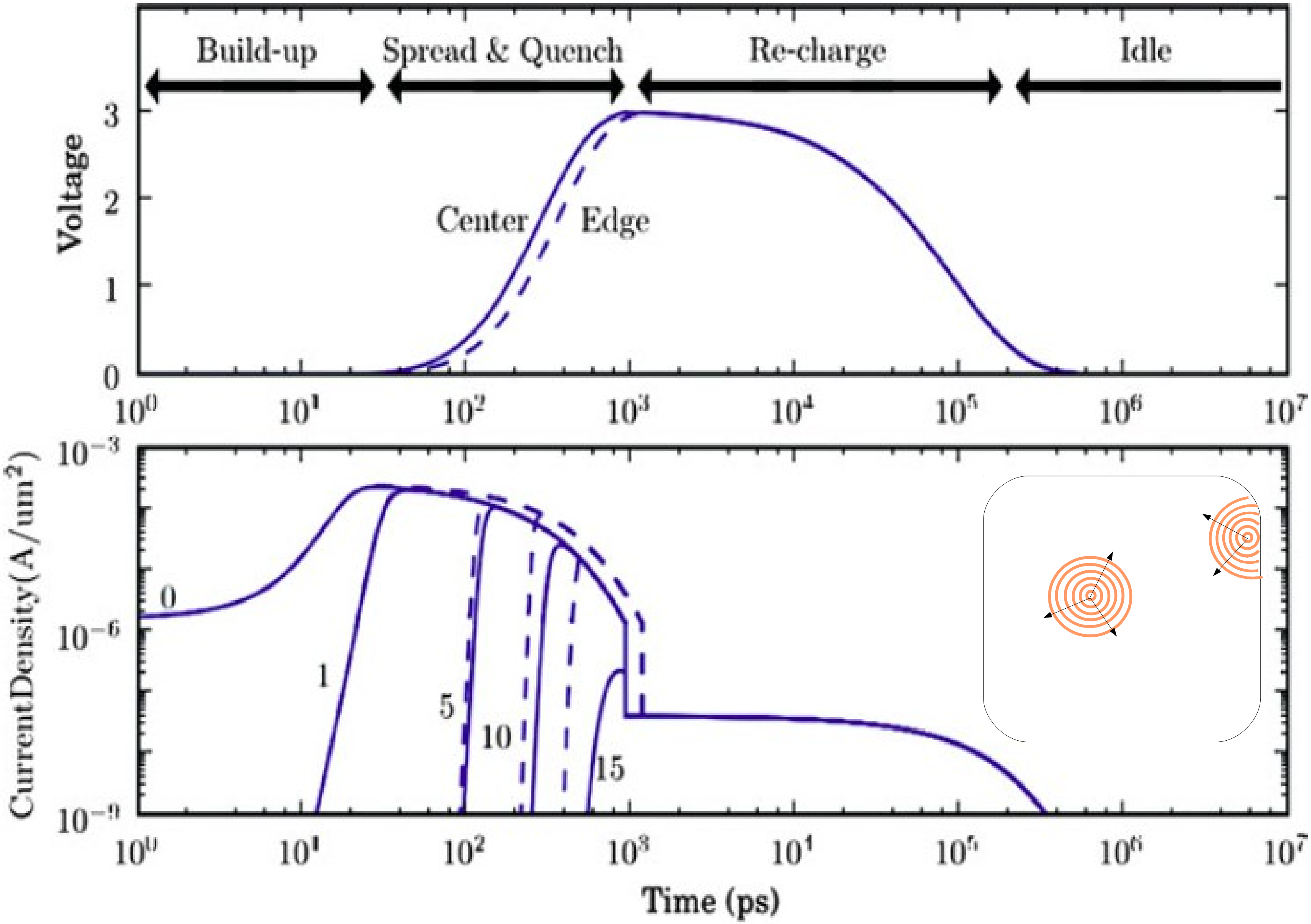

Pulse Shape – rise and fall edges

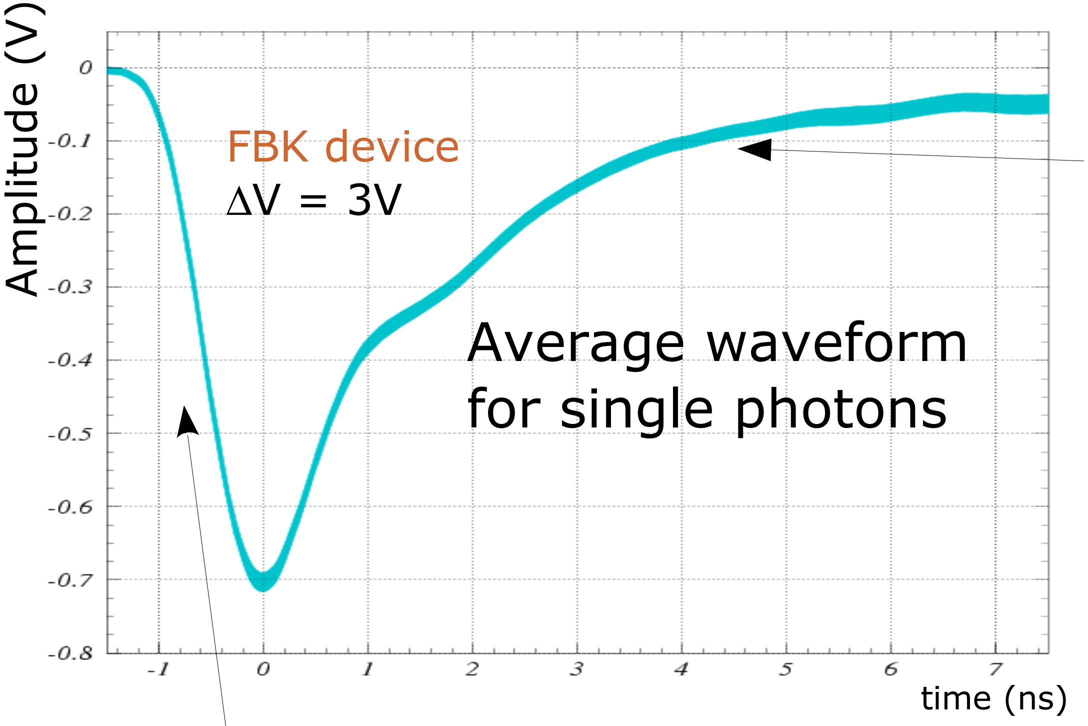

Falling signal shape fluctuates considerably (due eg to after-pulses) → signal tail is non useful for timing, if not detrimental

note: using Time-over-Threshold method for slew correction might lead to worse resolution

Reminder:

$$\frac{dI}{dt} \sim \frac{\sqrt{D}}{R_{sp}\sqrt{\tau}}$$

$$\tau \sim \frac{1}{1-(E_{max}/E_{breakdown})^{n}}$$

Rise-time depends on **ΔV**, **T** and **impact position** ie **signal shape is not constant**, then:
1) CFD method only partially effective in canceling time walk effects
2) any digital timing filter should account for shape variations (ΔV, T)

For comparison about waveform method and various digital algorithms
see Ronzhin et al NIM A 668 (2012) 94

Single Photon Time Resolution = gaussian + tails

Time resolution of SiPM is not just a gaussian, but gaussian + tails
(in particular at long wavelengths)

G.C. et al NIMA 581 (2007) 461

Data at **λ=400nm**

A simple **gaussian component** fits fairly

Data at **λ=800nm**

fit gives reasonable χ^2 in case of an **additional exponential term** exp(-|Δt|/τ) summed with a weight

- **τ ~ 0.2÷0.8ns** (depending on device) in rough agreement with diffusion tail lifetime: $\tau \sim L^2 / \pi^2 D$ wher L is the diffusion length
- Weight of the **exp. tail ~ 10%÷30%** (depending on device)

Gaussian + Tails (long λ)

rms ~ 50-100 ps

~ exp (-t / O(ns))
contrib. several %
for long wavelengths

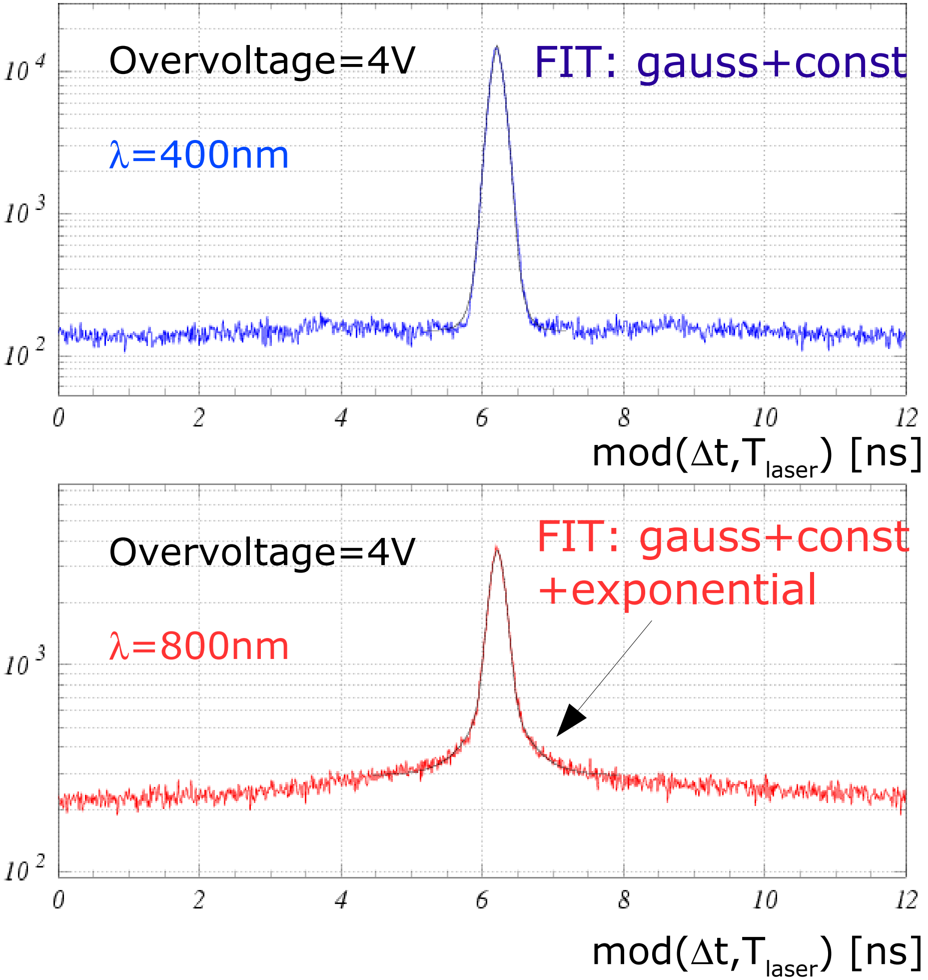

Distributions of the difference in time between successive peaks

Singel Photon Timing Resolution

(gaussian component)

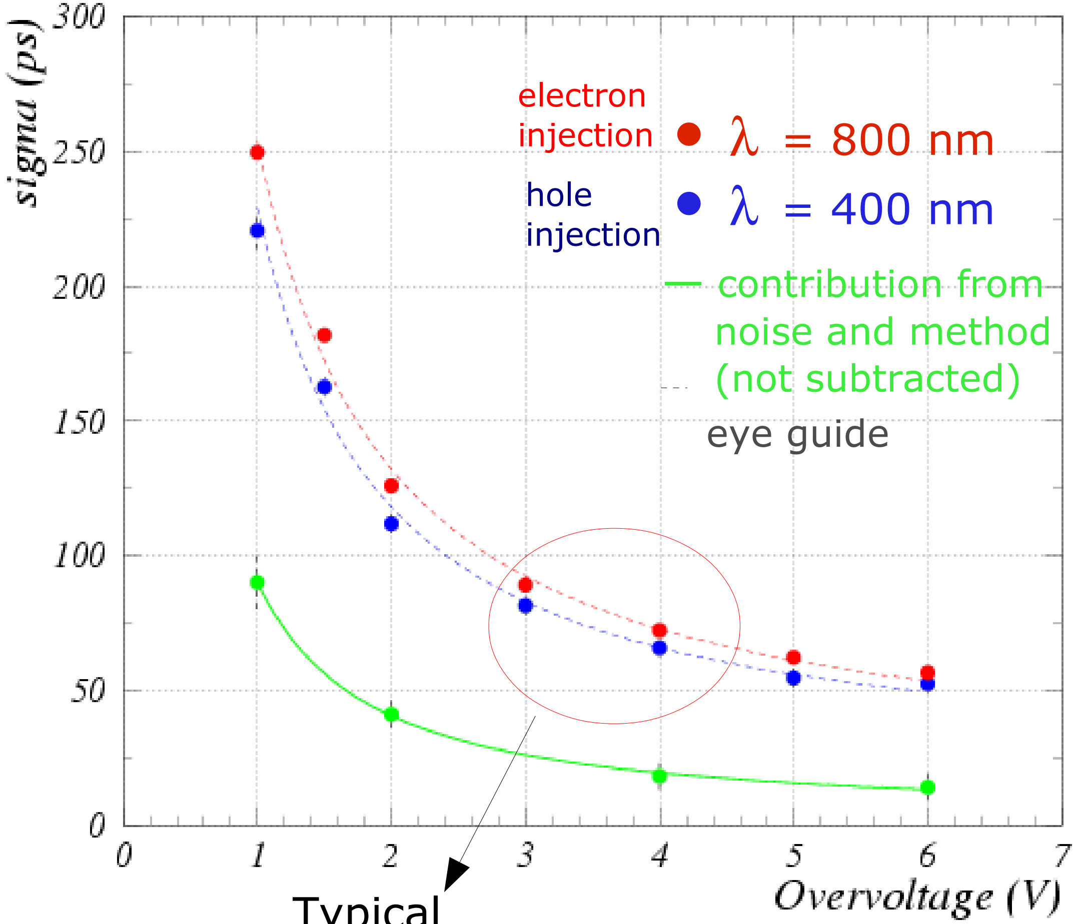

Typical working region

G.C. et al NIMA 581 (2007) 461

NOTE: good timing performances kept up to 10MHz/mm^2 photon rates

Multi-Photon Resolution

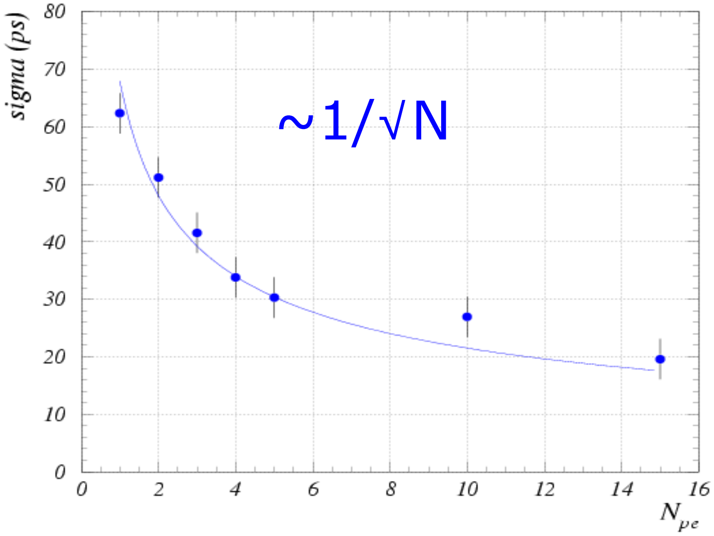

Note: SPTR differences (due to drift):

1) high field junction position

- shallow junction: $\sigma_t^{red} > \sigma_t^{blue}$
- buried junction: $\sigma_t^{red} < \sigma_t^{blue}$

2) n$^+$-on-p smaller jitter than p$^+$-on-n due to electrons drifting faster in depletion region (but λ dependence)

3) above differences more relevant in thick devices than thin

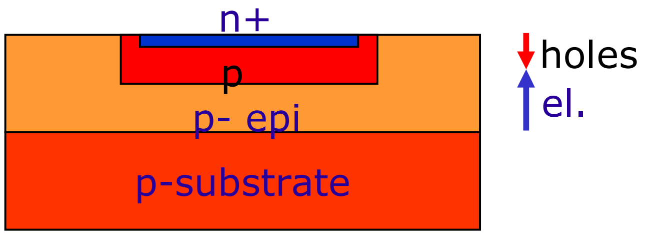

SPTR: position dependence → cell size

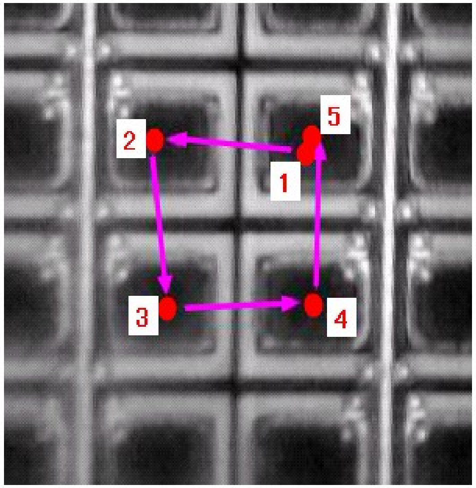

	FWHM (ps)	FWTM (ps)
1	199	393
2	197	389
3	209	409
4	201	393
5	195	383

K.Yamamoto PD07

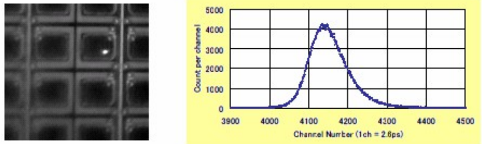	FWHM = 263 ps
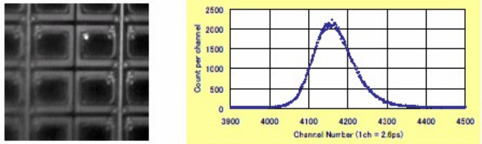	FWHM = 294 ps
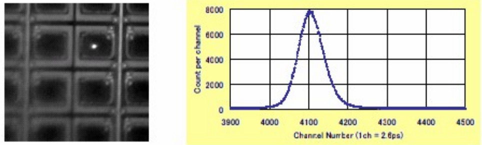	FWHM = 192 ps

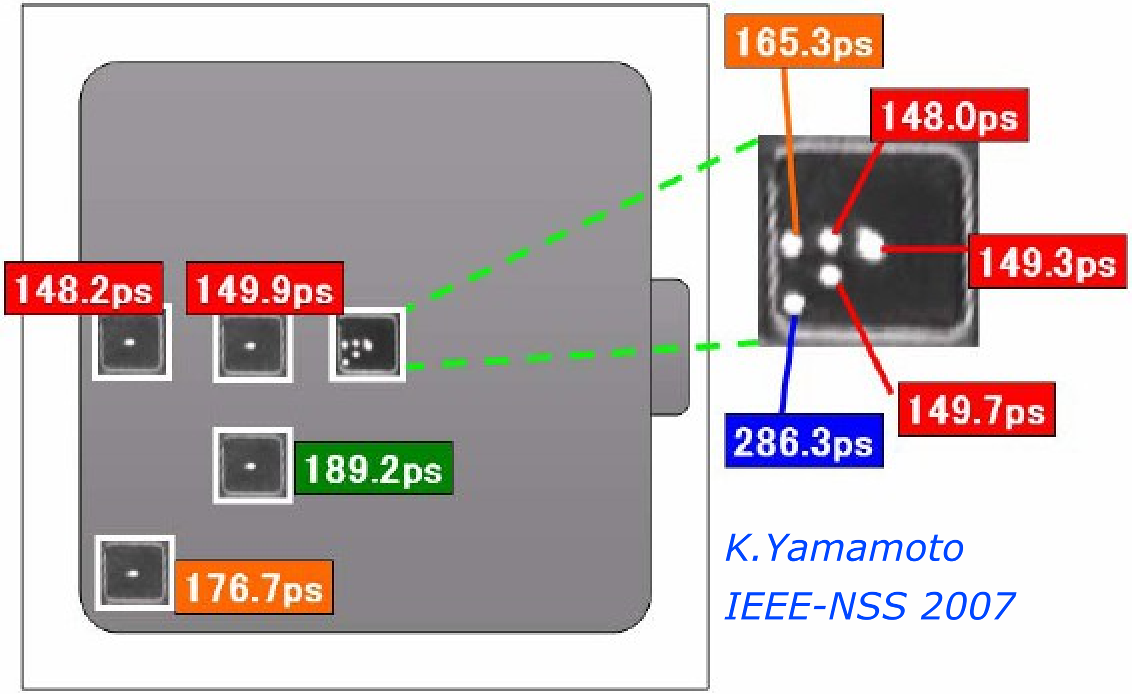

K.Yamamoto
IEEE-NSS 2007

Data include the system jitter
(common offset, not subtracted)

Larger jitter if photo-conversion at the border of the cell

Due to:

1) slower avalanche front propagation

2) lower E field at edges

→ cfr PDE vs position

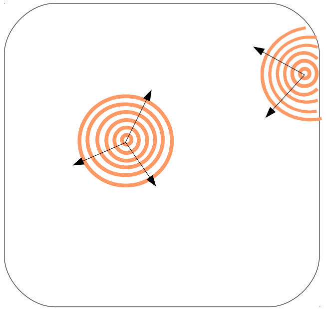

PDE vs timing trade off

C.H.Tan et al IEEE J.Quantum Electronics 13 (4) (2007) 906

k=ratio of hole (β) to electron (α) ionization coefficient (increasing with E field)

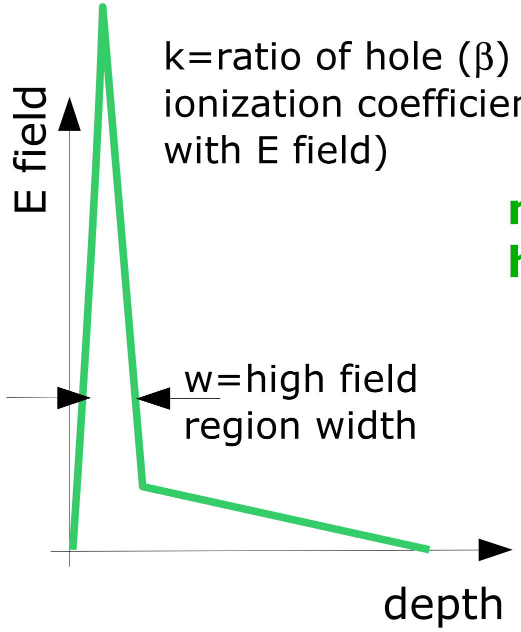

narrow avalanche region, high E:
- **small w**
- **high k = β / α**

better for **TIMING**

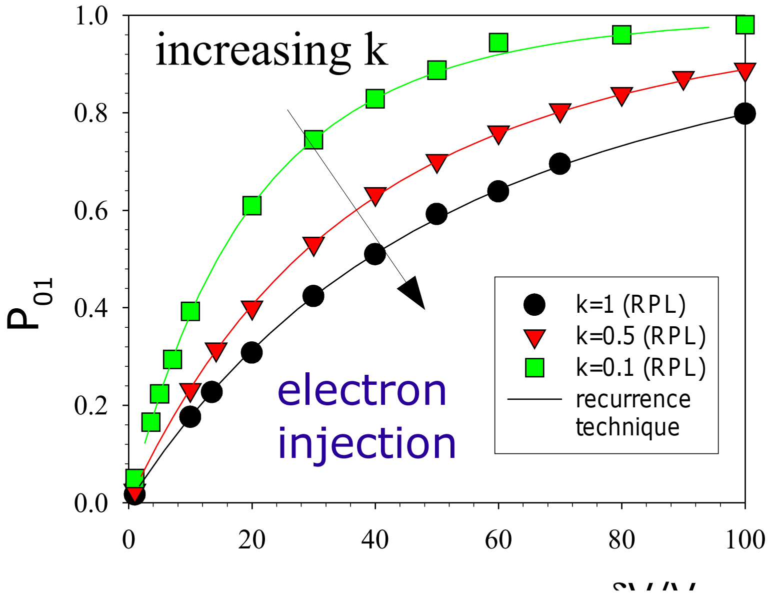

better for **PDE**

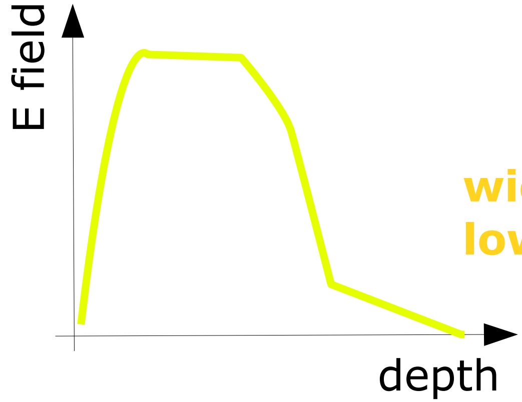

wide avalanche region, low E:
- **wide w**
- **small k = β / α**

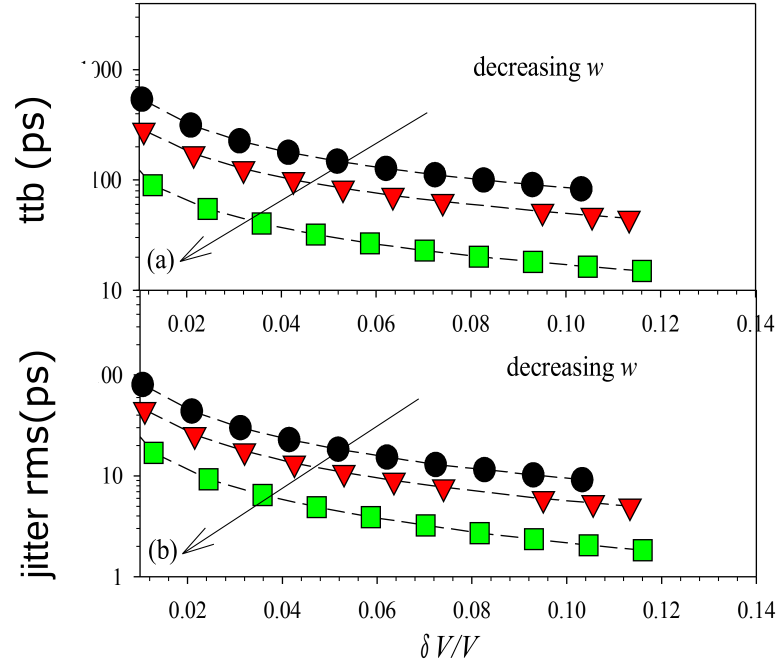

plots: courtesy of C.H.Tan

Technologies around the world

Pioneering work in '90s by Russian institutes

- **CPTA**, Moscow
- **JINR**, Dubna

Metal-Resistive-Semiconductor

- **MePhi/Pulsar** Enterprise, Moscow — **Poly-silicon resistor**

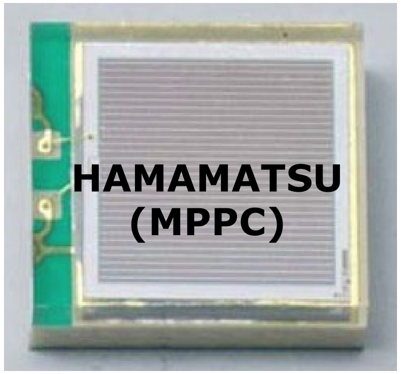

Recently more institutes/companies involved

- **Hamamatsu HPK**, Hamamatsu
- **FBK-AdvanSiD**, Trento — **SiPM Matrixes** **vias to avoid bonding**
- **SensL**, Cork
- **ST Microelectronics**, Catania
- **Excelitas** techn. (formerly Perkin-Elmer)
- **National Nano Fab Center**, Korea
- **Novel Device Laboratory** (**NDL**), Bejing

Poly-silicon resistor

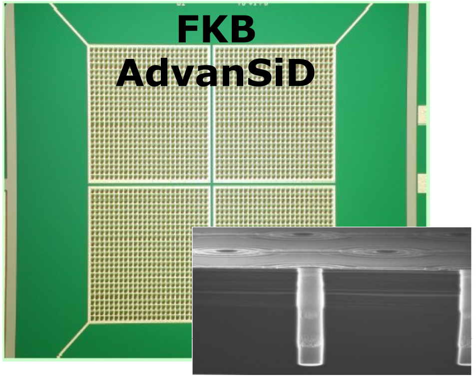

- **MPI-HLL**, Munich — **Resistor embedded in the bulk**
- **RMD**, Boston — **CMOS process**
- **Philips**, Aachen — **Digital SiPM (CMOS)**
- **Zecotek,** Vancouver — **Quenching with floating wells**
- **Amplification Technologies**, Orlando

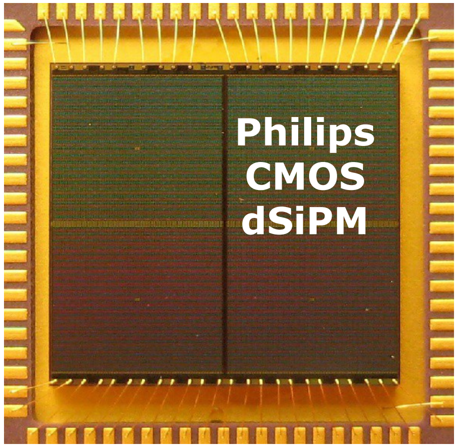

Some are commercially available, other prototypes

ZECOTEK MAPD-3N

ASD-SiPM4S

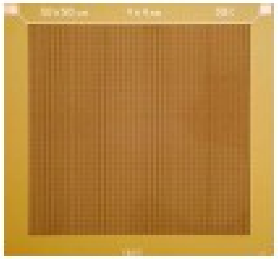

HAMAMATSU S10985

KETEK PM3350

STMicroelectronics

Producer	Reference	Area (mm^2)	PDE max @ 25 °C *	Dark Count Rate (Hz) @ 25°C *	Gain *
ZECOTEK	MAPD-3N	3 x 3	30% @ 480 nm	$9.10^5 - 9.10^6$	10^5
FBK - AdvanSiD	ASD-SiPM4S	4 x 4	30% @ 480 nm	$5.5\ 10^7 - 9.5\ 10^7$	$4.8\ \ 10^6$
HAMAMATSU	S10985-50C	6 x 6	50% @ 440 nm (includes afterpulses & crosstalk)	$6.10^6 - 10.10^6$	$7.5\ \ 10^5$
KETEK	PM3350	3 x 3	40% @ 420 nm	4.10^6	$2\ \ 10^6$
STMicrolectronics	SPM35AN	3,5 x 3,5	16% @ 420 nm	$7.5\ 10^6$	$3.2\ 10^6$

** datasheet data*

Ongoing R&D to increase the active area at KETEK, AdvanSiD, Excelitas (6 x 6 mm^2)

Other solution to get larger area : connection of several channels of a matrix

Hybrid Photo Detectors

1) Photo-emission from photo-cathode
2) Photo-electron acceleration to **$\Delta V \sim$ 10-20kV**
3) charge multiplication in Si by ionization
→ **reduced fluctuations** due to Fano factor (F~0.12 in Si)

$$G = \frac{\Delta V - V_{thr.}}{W_{Si}}$$

$$\sigma_G = \sqrt{F \cdot G}$$

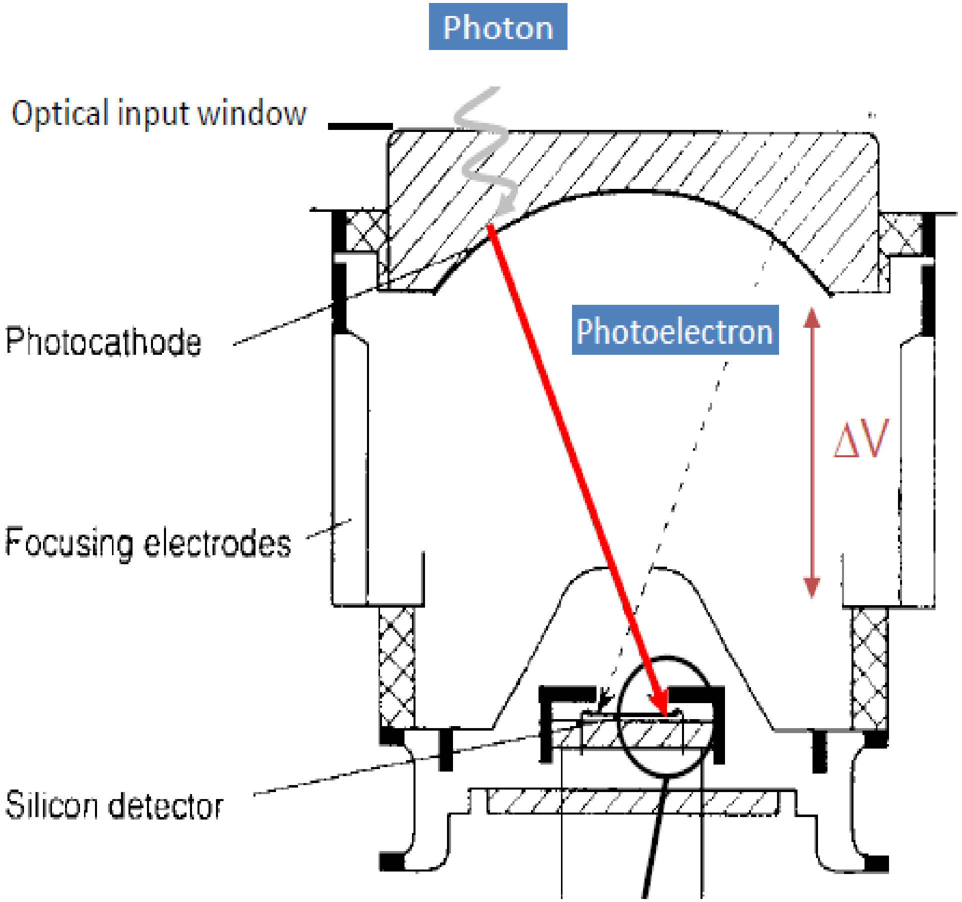

EDIT 2011 School at CERN - photodetectors

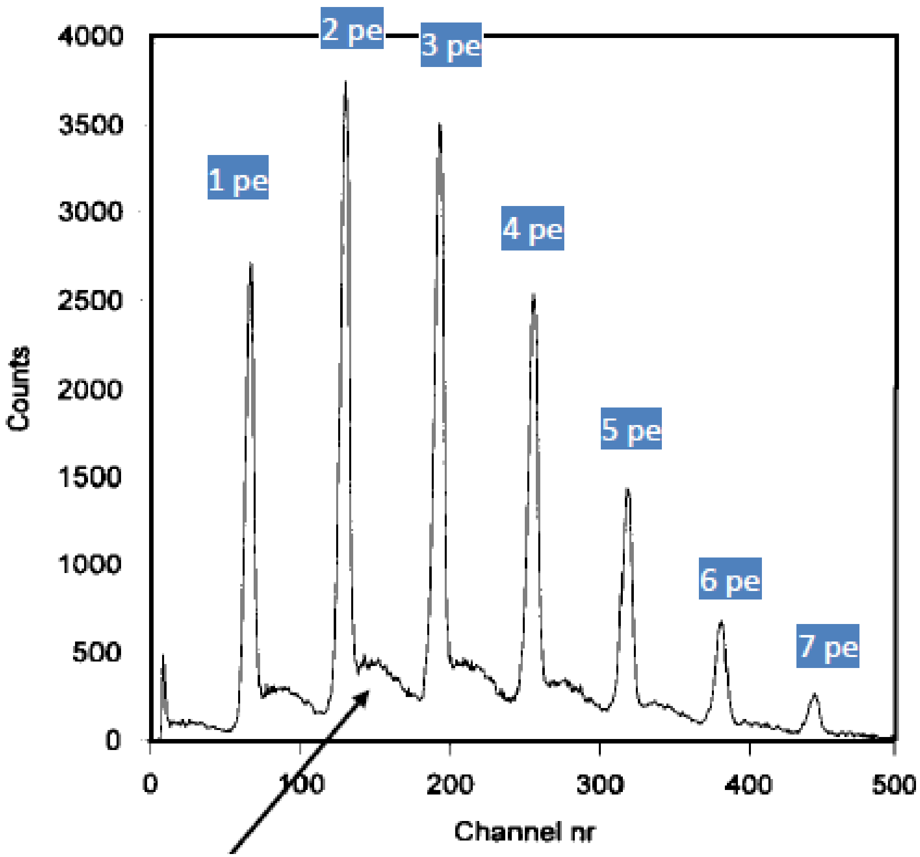

background from electron back-scattering at Si surface

Summary,
comparison
and conclusions

Quantum Efficiencies (HPK)

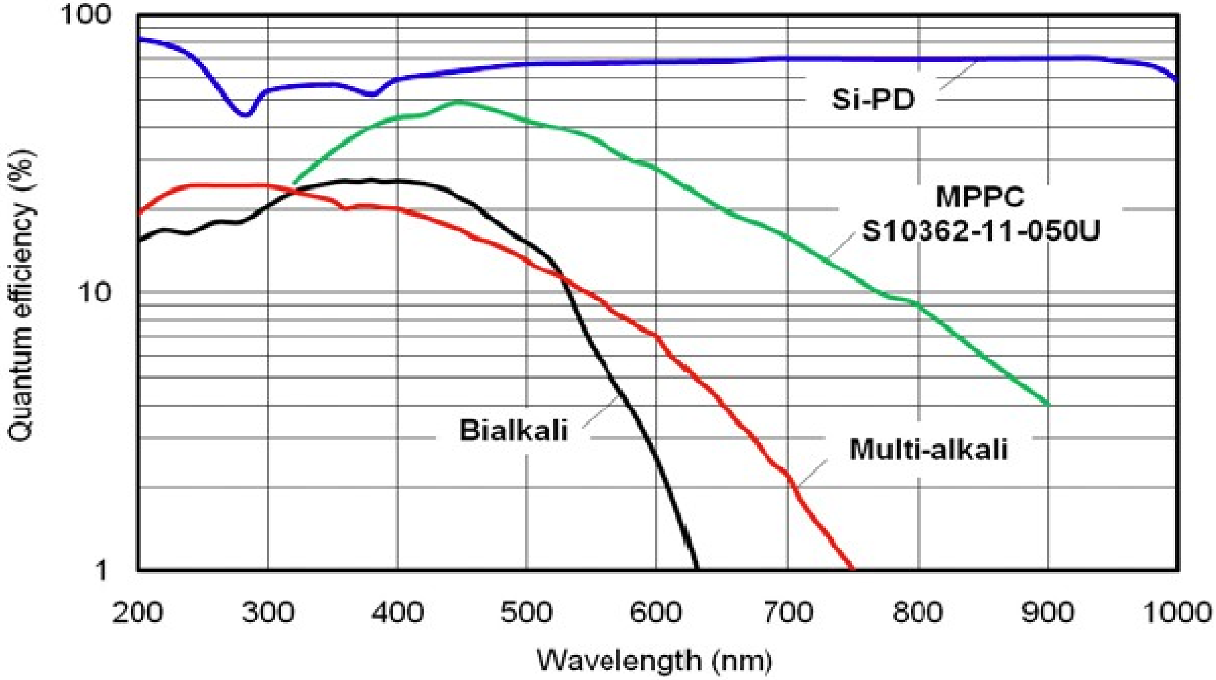

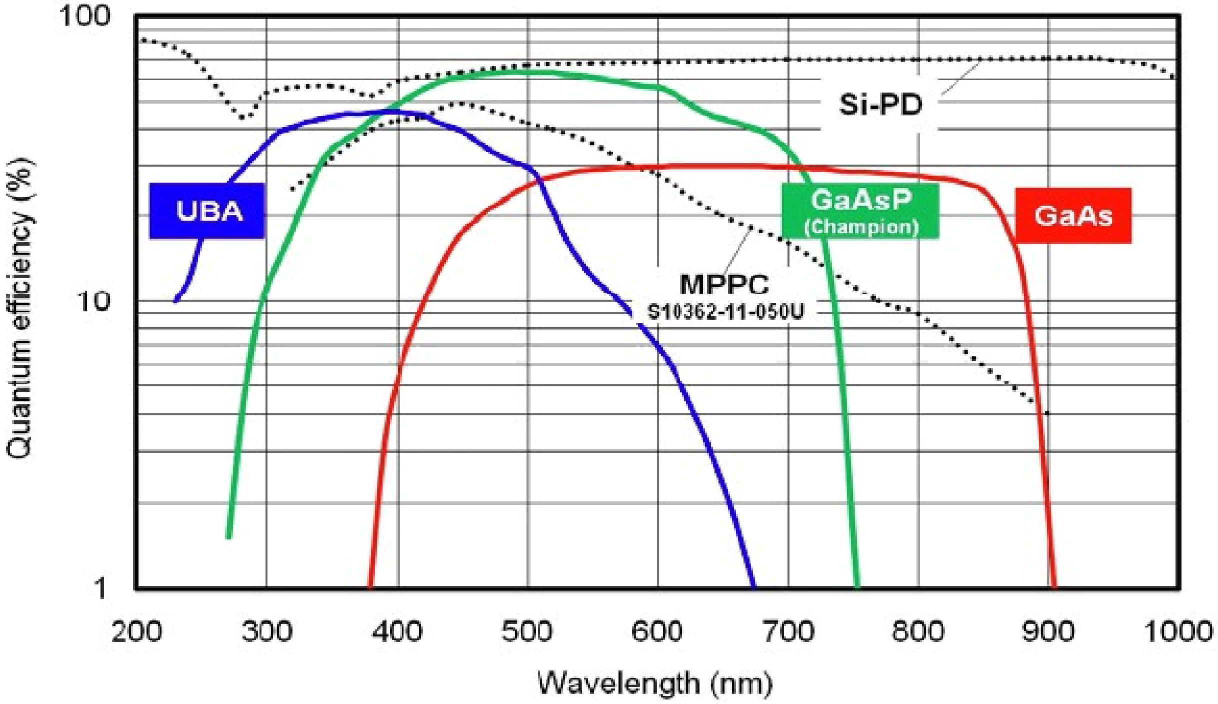

Summary Table

	QE	CE	δ_i	ENF	G	ENC	σ/E
Ideal	1.0	1.0	1000	1.0	10^6	0	$\sqrt{1/N}$
PMT	0.35	0.9	10	1.3	10^6	200	$\sqrt{3.8/N}$
PD	0.7	1.0	-	1.0	1	200	$\sqrt{1.4/N+(280/N)^2}$
APD	0.7	1.0	2	2.0	100	200	$\sqrt{2.9/N+(2.9/N)^2}$
HPD	0.5	0.9	1000	1.0	10^3	200	$\sqrt{2.2/N+(0.4/N)^2}$
HAPD	0.5	0.9	1000	1.0	10^5	200	$\sqrt{2.2/N}$
SiPM	0.7	0.4	1000	1.3	10^6	1000	$\sqrt{4.3/N}$
VLPC	0.7	1.0	1000	1.0	10^5	200	$\sqrt{1.4/N}$

K.Arisaka – Lecture at IEEE NSS 2012 (Anaheim)

Energy resolution vs #photons

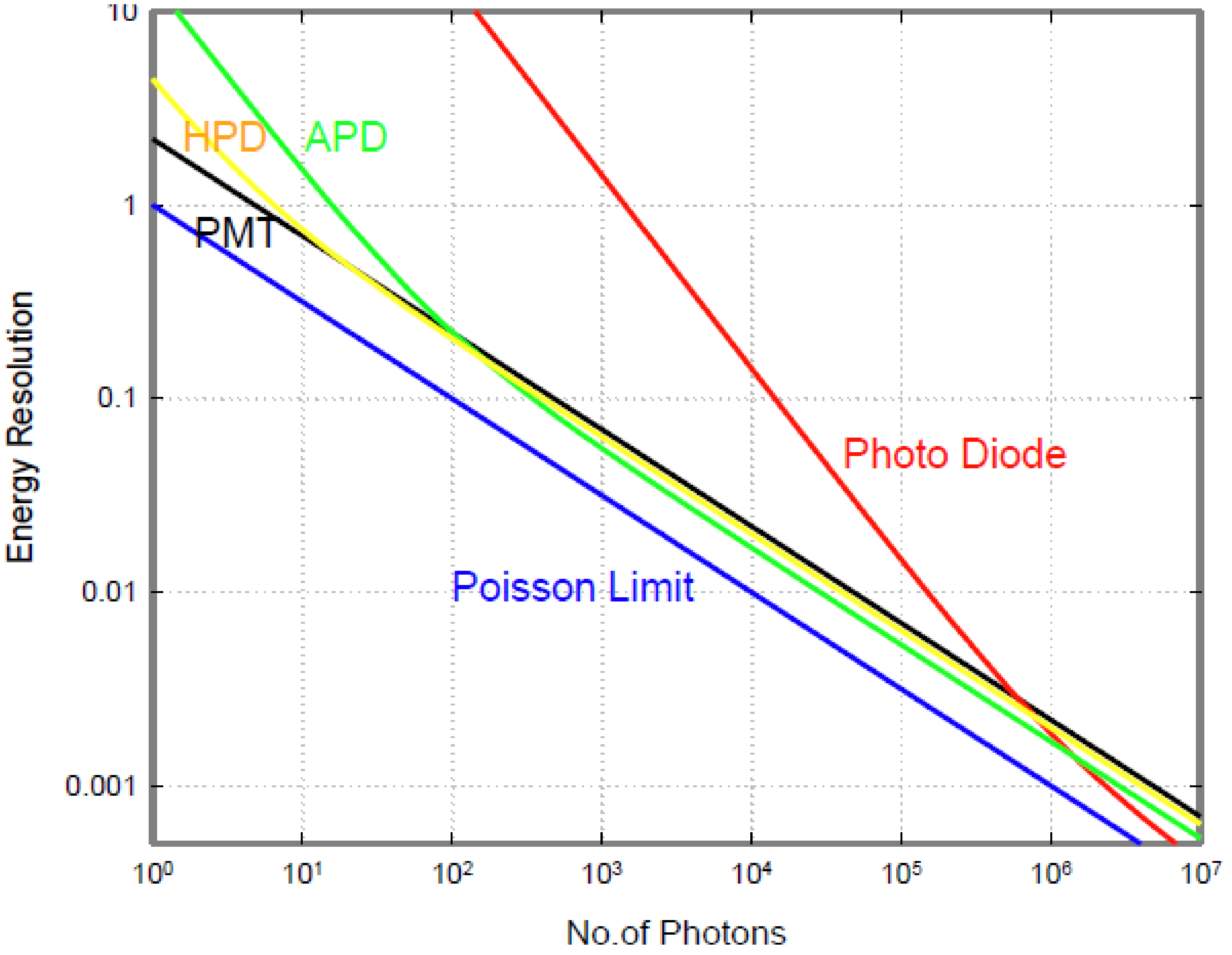

K.Arisaka – Lecture at IEEE NSS 2012 (Anaheim)

Resolution vs Poisson limit

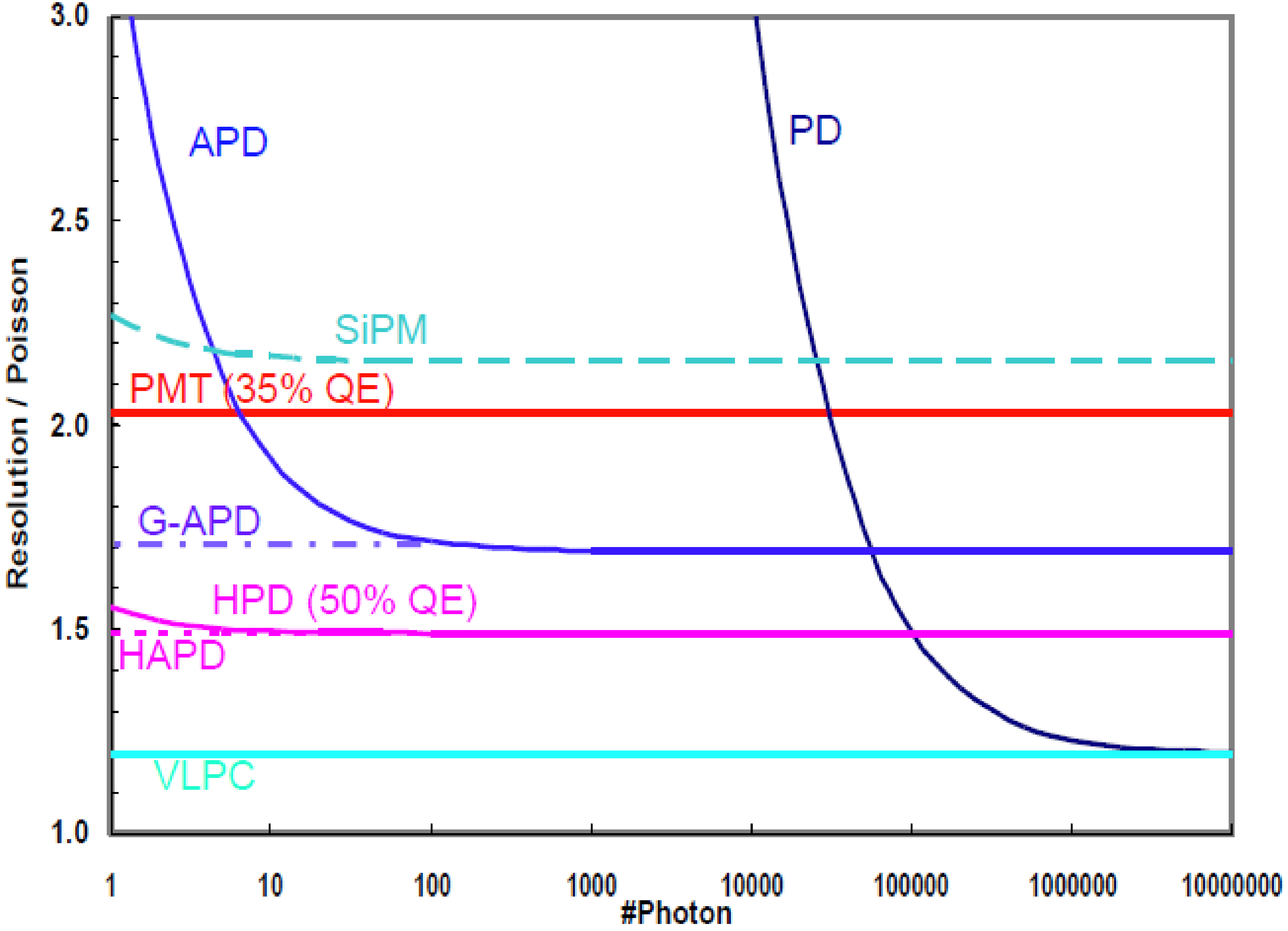

K.Arisaka – Lecture at IEEE NSS 2012 (Anaheim)

Timing (single photon) vs Area

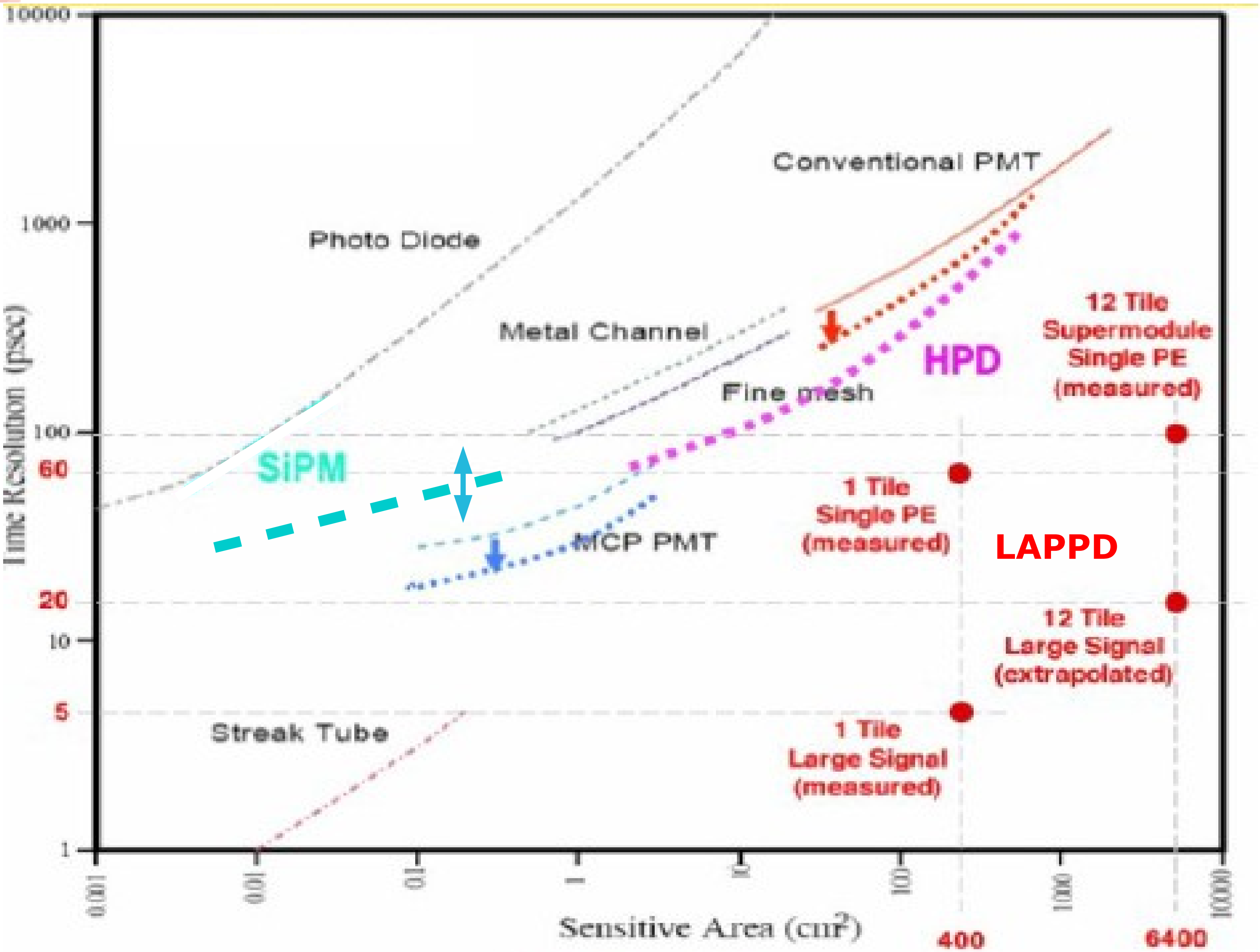

Market price

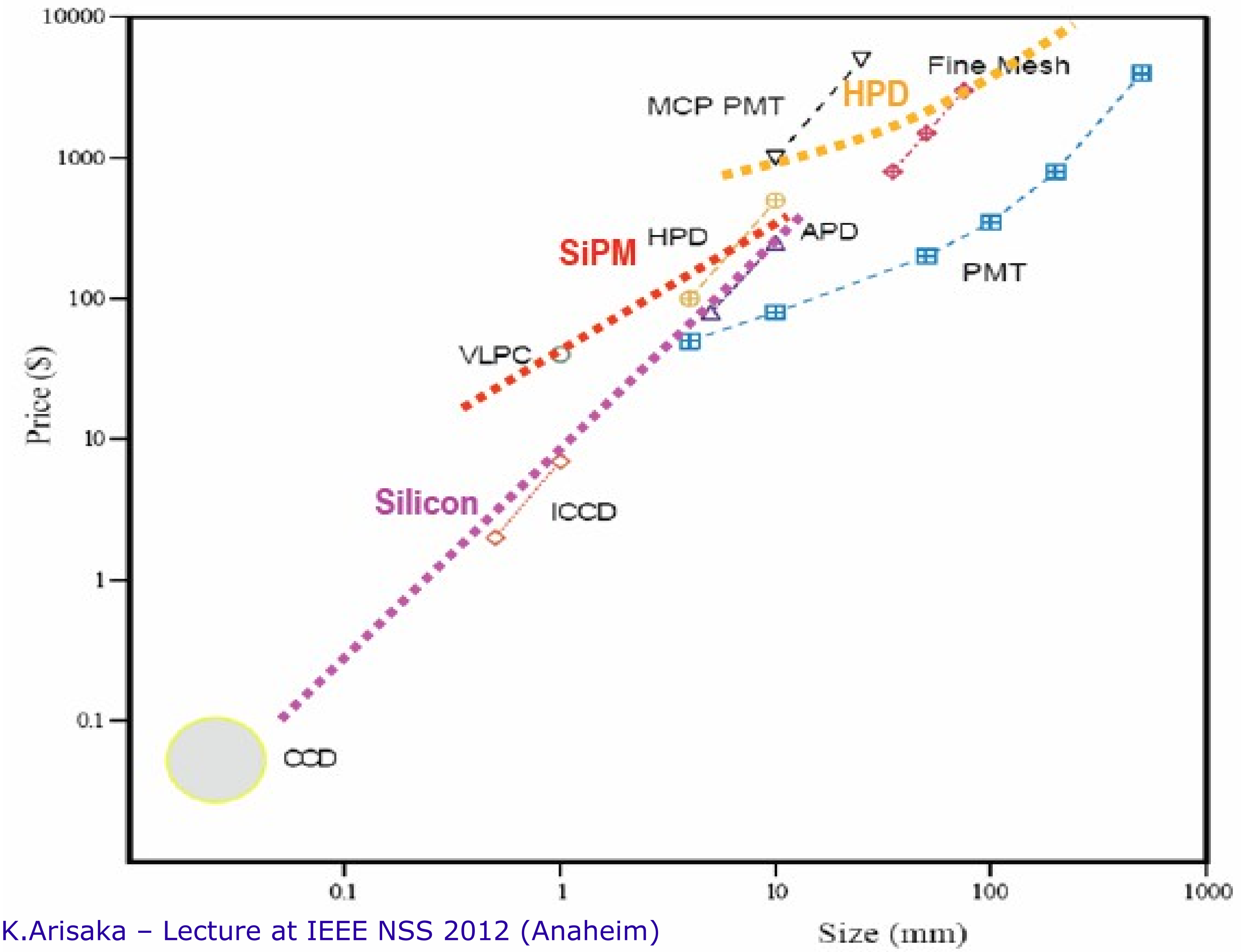

K.Arisaka – Lecture at IEEE NSS 2012 (Anaheim)

Conclusions – vacuum based PD

PMT: 80 years old... still the most used sensor for low-level light detection

Features
- sensitivity from DUV to NIR
- **high gain**
- **low noise**
  - → single photon sensitivity
  - → large area at low cost
  - → low capacitance
- imaging capabilities (large pixels)
- high frequency response
  - → fast speed
- stability

Issues
- intrinsic **limit QE < 40%**
- broad SER
- high voltage, bulky, fragile
- influenced by B, E fields
- damaged by high-level light
- ageing (eg. He)
- radiopurity

Developement

→ photocathodes: new materials and geometries → high QE
→ ultra-fast, large area, imaging MCP based PMTs
→ hybrids (eg photocathode + SiPM) → narrow SER

Conclusions – solid state PD

PIN photo-diode: successfully used, e.g. in HEP experiments
- **No internal gain**: necessary Q sensitive amplifier (noise, slow)
  → minimum of several 100 photo-electrons (p.e.) detectable
- Nuclear counter-effect

Avalanche photo-diode: used in big experiments (CMS at LHC)
- Internal multiplication: S/N improved → still >20 p.e. detectable
- Gain limited by the excess noise due to **avalanche multiplication noise**

GM-APD based PM: technology of **SiPM** is mature
→ candidates for more and more experimental setups
- **Dark noise** still the most limiting factor → **active area**
- **Low T**: SiPM perform ideally in the range 100K < T < 200K
  → quenching R should be tuned shorter recovery (ad hoc)
  → lower gain (small cells) might be desirable to mitigate after-pulses

Development of GM-APD in several directions still missing, e.g.:
- IR/NIR sensitive devices → possibly with different semiconductors
- DUV/VUV sensitive devices → relatively easy with SiPM
- Imaging (small pixels)

...Other imaging devices (CCD, CMOS, ...) not covered in this talk

Thanks for your attention

Additional material →